

Argonne National Laboratory

CREWE ELECTRON-ENERGY-ANALYZING
SCANNING MICROSCOPE

by

D. N. Eggenberger

The facilities of Argonne National Laboratory are owned by the United States Government. Under the terms of a contract (W-31-109-Eng-38) between the U. S. Atomic Energy Commission, Argonne Universities Association and The University of Chicago, the University employs the staff and operates the Laboratory in accordance with policies and programs formulated, approved and reviewed by the Association.

MEMBERS OF ARGONNE UNIVERSITIES ASSOCIATION

The University of Arizona
Carnegie-Mellon University
Case Western Reserve University
The University of Chicago
University of Cincinnati
Illinois Institute of Technology
University of Illinois
Indiana University
Iowa State University
The University of Iowa

Kansas State University
The University of Kansas
Loyola University
Marquette University
Michigan State University
The University of Michigan
University of Minnesota
University of Missouri
Northwestern University
University of Notre Dame

The Ohio State University
Ohio University
The Pennsylvania State University
Purdue University
Saint Louis University
Southern Illinois University
University of Texas
Washington University
Wayne State University
The University of Wisconsin

LEGAL NOTICE

This report was prepared as an account of Government sponsored work. Neither the United States, nor the Commission, nor any person acting on behalf of the Commission:

A. Makes any warranty or representation, expressed or implied, with respect to the accuracy, completeness, or usefulness of the information contained in this report, or that the use of any information, apparatus, method, or process disclosed in this report may not infringe privately owned rights; or

B. Assumes any liabilities with respect to the use of, or for damages resulting from the use of any information, apparatus, method, or process disclosed in this report.

As used in the above, "person acting on behalf of the Commission" includes any employee or contractor of the Commission, or employee of such contractor, to the extent that such employee or contractor of the Commission, or employee of such contractor prepares, disseminates, or provides access to, any information pursuant to his employment or contract with the Commission, or his employment with such contractor.

Printed in the United States of America
Available from

Clearinghouse for Federal Scientific and Technical Information
National Bureau of Standards, U. S. Department of Commerce
Springfield, Virginia 22154

Price: Printed Copy \$3.00; Microfiche \$0.65

ARGONNE NATIONAL LABORATORY
9700 South Cass Avenue
Argonne, Illinois 60439

CREWE ELECTRON-ENERGY-ANALYZING
SCANNING MICROSCOPE

by

D. N. Eggenberger

Electronics Division

December 1969

TABLE OF CONTENTS

	<u>Page</u>
ABSTRACT	13
1. INTRODUCTION	13
2. THEORY OF DESIGN	17
2.1 Conventional Picture	17
2.2 Low-energy Losses	17
2.3 Higher-energy Losses	17
2.4 Low Resolution	18
2.5 Display	19
2.5.1 Specimen Image	19
2.5.2 Energy-loss Image	19
2.5.3 Color Composition.	19
2.5.4 Energy Spectrum.	20
3. INSTRUMENTAL PRINCIPLES.	21
3.1 Small beam Image	21
3.1.1 Source.	21
3.1.2 Anode Lens	22
3.1.3 Vacuum.	22
3.1.4 Magnetic Lens	23
3.1.5 Spurious Charges	23
3.1.6 Magnetic Shielding.	23
3.1.7 Vibration.	24
3.2 Energy Analysis	24
3.2.1 Spectrometer	24
3.2.2 Slits	25
3.2.3 Detectors.	25
3.3 Display	26
3.3.1 Image Tube	26
3.3.2 Circuits.	26
3.3.3 Energy Spectrum.	26
3.3.4 Multichannel Analyzer	26
3.3.5 Line-sweep Display for Resolution Measurement . . .	27

TABLE OF CONTENTS

	<u>Page</u>
4. SOURCE	28
4.1 Requirements	28
4.1.1 Small Size	28
4.1.2 Small Energy Spread	28
4.1.3 Mechanical Stability.	28
4.2 Field Emission	29
4.2.1 Theory of Emission.	29
4.2.2 Source Size	31
4.2.3 Energy Spread	31
4.2.4 Making the Tips	31
4.3 Operating Experience.	33
4.3.1 Tip Loss by Electrical Breakdown	33
4.3.2 Erratic Current	34
4.3.3 Flashing	35
4.3.4 Tip Loss from Ion Pumps at High Pressure.	36
4.4 Design.	36
4.4.1 Tip Mount	36
4.4.2 Insulator	36
4.4.3 Adjustment.	36
5. ANODES.	39
5.1 Bias Potential.	39
5.2 Anode System	40
5.2.1 Empirical Designs.	40
5.2.2 Low Spherical-aberration Anodes.	41
5.2.3 Characteristics of Butler Anodes.	41
5.3 Design.	43
5.3.1 Material	43
5.3.2 Construction.	44
5.3.3 Anode Supports.	45
6. LENSES.	47
6.1 Magnetic Quadrupole-Octupole Lens	48

TABLE OF CONTENTS

	<u>Page</u>
6.1.1 Theory	48
6.1.2 Design.	49
6.1.3 Operation and Performance.	54
6.1.4 Computer Analysis Performed by Meads and Cohen.	54
6.1.5 Degausser	55
6.2 Annular Lens	56
6.2.1 Redesign	56
6.2.2 Results	57
6.3 Electrostatic Quadrupoles.	57
6.4 Single-field Condenser-Objective Lens	58
6.4.1 Design.	59
6.4.2 Construction.	59
6.4.3 Characteristics.	61
7. STIGMATORS	63
7.1 Electrostatic Stigmator.	63
7.2 Magnetic Stigmator	64
7.2.1 Design of Original Unit.	64
7.2.2 Results	64
7.2.3 Condenser-Objective Lens Unit	65
8. DEFLECTION.	66
8.1 Requirements	66
8.2 Electrostatic Deflection	66
8.2.1 Original Set	66
8.2.2 Single-level Set.	66
8.2.3 Short-plate Shielded Set	67
8.2.4 Stigmator-Deflector Unit	67
8.3 Magnetic Deflection	67
8.3.1 Double Deflection	67
8.3.2 Original Design.	67
8.3.3 Condenser-Objective Lens Unit	68
9. APERTURES.	69
9.1 Crossed Slits	69

TABLE OF CONTENTS

	<u>Page</u>
9.2 Lower Circular Series	69
9.3 Other Apertures	70
9.3.1 Fixed Upper Beam	70
9.3.2 Spectrometer Entrance	70
10. SPECIMEN HANDLING	71
10.1 Original Specimen Holder	71
10.2 Changer System	71
10.3 Immersed Specimen	72
10.4 Condenser-Objective Lens Unit	72
10.5 Types of Specimen	72
10.5.1 Aluminum	73
10.5.2 Carbon	73
10.5.3 Other Specimens	74
10.6 Effects	74
10.6.1 Contamination	74
10.6.2 Ultrahigh Vacuum	74
10.6.3 Burnup	76
11. SPECTROMETER	77
11.1 Choice of Type	77
11.2 Theory of Design	77
11.2.1 Plate Potentials	77
11.2.2 Focusing and Relativistic Defocusing	78
11.2.3 Energy Defocusing, Sensitivity, and Resolution	79
11.2.4 End Shields	80
11.3 Design and Construction	81
11.3.1 Plates	81
11.3.2 Frame	82
11.4 Resolution	83
11.5 Quadrupole Lens	83
11.6 Operating Experience	84

TABLE OF CONTENTS

	<u>Page</u>
11.6.1 Contacts to Plates	84
11.6.2 Cleaning by High Voltage	84
11.6.3 Apparent Gain in Energy	84
12. ENERGY SLITS	85
12.1 Requirements	85
12.2 Design	85
12.3 Rework for Higher Energy Resolution	86
13. DETECTORS AND LIGHT PIPES	87
13.1 Choice of Detectors	87
13.2 Light Pipes	87
13.3 Photomultipliers	87
13.4 Experience	88
14. DISPLAY SYSTEM	89
14.1 Image Display	89
14.1.1 Requirements	90
14.1.2 Storage Tubes	90
14.1.3 Electronics	90
14.2 Energy Spectrum	95
14.2.1 Circuits	95
14.2.2 Multichannel Analyzer	95
14.3 Color Display	96
14.3.1 Optical Composite	96
14.3.2 Color-television Composite	97
15. CAMERA SYSTEM	99
15.1 Storage-tube Photography	99
15.2 Remote Camera	99
15.2.1 Capabilities	99
15.2.2 Cameras	100

TABLE OF CONTENTS

	<u>Page</u>
15.2.3 Cathode-ray Tube	100
15.2.4 Dark Box	100
15.2.5 Circuits	101
15.2.6 Sample Photographs	104
16. VACUUM SYSTEM	105
16.1 Requirements	105
16.2 Chamber	105
16.2.1 Design	105
16.2.2 Materials	107
16.2.3 Components	107
16.3 Pumps and Gauges	108
16.3.1 Roughing Pumps	108
16.3.2 Ion Pumps	109
16.3.3 Nonmagnetic Pumps	109
16.3.4 Gauges	109
16.4 Cold Trap	110
16.5 Procedures and Experience	110
16.5.1 Pumpdown	111
16.5.2 Electrical Conditioning	111
16.5.3 Sorption Pumps	111
16.5.4 Ion Pumps	112
16.5.5 Flanges and Seals	112
17. BASE AND ACCESSORIES	113
17.1 Base	113
17.2 Telescope	113
17.3 Bake-out Oven	114
17.4 Test Fixtures for Gun	114
17.5 Filament-forming Fixtures	115
18. POWER SUPPLIES	116
18.1 High-voltage Supply	116

TABLE OF CONTENTS

	<u>Page</u>
18.2 Tip-bias Supply	116
18.2.1 Original Divider	117
18.2.2 Battery Bias Supply	117
18.2.3 Electrometer	117
18.3 Spectrometer Supplies	118
18.3.1 Requirements	118
18.3.2 Modifications	118
18.4 Magnet Supplies	119
18.4.1 Requirements	119
18.4.2 Modifications	120
18.5 Tip-flasher Supply	120
19. ENVIRONMENT	121
19.1 Magnetic Field	121
19.2 Vibration	123
ACKNOWLEDGMENTS	125
REFERENCES	126

LIST OF FIGURES

<u>No.</u>	<u>Title</u>	<u>Page</u>
1.	Crewe Electron-energy-analyzing Scanning Microscope	14
2.	Plasma-oscillation Losses in Aluminum.	18
3.	Electron-energy Losses in Teflon.	18
4.	Spectra of Energy Loss in Light and Heavy Elements	19
5.	Schematic Diagram of Crewe Electron-energy-Analyzing Microscope.	21
6.	Butler-anode System.	22
7.	Beam Patterns from Tungsten Tip.	30
8.	Electron-gun Cross Sections	37
9.	Focal Distance of Butler Anodes at Several Calculated Bias Potentials and Experimental Bias Potential of 1.31 kV	42
10.	Focal Distance of Butler Anodes at Several Calculated Bias Potentials and Experimental Bias Potential of 1.59 kV	42
11.	Magnification of Image due to Butler Anodes	42
12.	Spherical Aberration in Image due to Butler Anodes	43
13.	Basic Quadrupole Profile.	48
14.	Quadrupole-Octupole Magnet.	49
15.	Profiles of Quadrupoles and Shields.	50
16.	Poles and Shields	50
17.	Magnet Parts.	51
18.	Coils and Poles in Place	52
19.	Encapsulated Magnet.	54
20.	Electrostatic-lens Cross Section.	57
21.	Electrostatic-lens Components	58
22.	Electrostatic-lens Assembled.	58
23.	Single-field Condenser-Objective Lens, Cross Section	60
24.	Coil Jacket for Single-field Lens.	62
25.	Stigmator- and Deflection-coil Layout	64
26.	Core for Stigmator and Deflection Coils	65

LIST OF FIGURES

<u>No.</u>	<u>Title</u>	<u>Page</u>
27.	Storage-tube Images of Aluminum	75
28.	Energy Spectrum of Collodion.	76
29.	Spectrometer Geometry.	77
30.	Spectrometer Plates, Frame, and Component	81
31.	Detector-end Structure, Showing Location of Energy Slits	85
32.	Display Console Showing Multichannel Analyzer at Left.	89
33.	Block Diagram of Channel 2 Display	91
34.	Circuit Diagram of Video Amplifier.	92
35.	System for Producing Color Composites by Optical Method . . .	97
36.	Camera-system Block Diagram	102
37.	Sweep-drive Block Diagram.	103
38.	Camera-system Picture of Helix Aspersa.	104
39.	Microscope Chamber	106

1944

1945

1946

1947

1948

1949

1950

1951

1952

1953

1954

1955

1956

1957

1958

1959

1960

1961

1962

1963

1964

1965

1966

1967

1968

1969

1970

1971

1972

1973

1974

1975

1976

1977

1978

1979

1980

1981

1982

1983

1984

1985

1986

1987

1988

1989

1990

1991

1992

1993

1994

1995

1996

1997

1998

1999

2000

2001

2002

2003

2004

2005

2006

2007

2008

2009

2010

2011

2012

2013

2014

2015

2016

2017

2018

2019

2020

2021

2022

2023

2024

2025

2026

2027

2028

2029

2030

CREWE ELECTRON-ENERGY-ANALYZING SCANNING MICROSCOPE

by

D. N. Eggenberger

ABSTRACT

The limitations of electron microscopes and micro-probes in resolution, contrast mechanisms, and analyzing ability led to the design and construction of a new instrument that should extend the possibilities in these areas. Resolution improvement is obtained by a simpler optical system which focuses a "point" source to a "point" image on the specimen. A point source is approached by using cold tip emission rather than hot filament emission. Various types of contrast and some degree of specimen analysis are obtained by measuring the intensity of transmitted electrons with selected or characteristic energy loss. This makes possible high-contrast pictures among light elements without staining, as well as providing a possible means of identifying elements present in the specimen.

1. INTRODUCTION

This report describes a new electron microscope which provides a means of crude chemical analysis of a specimen and has the potentiality of achieving higher resolution than is presently reached by conventional instruments.

The conception as well as many ideas of detail of the microscope were those of Dr. A. V. Crewe, then Laboratory Director of Argonne National Laboratory.

Commercial transmission electron microscopes have no means of analyzing the specimen for its elements. They produce shadows delineating shape and density profiles, but analysis must in general be obtained by other means.

The microscope described here (Fig. 1) permits some degree of elemental analysis by measuring energy losses of the transmitted electrons. Since each element has its unique set of energy levels, some of the electrons that pass through the specimen will show losses of energy corresponding

to differences in energy levels of the specimen atoms. In particular, the energies associated with the complete removal of inner-shell electrons from atoms are large and spaced well apart among different kinds of atoms, and therefore quite easy to separate. Energy selection is performed by an electrostatic spectrometer.

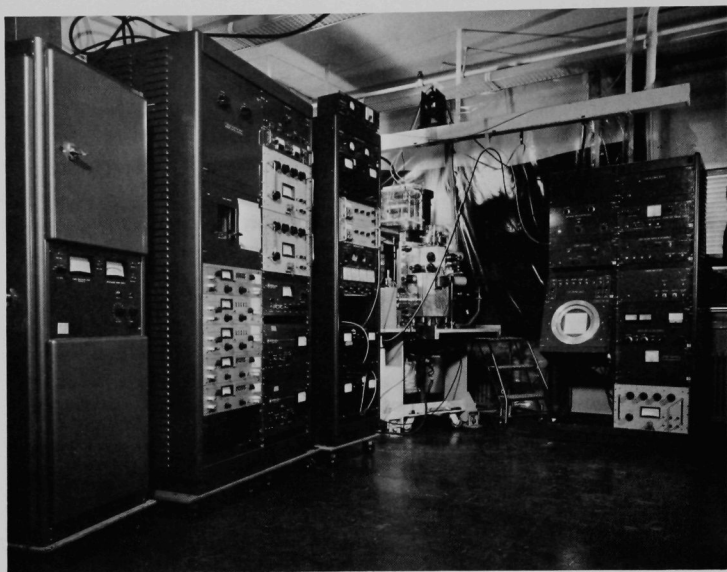


Fig. 1. Crewe Electron-energy-analyzing Scanning Microscope. ANL Neg. No. 143-1475.

To have a structurally detailed analysis of the specimen, it appears necessary to examine the specimen one point at a time. For that reason, a scanning electron beam is used, with the beam sweep synchronized to that of a storage-type oscilloscope display tube. The intensity of the display at any point is a function of the beam intensity measured through the spectrometer at the energy selected. Thus a picture showing the locations of a particular element can be seen.

Energy analysis can be made by measuring output beam intensity as a function of energy loss, in a different kind of display. Here the spectrometer is swept through a range of energy losses in synchronism with the sweep on an ordinary oscilloscope, with the output beam intensity as the dependent function. Thus a curve is displayed with peaks at the characteristic energy losses.

Higher spatial resolution is potentially possible for several reasons, the use of a very small source and of a simpler point-to-point focusing

system. Conventional electron microscopes collimate the electron beam to cover the entire specimen and therefore use a heated filament to provide sufficient intensity to get a satisfactory intensity in the image. Electrons transmitted through the specimen with little or no interaction are then focused into an image using three magnetic lenses--objective, intermediate, and projector. The resolution depends primarily on the quality of these three lenses.

In the new microscope, resolution depends on the size of the primary beam on the specimen. This size in turn depends essentially on the size of the source and the quality of the lens focusing the beam onto the specimen. Only a single lens should be needed, with a reduction in the number of lenses contributing their aberrations to the image as compared with a conventional microscope.

Magnification is virtually unlimited, since whatever area is being covered by the electron beam raster on the specimen is displayed on the full raster face of the display tubes. The specimen area can be reduced to any size desired by attenuating the potentials sweeping the microscope beam. However, the useful magnification is limited by the spot size of beam on the specimen.

Using a cold field emission source reduces the effective source diameter to the order of 30 Å. Heated filaments present an effective source size many times this figure, because of their greater physical bluntness and because of the effect of transverse thermal velocities given to the electrons.

Scanning microscopes of another type, commonly called microprobes, are being used. They do not fit the requirements set up in this project for several reasons. They generally are used for surface analysis by X rays or secondary electrons reflected from the surface layers. Their field has been in analysis for medium and heavy elements, although improved techniques have been gradually extending their capability into lighter elements. Also, resolution has so far been limited to about a hundred angstroms, because of the use of heated filaments and because electrons scattered below the surface of the specimen produce an effective reaction area larger than the actual beam-spot size.

In this microscope there does not appear to be any basic reason for not attaining resolution down to one angstrom or better eventually. Also, analysis for light elements is not difficult, because the K-shell energy separation among them is ample for easy selection.

The type of signal detection used makes it possible to count single electrons as well as to measure currents when the counting rate gets very high. With this high sensitivity, the primary current can be small (10^{-9} to 10^{-10} A is normally used) and specimen burnup is almost nonexistent, even for long observation periods.

This report records several aspects of the project, namely, purpose in Section 1, theory of design and instrumental principles in Sections 2 and 3, instrument details that are more or less unique in Sections 4 to 19, development phases, and early results.

Since the major objective is the development of an instrument, developmental stages are important in reaching this goal and are therefore described. A succession of changes in components have been made and will continue to be made as the characteristics of each are learned and new designs are made. These components are described along with their advantages and limitations.

The coverage is limited to the period that the project was at Argonne National Laboratory. This period started with the conception of the project late in 1962 and terminated with its removal to The University of Chicago in August 1967.

2. THEORY OF DESIGN

To provide different contrast mechanisms using selected electron energies and to perform an analysis of energies and possibly relate these to definite locations on the specimen, it is necessary to examine one at a time the elemental areas in the specimen. This led to using a small beam scanning the specimen, with the spatial resolution approximately equal to the diameter of the beam at the specimen.

The analysis parameter was chosen to be the characteristic energy losses in electrons transmitted through a thin specimen. A spectrometer separates electrons of different energies transmitted and permits signal output from a selected energy band. This permits a selection of contrasts. Information can be obtained in several forms, as discussed below.

2.1 Conventional Picture

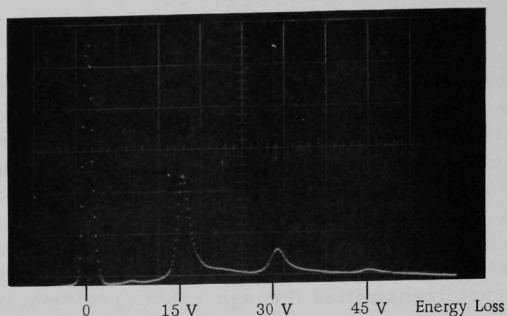
A conventional electron-microscope picture is obtained by observing the electrons that are transmitted at full energy (no loss). Good contrast is possible from light-element specimens without staining or shadowing with heavy elements.

2.2 Low-energy Losses

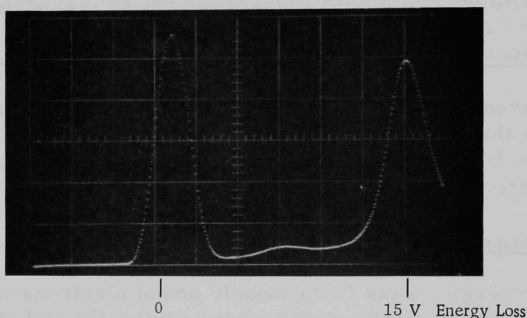
Low-energy losses from loosely bound electrons can be observed. In particular, some metals exhibit what are usually called plasma electron losses. For example, aluminum shows such an absorption at 15 eV and multiples of that (Fig. 2). Outer-shell electron-absorption peaks may be useful where only a few known elements are present and their spatial distribution is desired. However, these absorptions are less useful for general analysis, because of their abundance in elements, their small values, and the overlapping among spectra from different elements.

2.3 Higher-energy Losses

Higher-energy losses from K-shell interactions provide more clear-cut data for analysis than do the low-energy losses, because of the greater separation in energy in the former. For example, the K_{α} energy in carbon is 283 eV, in nitrogen 399 eV, and in oxygen 531 eV. These values indicate that identification of elements in organic materials should be possible in many cases by measuring energy-loss peak locations using an energy-selection device. An example of an energy spectrum obtained using a Teflon specimen in the microscope is shown in Fig. 3, with an oxygen K_{α} peak at 530 eV, and a weak but definite fluorine peak at ~680 eV.

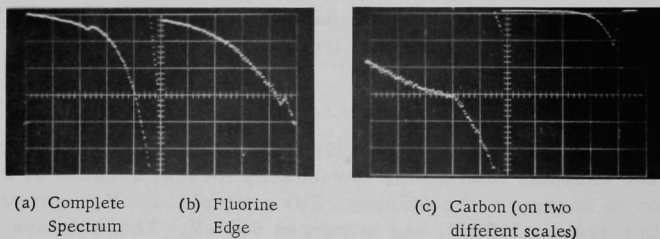


(a) Complete Spectrum



(b) Expanded Portion of Spectrum

Fig. 2. Plasma-oscillation Losses in Aluminum. ANL Neg. No. 201-7612.



(a) Complete Spectrum

(b) Fluorine Edge

(c) Carbon (on two different scales)

Fig. 3. Electron-energy Losses in Teflon. ANL Neg. No. 201-7611.

2.4 Low Resolution

At low resolution, one can gain some information from the energy-curve envelopes. The drawing of Fig. 4 shows that as one goes from lighter to heavier elements the maximum moves to higher energies and the peak broadens. The ratio of intensities at two values of energy losses, such as at E_1 and E_2 in Fig. 4 may provide useful information for qualitative analysis.

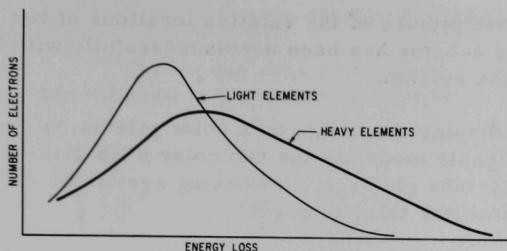


Fig. 4. Spectra of Energy Loss in Light and Heavy Elements. ANL Neg. No. 143-2878.

2.5 Display

Four modes of display, discussed in the paragraphs below, make it possible to look at the specimen in different ways.

2.5.1 Specimen Image

A black and white image on the face of a cathode-ray tube provides a conventional-

looking enlargement of the specimen. These are made by showing the intensity of full-energy electrons at each point of scan. Darker areas mean that fewer electrons penetrated the specimen due to either increased density or thickness.

2.5.2 Energy-loss Image

An image is made similarly to the specimen image above except that the intensity observed is that of electrons that have lost energy. The first difference is that the image is generally reversed. That is, open spaces that show white using full-energy electrons are now black because no electrons lose energy where there is no material. Thick areas may be black, the same as with full energy, because no electrons get through. However, thin areas that are partially transparent may be light, dark, or some shade of grey depending on the energy loss selected and the nature of specimen material.

A pattern of location of an element can be displayed, provided the specimen thickness is uniform and not excessive. This can be done by selecting a narrow energy-loss band corresponding to removing an inner-shell electron in that element. This display can be specific for a given element of low atomic weight, since the inner-shell energies are quite widely separated between elements that are adjacent to each other in the periodic table.

2.5.3 Color Composition

Selecting electrons at two energy losses permits two energy-loss images to be superposed if a different color is used for each energy.

In one scheme, the two images can be displayed on two cathode-ray tubes, each tube having a color filter different from that of the other. By an arrangement of mirrors, these images are combined on a ground-glass screen for visual observation or on a color film for a permanent record.

The color gradations provide a vivid picture of the relative locations of two components in the specimen. This scheme has been used successfully with the two storage-tube displays on the system.

An alternate scheme is to display the image on a color television tube. In this case, the intensity signals modulate the two color guns without using intermediate cathode-ray-tube pictures. A working system of this type was built using an RCA monitor television set.

2.5.4 Energy Spectrum

A quite different type of display permits a qualitative, and to some extent quantitative, analysis to be made of a portion of the specimen. The display is a curve on a cathode-ray tube showing intensity as a function of energy loss. If the energy-loss scale is calibrated, the energy losses of the peaks can be compared with known losses of elements to identify them. The peak height is related to the amount of material, but it is also affected by the specimen thickness and the scattering losses by other material. Therefore quantitative analysis may not be very reliable; however, the accuracy may be improved by choosing other base energies such that in the specimen thickness, few collisions occur in the secondary electrons.

The method for producing this display is to superpose a sweep potential on the spectrometer steady potentials. This sweep is in synchronism with that of the cathode-ray tube, and a succession of electron energies is swept across the spectrometer slit, with the intensity at any instant being measured as the y-coordinate on the cathode-ray tube (the x-coordinate represents energy). Usually, the microscope beam sweeps are shut off for this observation of a particular spot on the specimen. If the specimen is swept also, one gets a general average curve, but it is so broadened as to be rather useless.

3. INSTRUMENTAL PRINCIPLES

The unique requirements of this instrument resulted in a design that differed in a number of ways from conventional electron microscopes and microprobes. The various design features will be listed and described generally under the functional requirement. (A schematic diagram of the Crewe electron-energy-analyzing microscope is shown in Fig. 5.) Later in this report each item will be taken up again in detail.

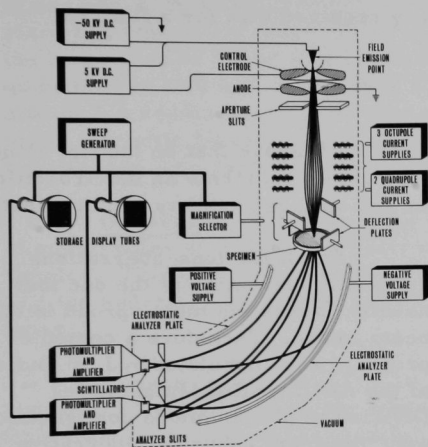


Fig. 5. Schematic Diagram of Crewe Electron-energy-analyzing Microscope. ANL Neg. No. 143-1740.

3.1 Small Beam Image

The resolution, and consequently the beam-image scanning spot, was initially planned to be 10 \AA , but it was later decided that the goal should be 1 \AA . Optically, the needs are a small source, small aberrations in all focusing elements, small magnification, monochromatic electrons (or achromatic lenses) and absence of distorting fields, either electric or magnetic. Mechanically, the requirements are stability and

freedom from vibrations. The image spot can have a virtual size larger than its actual size if the beam is vibrated laterally by changing fields or by movements in the optical elements due to mechanical vibrations.

3.1.1 Source

The smallest known sources for electron beams are cold-emission tips. These are usually made of tungsten, etched to a sharp point, and then thermally smoothed. Well-formed tips of several hundred angstroms radius may have a virtual source size about 30 \AA diameter, since electrons are ejected along the field lines, which are nearly normal to the hemispherical surface. With modest demagnifications, images of a few angstroms, or even 1 \AA , in diameter should be possible.

A cold-emission source produces more nearly monochromatic electrons than does a hot filament. In cold emission, the spread in energy can be less than an electron volt (at low currents).

Field emission from a heated tip, commonly called the T-F (temperature-field) mode of emission, is not as satisfactory as cold emission since a wider thermal energy spread is developed and also

increased lateral velocities (i.e., velocity components normal to the field lines at the emitting surface) produces a larger virtual source size.

Two complications arise from the use of cold-emission sources, namely, a bias electrode is needed between the tip and accelerating anode, and a much higher vacuum environment is required than for a filament source.

3.1.2 Anode Lens

The bias anode at a potential of 1 or 2 kV above that on the tip, along with the accelerating anode at much higher potential, forms an electrostatic focusing system with its own aberrations and voltage-stability requirements.

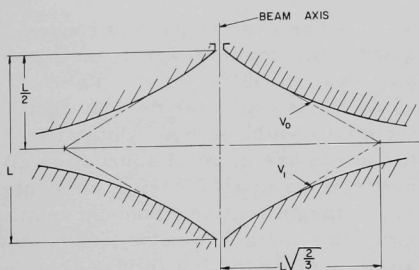


Fig. 6. Butler-anode System. ANL Neg. No. 201-6150.

Of all the lens aberrations, spherical aberration is the one that usually causes the most spread in the beam image. Therefore a computer program was formulated by J. W. Butler of the ANL Applied Mathematics Division to plot an anode configuration with minimum spherical aberration.¹ A radial-section plot of the desired anode surfaces is shown in Fig. 6. The two anode surfaces are mirror images of each other.

Since focal length of the anode lens is dependent on both potentials, stability of these is important. At present, the accelerating potential is furnished by an electronic supply regulated to a few parts per million, and the bias potential is supplied by batteries.

Sources and anodes are described more fully in Sections 4 and 5.

3.1.3 Vacuum

For continued stable-current operation of a cold-emission source, a pressure of about 10^{-9} Torr or less is required to preclude instability from contamination and to prevent premature destruction of the tip by ion bombardment. The entire electron-beam system is enclosed in one vacuum chamber. The beam is terminated at a scintillator detector mounted on a quartz light pipe, which provides an optical path through the vacuum-chamber wall. To avoid organic contamination, the system was designed with sorption pumps for the roughing pumpdown stages and ion pumps for the final stage.

Further details of the chamber and the vacuum system are presented in Section 16.

3.1.4 Magnetic Lens

The requirements of the lens are that it demagnify and focus the monoenergetic beam of electrons from the source to a spot on the specimen. In one sense, this requirement is simple in that a single lens could suffice, since the area of coverage on the specimen is very small as contrasted to the large area of image in a conventional microscope. However, the requirement is still severe because of the aberration qualities needed if the goal of 1 Å resolution is to be attained. Two approaches have been made to the magnetic lens--a multipole (quadrupole-octupole) design, and a single annular-gap lens design. Details of the lenses are contained in Section 6.

3.1.4.1 Quadrupole-Octupole Lens. The first lens design contained a pair of quadrupoles with three octupole correctors interleaved among the quadrupoles. This choice was made because of some theoretical indications that the spherical aberration could be reduced below that of annular-gap lenses.

3.1.4.2 Annular-gap Lens. For an alternate approach, a lens from a conventional electron microscope was modified for use in this microscope. Operation of its one coil is simpler than that of the multicoil quadrupole unit, and its properties are better known. Thus it serves as an interim lens while other characteristics of the microscope are being studied.

The first annular-gap lens was an intermediate lens from an RCA EMU-3G electron microscope. Since its limit of resolution is about 40 Å, a second lens of shorter focal length, a Ruska-type unit with specimen in the center of the magnetic pole gap, was designed and was calculated to reach a resolution of about 5 Å.

3.1.5 Spurious Charges

To avoid beam distortion by electric charges, special care had to be taken in design so that only conducting metal surfaces could "see" the beam. Also, extreme cleanliness is necessary to prevent any organic or oxide film from forming on surfaces facing the beam, so that charges cannot build up there.

3.1.6 Magnetic Shielding

Alternating or otherwise varying magnetic fields move the electron beam through the Lorentz force. This has the effect of increasing the apparent size of the image spot during the time of observation and thus lowering the resolution. Therefore the design incorporated Mumetal shields inside the vacuum chamber surrounding the beam from the source to the magnet and from the magnet to beyond the specimen. The iron in

the magnet acted as a shield in that portion of the beam path. A compromise was necessary between shielding and vacuum pumping requirements resulting in shield cans with numerous holes in the shielding surfaces. Synchronizing the horizontal scan with the power line frequency improved the picture, as explained in Section 19.1.3.

Steady magnetic fields are not troublesome if weak, since they can be compensated quite easily by small permanent magnets.

3.1.7 Vibration

Mechanical vibration between parts of the electron beam system can wiggle the beam, thus making the image spot effectively larger and lowering the resolution. The design therefore included a framework and mountings for components that are rigid structurally. Also, shock-absorbing pads form the feet of the instrument.

Two components are particularly susceptible to vibrating--the emission tip and the specimen mounting. There is little to be done to make the tip more rigid, since it is inherently a long, thin cantilevered piece. One specimen carrier, designed to be immersed inside the lens pole pieces, was made to rest against the poles supported by a light spring which decouples the carrier from the specimen changing and adjusting mechanism. In this way, vibration coming through the magnet moves the specimen with it, avoiding relative motion between them.

Shielding and vibration are discussed more fully in Section 19.

3.2 Energy Analysis

The energy-analysis system involves entirely different instrumentation than do conventional electron microscopes or microprobes. Basically, a sorter of electrons by energy and a detector capable of measuring intensity of any selected energy beam are needed.

3.2.1 Spectrometer

An electrostatic electron-energy analyzer was chosen for two reasons. First, the dimensions and potentials needed for 50-keV electrons were all reasonable. Second, it was desirable to be able to dial in precise quantities and relate them to energies consistently. Potentials on electrostatic-analyzer plates fulfill the latter requirement, but currents in magnetic spectrometers do not, because of hysteresis in the iron magnetic circuit. Spherical rather than cylindrical surfaces were chosen because of the easier construction of the former using conventional lens-grinding techniques. For stability, quartz was used for the plates, and conducting films of evaporated Inconel form the electrode surfaces.

Details of the spectrometer are in Section 11.

3.2.2 Slits

The minimum slit opening was initially planned for a 10-eV bandwidth of electron energies at 50 keV. This was felt to be adequate resolution for analyzing by K-shell energy losses, where the difference between two adjacent light elements is much larger than 10 eV. For example, these energies in carbon and nitrogen are 116 eV apart. The slits were designed to accept a band as wide as 100 eV for wide peak measurements.

Two outputs were designed into the instrument so that simultaneous comparisons could be made on two energy losses. The separation between slits is variable between 200- and 1100-eV energy. The comparison between the two outputs is vividly displayed in color, using two color filters, one for each output, and superimposing them.

Experiments show the spectrometer to be capable of much higher energy resolution than 10 eV. The slits were reworked to close to about 0.3-eV bandwidth.

More details of the slits are given in Section 12.

3.2.3 Detectors

Scintillators sensitive to electrons in the energy range of approximately 10-50 keV and capable of existing in a vacuum of 10^{-9} Torr limited the selection of materials. Some preliminary tests of scintillating material in a vacuum chamber indicated that cesium-iodide and Pilot B would be acceptable. These tests were done by W. C. Kaiser and his group of the Electronics Division. Both these materials were used and have proven to be satisfactory. Each scintillator is a thin plate and is bonded with epoxy cement onto the end of a quartz light pipe.

The quartz light pipes are shaped to transmit light to Amperex XP1010 photomultiplier faces outside the vacuum chamber, and have flanges such that a Viton O-ring seal is made to the chamber.

There are two detector systems, each with a scintillator, light pipe, seal, photomultiplier, and display system. They are not identical, however. The detector and light pipe behind the movable slit are larger than those in the other detector system in order to cover the area that can be seen by this slit.

3.3 Display

Output information can be shown in several forms, as a direct-viewed image or as photographs of this image, and as energy spectra either directly viewed or recorded. In addition, line-sweep displays are used for resolution measurements. The display system is described in more detail in Section 14.

3.3.1 Image Tube

A storage-type tube was selected to retain the image and permit integration time because of the very low levels of signal. Picture frame times of 0.1, 1, and 10 sec. are provided. Signals can be superimposed on the images already present to increase the integration time to the order of minutes.

3.3.2 Circuits

Three major considerations were involved in circuit design--first, processing very small signals with as high signal-to-noise ratio as possible; second, providing supplies and foolproof protection for the storage tube; and, third, providing linear sweeps for the storage tube and microscope beams. This system is described in Section 14.

3.3.3 Energy Spectrum

Analysis of the specimen through energy-loss information is best displayed by a plot of electron beam intensity versus energy loss. At first this was done point-by-point by either moving the slit or changing spectrometer potentials for varying the energy-loss coordinate. Later, these plots were observed directly on an oscilloscope tube by adding the tube horizontal-sweep potentials to the steady spectrometer plate potentials. By this means, the various energies of electrons are swept across a stationary slit.

3.3.4 Multichannel Analyzer

The beam current is usually in the order of 10^{-10} A, and only a very small portion of that suffers a K-shell energy loss. Therefore, the signal-to-noise ratio is often quite low, even though the system is capable of displaying individual electron detections. To improve the signal-to-noise ratio, a multichannel analyzer is used to accumulate data from repetitive sweeps of the energy spectrum. Thus a better display of intensity versus energy loss is obtained than by observing it directly on an oscilloscope.

3.3.5 Line-sweep Display for Resolution Measurement

Resolution measurements are made by sweeping the electron beam across a sharp edge in the specimen and displaying the output amplitude versus beam position. On an oscilloscope, the signal intensity will appear at one level when the entire beam goes through the specimen, and at another, higher, level when it goes through the opening. The rise time in going from one level to the other is the time that the beam is crossing the edge; from this information the beam width can be calculated. The beam-spot size is measured in two orthogonal directions by interchanging the sweep signals between the two pairs of deflection plates, thereby rotating the beam sweep 90° .

4. SOURCE

4.1 Requirements

4.1.1 Small Size

In the scanning type of electron microscope, the spatial resolution is essentially equal to the diameter of the beam at the specimen. The initial goal was to resolve to 10 \AA . However, there is no apparent theoretical reason why a much higher resolution cannot be achieved. In particular, at 1 \AA resolution, one should approach the possibility of delineating individual atoms in a specimen.

In either case, a very small source size is required, even with considerable demagnification by a lens. Assuming a lens magnification of 0.03, to get 1 \AA resolution, a source size of 30 \AA diameter is needed, if no lens aberrations were present. With some inevitable aberrations in focusing, either a smaller source or more demagnification is necessary.

4.1.2 Small Energy Spread

Since one use of the microscope was anticipated to be analysis by measuring energy losses in electrons, any spread in source energy would degrade the results by adding to the spread in energy of the transmitted electrons. It is necessary to keep this spread as small as possible for at least four reasons. First, a spread produces uncertainty in the energy of the loss peak, and where several peaks are close together, an accurate knowledge of the energy may be needed for quantitative analysis. Second, if several peaks are close together, they may merge and lose their identity as separate energy losses. Third, a very weak peak, by being broadened, may become submerged in the background and be lost. Fourth, chromatic aberration in the lens will enlarge the beam diameter and impair the resolution.

4.1.3 Mechanical Stability

Movement of the source in the scanning mode of operation worsens the resolution, because the spot moves and destroys the correlation between the spot locations in specimen and display. The effect depends to a large extent on the frequency of vibration as well as on the amplitude. At vibration periods short compared to the time the beam spot moves one diameter, the spot will be effectively smeared out with corresponding loss of resolution. At periods long compared to the time of movement of one spot diameter, the effect is to distort the scan line transversely, longitudinally, or both. In the fortuitous circumstance that the vibrations would have a harmonic synchronization with the line-sweep frequency, the effect would be only a slight distortion of the image. In general, however, this would not be so,

and the nonsynchronous matching of adjacent lines would degrade the resolution of the image.

Mechanical stability of the electron source, relative to the rest of the optical system and specimen, is thus important, and rigid supports for the source and other components are required.

4.2 Field Emission

The requirements of small source size and low energy spread are best met in cold field-emission tips. Mechanical stability perhaps suffers because of the long thin tip, but the overall requirements definitely indicated that this type of source was necessary. One other drawback, which was quite successfully solved, is the necessity of operating the cold emission tip in a pressure of 10^{-9} Torr or less to avoid its premature destruction by ion bombardment.

4.2.1 Theory of Emission

In very high fields at the surface of a metal, electrons can penetrate the surface barrier (which is deformed by the field) by tunneling. This is a quantum-mechanical process and differs from photoelectric and thermal emission in that the latter electrons must surmount the barrier rather than tunnel through it. The fields required for emission currents are of the order of $3-6 \times 10^7$ V/cm at the surface, and electrons from the conduction band then have an appreciable probability of tunneling out.

Such high fields are obtained by making the radius of an electrode sufficiently small. If two concentric spheres have a potential difference V_b between them, the field E at the surface of the inner sphere of radius R is

$$E \approx V_b/R \quad (1)$$

if R is very small compared to the outer electrode radius. The tapered shank on the hemispherical tip alters this relation and the field near the tip axis is determined to be (Ref. 2, p. 45)

$$E \approx V_b/5R. \quad (2)$$

The current function over a small range from the start of emission is

$$i = V_b^2 a \exp(-b\phi^{3/2}/cV_b), \quad (3)$$

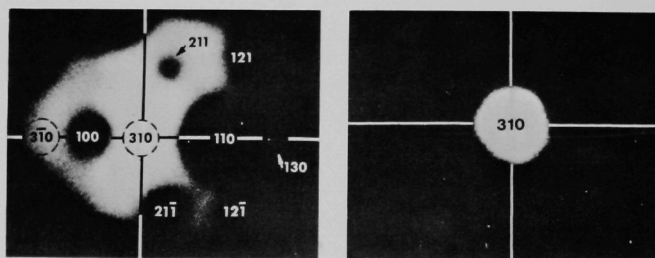
where a , b , and c are constant or nearly so, ϕ is the work function, V_b is the bias potential, and i is the total current.

The bias potential is of the order of 1 or 2 kV for most tungsten tips. The relation between bias and tip radius is given by Eq. 2. Measuring the potential at which emission begins, which requires about 3×10^7 V/cm field for tungsten, permits the tip radius to be calculated. A 1000-Å radius tip will thus emit at ~ 1500 V.

The current-versus-voltage function demonstrates the need for good regulation of the bias potential when steady current is desired. From Eq. 3, it appears that once field emission starts, the current rises approximately quadratically with field or voltage.

The brightness of a cold-emission tungsten source can be several orders of magnitude above that possible from heated filaments. Current densities up to about 10^5 A/cm² can be obtained in steady operation. In microsecond pulses at 1000 per second, currents of 10^8 A/cm² have been obtained (Ref. 2, p. 53).

The density of emitted current is strongly dependent on the work function of the crystal surface, which in turn depends on the type of crystal face that is exposed. On an etched tungsten tip, many faces are exposed and the emitted current at a given potential exhibits a wide variation in different directions. On a fluorescent screen facing the tip this pattern can be readily seen (Fig. 7), with some areas quite bright at the same time as others are completely dark. (Figure 7a shows a usable but not desirable beam pattern; Fig. 7b shows a desirable beam pattern.) Therefore, it is necessary to have the tip oriented in such a way that a bright portion of the solid angle is in line with the instrument beam axis.



(a) Usable but Undesirable
Beam Pattern

(b) Desirable Beam Pattern

Fig. 7. Beam Patterns from Tungsten Tip. ANL Neg. No. 143-2560.

Unfortunately, the wire-forming process usually orients the crystals so that the 110 plane is perpendicular to the wire axis. This plane has a high work function and is a poor emitter. Therefore, the emitter tips are usually made from wire that has been reoriented so that a lower work-function plane is perpendicular to the wire axis. The 310 plane is commonly used as the emitting plane in tungsten (see Section 4.2.4).

A tip with the poor-emitting 110 plane perpendicular to the axis could be tilted to put a good-emitting plane normal to the lens axis. This was not tried, because of the possibility of the slanting tip wire disturbing the electric field so as to enlarge the effective beam source size.

4.2.2 Source Size

After proper forming, a tungsten field-emission tip is nearly hemispherical. Etching produces crystalline faces in a polyhedron approximately hemispherical in shape on the end of a long cone. Heating to temperatures a few hundred degrees below the melting point allows the atoms to migrate and the sharp corners between faces to become rounded.

The radius of this hemisphere can be as small as a few hundred angstroms. Electrons emitted normal to this surface are on paths that extrapolate back through the center of the sphere bounded by the surface. Therefore the virtual source is ideally a point at the center. The actual virtual source size is approximately 30 \AA (Ref. 2, p. 57).

4.2.3 Energy Spread

The spread in energy of electrons emitted under field emission conditions is much smaller than the spread in hot-cathode emission, largely because of smaller thermal energy variations of the electrons. This spread is superimposed on the acceleration energy.

The total energy spread at room temperature depends on the field at the surface, being larger at higher fields. At moderate fields, $\sim 4 \times 10^7 \text{ V/cm}$, essentially all the electrons are in a range of energies $\Delta E \approx 1 \text{ eV}$. However, nearly two-thirds of them lie in a range $\Delta E = 0.2 \text{ eV}$ (Ref 3, Fig. 7), and about 80% lie in a range $\Delta E = 0.3 \text{ eV}$.

4.2.4 Making the Tips

A tip is made from a short length, about $1/8 \text{ in.}$, of 5-mil-diam tungsten wire. This is spot-welded near one end to the apex of a V-shaped filament of 8-mil-diam tungsten wire. (See Section 17.5 for equipment for forming the filament.) The tip is then etched on the free end of the 5-mil wire (Section 4.2.4.1). The final step is to round the tip end by heating to a few hundred degrees below the melting point of tungsten, either by sustained heating or, more generally, by flashing (Section 4.2.4.3).

4.2.4.1 Etching Process. An electrolytic etch is performed on the tip wire by dipping the free end of the tip, pointing vertically downward, into a 1N NaOH solution and applying a dc potential of about +10 V to the tip, with the negative pole connected to the solution. A concave annular ring is

etched around the wire with the thinnest part just below the liquid surface. After a few minutes, the wire is etched through and the bottom piece falls. The current is then shut off within a microsecond of the break time by means of an electronic trigger switch. If shutoff is delayed, the tip becomes blunter. This method produces a short etched length of wire.

Variations in method were used, such as having drops of liquid in two wire rings, using ac electrolysis, etc., but the tips produced were of a much longer taper and more fragile than those made as described above.

4.2.4.2 Material. Tips made from ordinary tungsten wire usually will have a poor-emitting 110 plane at the end after etching. Sometimes bending the wire a few times before etching will reorient the crystal structure, but getting a good tip by this means is rather uncertain.

Deposition of other materials such as zirconium or cesium onto the tungsten surface may produce more cold emission of electrons. However, these generally have to be deposited in the vacuum in which they are to be used. The added complexity in the microscope precluded the use of this method.

A source of oriented wire was obtained initially by cutting out "wires" from a billet of single-crystal tungsten by electric-discharge machining. A crystal in the form of a bar $1/2$ in. in diameter was obtained from Linde Division of Union Carbide. Using X-ray reflection, R. M. Mayfield and L. T. Lloyd of the Metallurgy Division oriented the crystal. The Central Shops Department then cut out wires by electric discharge machining, using stainless steel hypodermic-needle tubing as a tool.

Techniques for making zone-refined tungsten wire in diameters small enough, with some grinding and etching, to be used for cold-emission tips was developed in the meantime by Field Emission Corporation. These were purchased with the 310-plane orientation perpendicular to the axis. This plane was claimed to be better for emission than some other planes used for this purpose. This source of tip material was found to be satisfactory and was eventually standardized upon for the microscope.

4.2.4.3 Forming the Spherical Surface. The result of etching is a tip with a generally hemispherical shape, but is actually a polyhedron with numerous crystal planes on the surface. The sharp edges where planes meet produce high fields, and the overall field pattern is irregular, resulting in a virtual source that is quite large.

If the tip is heated to slightly below its melting temperature ($\sim 200^{\circ}\text{C}$ below), atoms can migrate along the surface and move so that the surface becomes quite smooth. This takes place in a short time, usually a few flashes of 0.2-sec time width are sufficient.

4.2.4.4 Sharpening the Tip. Migration of atoms caused by surface tension takes place toward the shank during heating, resulting in the tip radius becoming larger. However, the direction of migration can be stopped or even reversed if an electric field of sufficient strength is applied at the tip. The direction of this field is opposite that used for electron emission; that is, the tip is positive with respect to the bias anode.

The field, E_0' , in statvolts per centimeter, at which the electrostatic field force on a surface atom just balances that due to surface tension is given by (Ref. 4, Eq. 9)

$$E_0' = (8\pi\gamma/R)^{1/2}, \quad (4)$$

where R is the tip radius in centimeters and γ is the surface tension of tungsten in dynes per centimeter. The latter is given as $\gamma = 2900$ dynes/cm at 2000°K (Ref. 4, Eq. 10). Rearranging and converting units to E_0 in volts per centimeter makes the expression become

$$RE_0^2 = 6.5 \times 10^9 V^2/\text{cm}. \quad (5)$$

Using Eq. 2 with $E = 3 \times 10^7$ V/cm as the operating field, we obtain

$$V_f = 33\sqrt{V_b}, \quad (6)$$

where V_f is the reverse potential for no migration, and V_b is the operating potential for electron emission at low current.

Migration will be toward the tip and will then build on it to form a sharper tip during heating if the reverse potential is greater than that determined from Eq. 6. This process has a limited application, but has been used to decrease the tip radius by nearly a factor of 2. Tip growth is not smooth; some crystal planes grow faster than others so that a rough surface is formed. To smooth the surface, the tip is then flashed (as discussed in Section 4.3.3).

4.3 Operating Experience

This section is essentially a chronicle of unusual or unexpected operating experiences that affect the source.

4.3.1 Tip Loss by Electrical Breakdown

One of the more serious problems encountered in operation is loss of the tip whenever an electrical breakdown occurs inside the microscope. Not only is the cost of the tip involved, but hours of operating time are lost because the microscope must be opened to change the tip and then baked and pumped down again to 10^{-9} Torr.

Usually the breakdown is from the first, or bias, anode to the accelerating anode at ground potential. This momentarily puts the bias anode at near ground potential through the low-resistance arc. The tip then sees nearly accelerating potential (in the tens of kilovolts) rather than the bias potential (of the order of 1 kV). The tip is thus destroyed by its own excessive emission current.

These breakdowns usually occur on first raising the accelerating potential after the microscope has been opened. After a seasoning period at operating potential, the danger of a breakdown becomes remote. To protect the tip during the seasoning period, it would seem that if the tip and first anode were connected directly together, the tip should always face zero potential difference and be protected. However, all such attempts were unsuccessful, even when the connecting link was placed inside the main insulator at the feedthrough conductors (which was as close as we could get to the tip and anode). Apparently the small charge in the remaining conductor and tip allows a momentary high current to flow that is sufficient to destroy the tip.

A more nearly successful method of protecting the tip is to insert a series resistor of $5 \times 10^{10} \Omega$ in the high-voltage cable at the microscope. The current in the arc is limited so that the bias anode does not make a severe enough potential excursion to damage the tip. Few tips have been lost during arcover since this resistor has been used. After the seasoning period, the resistor is removed, since leaving it in would cause the tip potential to fluctuate with variations in current resulting in undesirable variations in energies of the electrons. Of course, the tip is vulnerable to loss during operation if a breakdown occurs, and this has been the primary remaining source of tip loss.

4.3.2 Erratic Current

The tip current is monitored continuously by an electrometer in the bias potential circuit. At a pressure of 10^{-9} Torr in the microscope as read from the ion-pump currents, there is some instability. Some periods of operation may last as long as several hours, others only a few minutes, before it becomes necessary to clean up the tip by flashing it with a current pulse through the tip support wire. The pattern of fluctuation is for the current to gradually rise, with the rate of rise increasing with time. The result is a catastrophic destruction of the tip unless it is flashed. Along with the overall rise in current, the short-time fluctuations become more violent also.

Why our experience with erratic current contrasted with that of workers in field emission work at 10^{-9} Torr was eventually answered by an experiment done in a small test chamber (see Section 17.4). This is a small

vacuum chamber, free of internal pumping obstructions, mounted on a large ion pump. By observing the current-versus-time characteristics of an emission tip as a function of pressure in the chamber, we could duplicate the behavior experienced in the microscope, but the pressure was 10^{-7} Torr or higher. The conclusion was that the pressure around the tip is considerably higher than that indicated by the pump current. Although there are numerous large holes in all the components around the tip, obstructions to direct-line pumping make possible a pressure difference of one or two orders of magnitude.

4.3.3 Flashing

Flashing the tip consists of sending a current pulse through the filament wire supporting the tip. The tip itself is heated by conduction from the filament. Flashing is used for two different purposes--to form the tip (see Section 4.2.4.3) and to clean it.

The heating step in forming the tip is necessary because the result of etching is a polyhedron tip surface, consisting of the crystal planes. Heating the tip to a few hundred degrees below the melting point allows surface migration of the atoms so as to smooth the surface to a hemispherical shape. This can be done by flashing as well as by sustained heating.

Cleaning the tip by heating is necessary periodically during operation to remove gas or oxide layers on the tip which cause erratic current emission (Section 4.3.2). After heating, the current immediately becomes steady.

The flash pulse consists of a current of about 8 A lasting for 0.2 sec when an 8-mil-diam filament wire is used. Both current and time period are adjustable in the supply built for this purpose (Section 18.5), but the values above appear quite satisfactory.

In earlier operation of the microscope, flashing required that the high voltage be shut off and then a plug from the flasher power supply was inserted into the high-voltage box containing the bias supply to perform the flash. Then the high voltage had to be brought to operating level again. This process was time-consuming and interrupted operations.

The system was revised to permit flashing with the high voltage on. This method requires a transformer with isolation between primary and secondary to withstand the high voltage and to hold leakage to either secondary or ground to 10^{-8} A levels or lower. Otherwise, disturbances in the electron energy would occur due to fluctuations in the high voltage. The transformer used is an Electran custom-built unit with 10 V, 10 A output and isolation for 60 kV.

4.3.4 Tip Loss from Ion Pumps at High Pressure

Occasional loss of the emission tip occurred when the ion pumps were turned on. Sometimes a flash of light was noted in the microscope. This proved to be a glow discharge that traveled out from the pump at pressures in the order of a few times 10^{-3} Torr. This problem was solved by simply pumping longer with the sorption pumps to lower the pressure to about 10^{-3} Torr. Another solution considered, but not used, was to install coarse screens at the mouth of each pump to stop the glow discharge in the pump from spreading.

4.4 Design

Cross-sectional views of the electron gun are shown in Fig. 8.

4.4.1 Tip Mount

The insulators used for the tips are ceramic discs used in a Siemens beam welder. Collets of stainless steel were designed to hold the two ends of the tip support wire rigidly. The wire must be held inflexibly, because it becomes quite brittle where the tip wire is spot-welded to it. The other ends of the collets are designed to be pushed into spring-clip contacts (as shown in Section A-A of Fig. 8).

4.4.2 Insulator

The insulator to carry the vacuum-seal electrical feedthroughs for the tip and bias anode is designed to operate at 50 kV. This was made in the Chemistry Division Glass Shop by J. C. Hodur and his group. The double-wall construction (seen in Fig. 8) was to make the glassworking simpler, with the close tolerances required in alignment of the three feed-through pins and the tip-supporting structure.

4.4.3 Adjustment

Three types of adjustment of the insulator holding the tip are possible--tilt, lateral, and vertical. A stainless steel bellows provides the flexible seal.

Tilting is done by means of four adjusting screws at the top of the insulator assembly. The tip is swung into axial alignment with the anodes by observing the signal output of the microscope. Alignment is quite critical, and a few degrees of screw rotation means the difference between a strong signal and no signal.

Lateral motion was provided because of uncertainty initially as to the angular alignment required between tip axis and anode axis. This

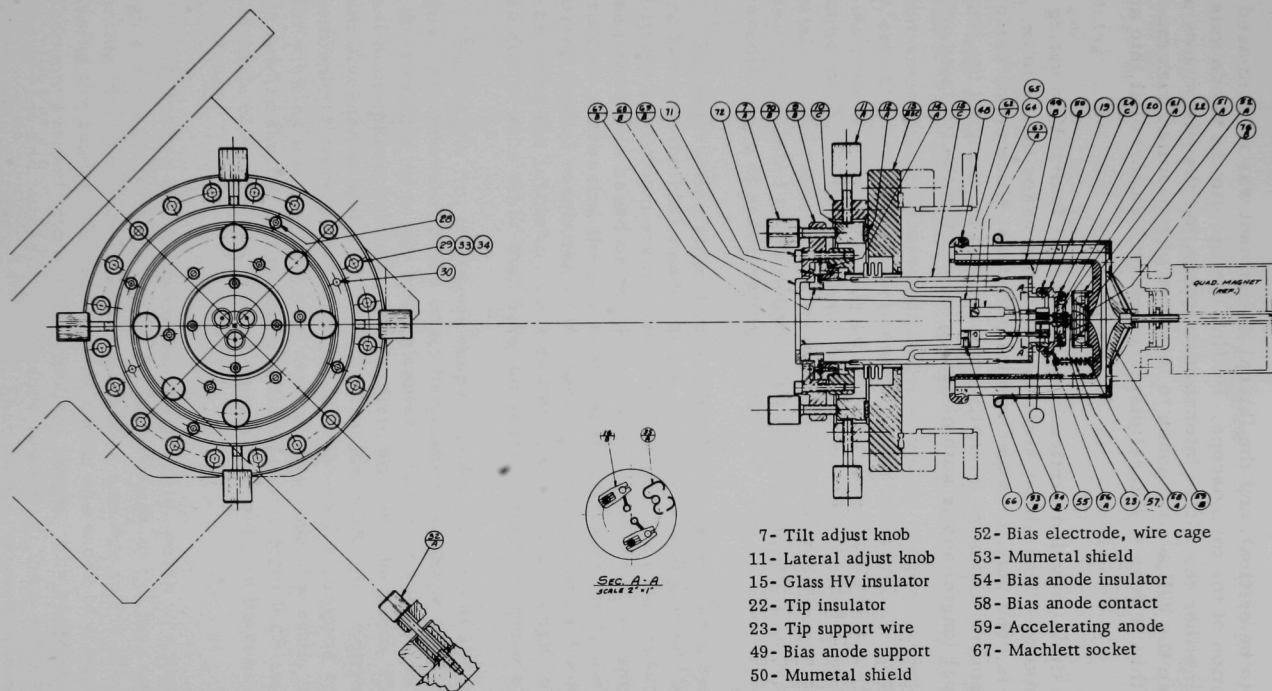


Fig. 8. Electron-gun Cross Sections

proved not to be critical, and the lateral adjustment was seldom used after early operation of the microscope. Putting the tip into the anode axis could be done with either the tilt or lateral adjustment, but the tilt screws are used because the bellows responds to this type of movement with much less resistance than it does to lateral displacement, which forces it into an S shape.

The tip is adjusted vertically by turning all four tilt-adjusting screws the same amount. This either stretches or compresses the bellows. This adjustment is used only for experimental purposes, since small variations in tip height (source distance) is easily compensated by changing the lens current (focal length) and is automatically included in the focusing procedure.

5. ANODES

Two anodes are needed for a field-emission tip to be used in an electron gun where specified energies of electrons are required. The potential on the anode facing the tip is fixed by the tip characteristics and the emission current. Acceleration to a given energy must then be done by a second anode at the desired potential.

5.1 Bias Potential

The bias is the potential of the first anode relative to the emitter tip, and it determines the current from the tip. Measurable emission current starts (from tungsten) in fields at the tip surface of about 3×10^7 V/cm, and then rises nearly quadratically with field or voltage. Thus the bias potential must not only be well regulated, but must also essentially surround the tip so that it cannot be influenced by the high accelerating potential. In the conventional method of connecting the power supply, the emitter is connected to the negative high potential, and it sees all grounded microscope parts at accelerating potential.

Tip destruction almost invariably occurs whenever a breakdown occurs between the bias anode, or its connection, and ground (Section 4.3.1). Usually the breakdown occurs between anodes. The close spacing (~ 4 mm) between anodes is based on the design of the anodes for low spherical aberration. Increasing the gap would increase distortion in the beam, thus impairing spatial resolution in the specimen. Other paths for arcover, such as along the insulator, were designed to be long enough so that tip losses due to arcs other than between anodes have been quite rare.

Facing the tip, the anode shapes used have been of several different designs. All, however, had a basic hemispherical shape of 1-cm radius with the emitting tip at the sphere center. The first anode was a simple Inconel hemisphere with a 0.33-mm-diam hole for the beam, thus admitting a beam divergence of $0.033/1 = 0.033$ radian full angle. Equatorially around the hemisphere were eight 0.125-in.-diam holes for pumping out the inside and for viewing the tip. The next design, with cupped anodes, had the same design toward the tip, but had an additional set of eight 0.25-in.-diam holes on a latitude that cleared the eight equatorial holes, to increase the pumpout conductance.

Difficulties due to tip current instability, which was presumably due to high gas pressure in that area, led to redesign of the bias anode. Assuming that the cause of higher pressure was due to the electron beam degassing the anode surface, the next anode was made of a thin sheet of molybdenum formed into a hemispherical shape. The purpose here was to be able to heat and outgas it just before installing, then, after the microscope pressure reached $\sim 10^{-6}$ Torr, heat the tip filament and outgas the

cup again with a high beam current. While this method appeared to be an improvement, the next step was to build an open-mesh hemisphere out of fine molybdenum wire. The wire was 0.003 in. diameter and the openings about 0.1 to 0.2 in. in size.

The hemispherical shape with the tip at the center produces a radial field and keeps the electrons along straight radial paths from the tip surface. If the anode were flat, field lines would bend so as to become normal to the surface at the plate. If electrons follow these lines, they would appear to come from a larger source and thus degrade the resolution. Actually, the electrons paths would be influenced very little by the field shape at the anode, because they reach essentially their full energy not far from the tip. As an example, with an inner sphere of 10^{-5} -cm radius (1000 Å), an outer sphere of 1-cm radius, and a potential of 50,000 V between them, an electron reaches 45,000 eV energy only 1 micron radial distance from the center (90% full energy 9000 Å from the tip surface) and 49,995 eV at 1-mm travel. Actual tip and anode configurations alter these figures, but the orders of magnitude are similar.

The bias potential supply is described in Section 18.2.

5.2 Anode System

Both faces of the bias anode require surfaces to form properly designed fields. The face toward the tip is hemispherical and was discussed in Section 5.1. The other face looks toward the accelerating anode, and this combination, with the potential difference, forms an electrostatic lens containing its own aberration defects which degrade the resolution.

5.2.1 Empirical Designs

The first anode designs were empirical and were replaced as soon as a satisfactory analytical design was made.

The first set consisted of concentric spherical surfaces with the tip at the center. The bias anode was hemispherical, 1 cm in radius, and convex toward the other anode. The accelerating anode was 4 cm in radius, concave, and covered a half-angle from the beam axis of $\sim 50^\circ$.

In the next set, each anode was a near-hemisphere cup with concave surfaces facing each other. The purpose of this design was to reduce the electric fields on each side of the aperture in the anodes. Anode apertures act as lenses, and such lenses have large aberrations. Making the field on each side of the aperture zero eliminates this lens action. The surfaces were spherical with 14-mm radius and were mounted with centers coincident. A 3-mm annular gap separated them; thus neither cup was a full hemisphere.

All the above anodes, as well as the later ones, were made of Inconel because of its nonmagnetic character. Care was taken throughout to avoid as nearly as possible any chance of a permanent or induced magnetic field being formed in the beam.

5.2.2 Low Spherical-aberration Anodes (Butler anodes)

Since the electron beam is processed by the anode fields as a lens, it is important that distortion be minimized here as well as elsewhere along the beam. All mechanical contributions to distortion were made as small as possible by machining and polishing to as low tolerances as reasonably possible. For example, the eccentricities of the beam apertures were kept below 0.0001-in. variation in diameter.

However, after all possible mechanical imperfections are successfully avoided, there still remain the inherent aberrations of the lens. Of these, spherical aberration usually causes the most serious beam spreading. (Chromatic aberration is small here, because the energy spread is very small (see Section 4.2.3).) Therefore, a lens anode design was made to minimize spherical aberration. The method was worked out by J. W. Butler of the Applied Mathematics Division and the resulting anode system has become known as the Butler gun.¹

Basically, the procedure was to set up an equation for the path of an electron as a function of the spherical aberration constant, C_s .⁵ Then a computer program was designed to solve for coordinates of a radial section of each anode such that C_s is at a minimum. A symmetrical design (one anode the mirror image of the other) was assumed with 2-cm spacing on the axis. The source was assumed to be just immersed. A cross-sectional drawing of the resultant anode shapes is shown in Fig. 6.

5.2.3 Characteristics of Butler Anodes

The design theory made possible the calculation of some performance characteristics of the electron gun.

5.2.3.1 Focal Length. The calculated shape of the anode depends on its size and in this case the axial distance between apexes of the two anodes was fixed at 2 cm. The focal distance from the second anode aperture was derived as a function of the accelerating potential, V_0 , holding the bias potential, V_1 , as a variable parameter. These values are shown in Figs. 9 and 10, along with experimental values measured at $V_1 = 1.31$ and 1.59 kV, respectively. It appears from these curves that the theory predicts the gun operation quite well at 1.31 kV, but deviates some at 1.59 kV, insofar as focal length is concerned.

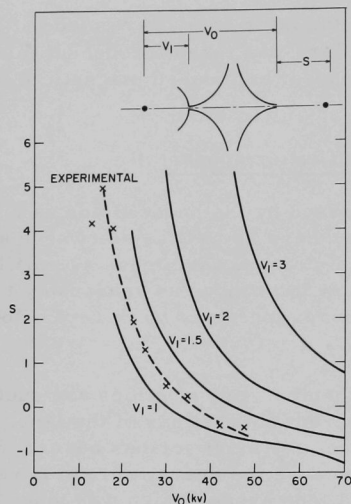


Fig. 9. Focal Distance of Butler Anodes at Several Calculated Bias Potentials and Experimental Bias Potential of 1.31 kV. ANL Neg. No. 201-6963.

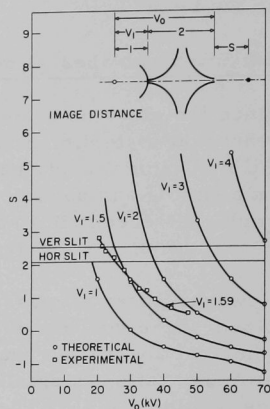


Fig. 10. Focal Distance of Butler Anodes at Several Calculated Bias Potentials and Experimental Bias Potential of 1.59 kV. ANL Neg. No. 201-6813.

5.2.3.2 Magnification. Calculated magnifications as a function of acceleration potential, with bias potential as variable parameter, are shown in

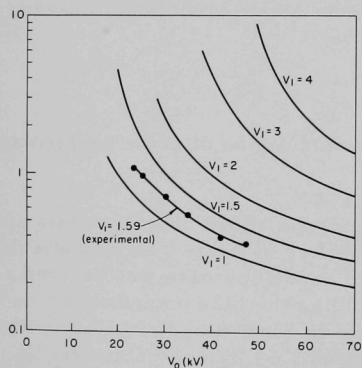


Fig. 11. Magnification of Image due to Butler Anodes. ANL Neg. No. 201-6811.

Fig. 11, along with a curve of experimental values taken at $V_1 = 1.59$ kV. The agreement between calculated and experimental values is fairly good, considering the difficulty of making these measurements.

5.2.3.3 Aberration. A calculated set of values for spherical aberration is shown in Fig. 12. It is apparent from these curves that it is desirable to keep the accelerating potential and the bias potential high to reduce the aberration. However, the choice of these values is limited by other factors.

The bias potential is limited to a small range determined by the size of the emitting tip, because of the steep function of emitted current with potential. Tip size can be controlled to some extent, but when the tip is installed, the bias

determined. Heating or flashing the tip can enlarge the size of the tip and increase the bias, but this is not very predictable and includes a hazard in that the tip may be ruined. To bring the focal point to a position so that the lower lens can focus the beam on the specimen with sufficient demagnification, the accelerating potential is then determined as in Figs. 9 or 10. To keep the focal distance short, the ratio V_0/V_1 must be made large, contrary to the requirement for lowering the spherical aberration constant. Thus a compromise with aberration is made. Typical values for V_0/V_1 are 15 to 25.

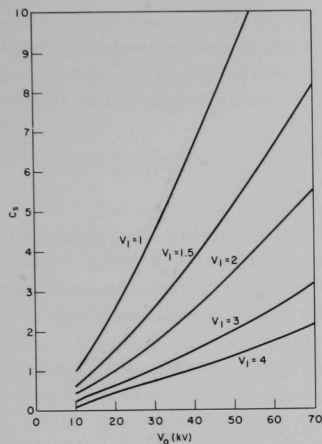


Fig. 12. Spherical Aberration in Image due to Butler Anodes. ANL Neg. No. 201-6812.

5.3 Design

5.3.1 Material

The choice of material for the anodes was limited by requirements of low magnetism, vacuum, and arcing.

5.3.1.1 Low Magnetism. The usual choice of 300 Series stainless steel for high vacuum parts was not satisfactory, because of the non-magnetic requirement. Though they are nominally nonmagnetic, tests on some pieces of Type 304 stainless steel using a Hall probe disclosed the presence of permanently magnetized spots. Annealing the pieces would probably remove the magnetism, but this was not done because of the danger of warping the parts, and there was no assurance that the permeability would be sufficiently close to unity for our requirements.

Inconel appears to have a satisfactorily low permeability as well as Curie point (-40°C). Inconel X is better, but was not readily available in sizes large enough. Other materials such as OFHC copper and beryllium copper would probably be satisfactory.

5.3.1.2 Vacuum. Vacuums of 10^{-9} Torr limit the choice of materials to those that have a very low vapor pressure and are not porous. Porosity that permits leakage through the chamber walls is obviously not permissible. A material that slowly releases molecules from pores, but is not permeable, is not very satisfactory because of the long time needed for pumpdown. Some speedup in time is gained by baking but for internal parts such as the anodes, heating may be difficult. Several metals, including the 300 Series stainless steels, Inconel, OFHC copper, and beryllium copper fulfill this requirement satisfactorily.

5.3.1.3 Arcing Resistance. The ability of a metal to resist development of a spark across a gap between pieces is probably related to the propensity

for the metal to grow whiskers. Definite information on relative arcing resistance is difficult to find, but Inconel, the metal chosen for the original electrodes, has been satisfactory in this respect.

It has been reported that the alloy of titanium containing 7% aluminum and 4% molybdenum is exceptionally resistant to arcing. This material was used for the anode inserts in a second gun system designed for 100-kV acceleration and has proven to be satisfactory.

5.3.2 Construction

5.3.2.1 Machining Methods. The first set of Butler anodes was made by using a template for a guide in cutting the surface shape in a lathe. For the next set, a tape was prepared for the tape-programmed lathe in Central Shops to cut the surface. Polishing was done by hand in both methods.

This tape was used to make anodes for other electron-gun systems, with a considerable saving in cost over the first manually machined set.

5.3.2.2 Testing. The characteristics of the anode system were tested in the scanning microscope itself.

The focal distance as a function of potentials was measured by scanning a narrow aperture slit (Section 9.1) manually across the beam to determine the width of the conical beam at that level. The location of the apex of this cone, the focal point, was then calculated. Several focal distances could be checked independently using the size of the specimen image as a gauge. With the lower (magnetic) lens off, a focused beam can be produced at the specimen as indicated by a sharp image of the specimen. Another check point is the central plane of the magnetic-lens field, near which it becomes impossible to focus the beam on the specimen. If the anode focus is anywhere between the magnetic-lens central plane and the specimen, it is not possible to focus the beam on the specimen with the magnetic lens. The lens plane point is not sharply defined, since the magnetic lens cannot be made strong enough to produce a focus on the specimen when the anode focus is some short distance toward the anodes from the central plane of the magnetic lens, but a fair estimate of the focus location can be made.

Aberrations are measured by getting a beam cross-section pattern using the aperture slits. The beam is focused at the specimen, and the variation in image intensity is plotted as a function of positions of the two orthogonal slits. The beam has a diameter at the slit level on the order of 1 mm, and the narrow slits are 0.05 mm in length. Therefore, the beam cross section can be resolved into several hundred areas by this method. Alternatively, the shape of the focused beam can be seen directly on the display image if a very small hole (small compared to the beam size) is

available in the specimen. The shape of the display image of the hole, produced as the beam sweeps through a raster, is essentially the shape of the beam cross section, and the brightness of various areas in this image is a measure of the corresponding intensities of the beam areas. The latter measurement is made with the magnetic lens off if the aberrations of the anode system is desired; otherwise one gets a combined aberration figure for the entire optical system.

5.3.3 Anode Supports

The accelerating anode is at ground potential and is mounted directly on top of the magnet support, and there is no electrical problem involved. The bias anode is at nearly accelerating potential (negatively) with respect to ground, and several methods were tried to mount it. Since it is not far (a few kilovolts at most) from the emitter in potential, its potential connection is brought through the same high-voltage feedthrough insulator as that for the emitter, in all the mounting types.

5.3.3.1 Concentric and Cup Anodes. The first anode, a concentric style (Section 5.2.1), and the next, the hemispheric type, were mounted on the bottom of the insulator, surrounding the emitter. Therefore, the bias anode could be moved laterally relative to the other anode by means of the insulator adjusting screws. The tip was fixed with respect to the bias anode, and they moved together in the adjusting procedure. When the anode was mounted over the tip, they were aligned so as to be coaxial with each other by means of adjusting screws, but after the insulator was mounted in the microscope, this setting could not be changed.

The primary disadvantage of this type of mount is that if the emitter tip bends, which it often does when it is flashed, there is no way to correct it without opening the microscope. Although this system permits both emitter and bias anode to be isolated by one insulator, later anodes were mounted separately, even though separate high-voltage insulation then had to be provided.

5.3.3.2 Long Insulator. The first system using Butler anodes had the bias anode hanging on a cylindrical insulator, which in turn was supported by the accelerating anode (as shown in Fig. 8). This design made possible accurate alignment between the anodes before they were mounted in the microscope. Now adjusting the main insulator moved only the emitter tip.

The insulator was made from a 4-in.-diam, 4-in.-long quartz cylinder, the long length being to avoid electrical leakage since the potential between anodes may go as high as 50 kV. This design produced a bias anode in the form of a cup. Holes were made in both the insulator and the cup in a number of places around the circumference for pumping out the interior. The electrical connection to the anode came through the main insulator, and contact with the anode was made through a spring connector.

This system worked quite well and was used for several years. Its drawback was the interference with attaining a low pressure around the emitter, and it was replaced with a short insulator unit.

5.3.3.3 Short Insulator. Making the insulator between anodes in the form of a short spacer opened a clear path for pumping from the emitter area to the cold baffle. Some hesitation was felt as to the possibility of an insulator ring only 0.697 in. long allowing too much leakage current. The system has operated quite satisfactorily by avoiding shapes in the anodes that would cause high fields and by keeping the insulator clean.

The insulator ring was cut from a 99% Al_2O_3 alumina cylinder and was sandblasted lightly. The anode surfaces near the insulator were made flat to avoid high fields, so there were no guide or alignment rings. Therefore, the anodes were aligned optically with the insulator in a sandwich form, and the parts were cemented together. After some tests on several adhesives, including epoxies, both for their adhesive strength and their effects on attaining an ultrahigh vacuum, the choice made was Eastman 910. This material has proven to be highly satisfactory in this application. If high-temperature bakeout is required, other materials may be necessary.

6. LENSES

The function of the lens is to focus the electron beam to a point on the specimen. Since the effective source size is of the order of 30 Å diameter, a demagnification of 30 would, in principle, produce a 1-Å-diam spot. This amount of demagnification is well within the range of one lens; so the basic plan was to design the microscope with a single lens. Aberration correction, however, may require additional lens components.

Since resolution is essentially equal to the beam image size, the diffraction and aberration requirements of the lens are stringent if a resolution of a few angstroms is to be attained. The three principal contributors to enlarging the beam image size are (1) spherical aberration, (2) diffraction (not strictly a lens defect), and (3) chromatic aberration.

Spherical aberration increases with increased aperture size according to the relation

$$\delta d_s \propto C_s \alpha^3, \quad (7)$$

where δd_s is the image size due to spherical aberration if a perfect lens would produce a point image, C_s is the spherical aberration constant, and α is the cone apex half-angle of the beam at the specimen. Since δd_s goes up as the cube of aperture size, the aperture should be as small as possible if spherical aberration is to be minimized.

Diffraction contributions, δd_d , to image size are given by

$$\delta d_d \propto 1/\alpha. \quad (8)$$

Therefore, to reduce this effect, the aperture should be made as large as possible. Choice of aperture must then be a compromise between spherical aberration and diffraction effects. In this microscope the effects were selected such that $\delta d_s = \delta d_d$ at $\alpha = 5 \times 10^{-3}$ rad, and the first design used this angle for choosing the size of the aperture at the output of the lens. Further improvement can then be made only by improving spherical aberration in the lens, or by compensating for it (such as with a Deltrap corrector).

Chromatic aberration requirements of the lens are essentially eliminated by having monoenergetic electrons in the beam. The contributions to variations in energy are (1) instability in the high-voltage power supply, and (2) variations in energy of electrons as they are emitted from the source.

The power-supply stability is rated at 50 ppm over an hour including ripple and dc change and has been observed to be much more stable than its rating. It thus contributes <1 eV to the energy variations. The energy

spread between a great majority of cold-emission electrons is considerably less than 1 eV. Therefore, the total spread is of the order of 2 eV in 50,000 eV, at most. The power-supply contribution to instability can no doubt be reduced considerably by upgrading the supply.

6.1 Magnetic Quadrupole-Octupole Lens

Since spherical aberration would produce the worst image spreading, the initial choice of lens was an attempt to minimize this factor.

Some work by Septier⁶ indicated that the spherical-aberration coefficient of a quadrupole doublet was at least as good as that of solenoidal lenses. This was the primary reason for choosing a quadrupole lens. Also, conventional lenses have been studied quite thoroughly, and their characteristics are quite predictable, but, the characteristics of small quadrupoles were relatively unknown and thereby offered a promising item for development. A secondary advantage of quadrupoles is their low power requirements (a fraction of a watt as contrasted with tens of watts for a conventional lens), which lessen the effects of thermal distortion.

6.1.1 Theory

Multipole magnetic lenses have poles pointing radially inward toward the lens axis and produce fields with large circumferential components. Since successive poles around the axis alternate in sign, these field components between the poles alternate in direction (as shown in Fig. 13). Thus charged particles moving axially will be forced toward the axis in one gap, forced away in the next gap, and so on around the multipole. The beam image is lobed in appearance, alternately focused and defocused as one proceeds around the axis.

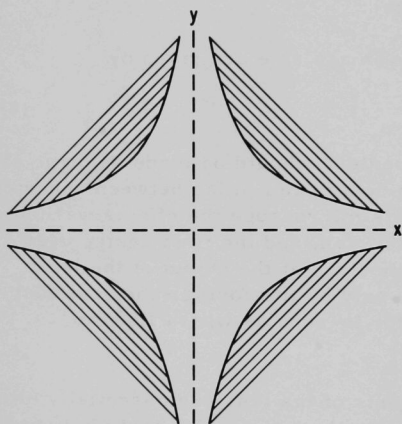


Fig. 13. Basic Quadrupole Profile.
ANL Neg. No. 143-2421.

Quadrupoles produce a first-order focused image, but with spherical aberration. The field $B_Q = kr$ is linear with radial distance from the axis. Two sets of poles are needed for a complete system. Sextupoles produce a first-order image with chromatic correction, and the field as a function of radius is $B_S = kr^2$. Octu-

poles provide correction for spherical aberration, since their fields, $B_O = kr^3$, are cubic functions of distance from the axis, and the image spread due to this aberration is proportional to the cube of beam angle

with axis or cube of radial distance from axis. Therefore an octupole can be adjusted to compensate for spherical aberration. For complete correction around the axis, three sets of octupoles are needed.

Since the electron beam in the microscope is quite monoenergetic, there is no need for sextupoles for chromatic correction. Therefore, the

initial design included two sets of quadrupoles and three sets of octupoles (as shown in Fig. 14).

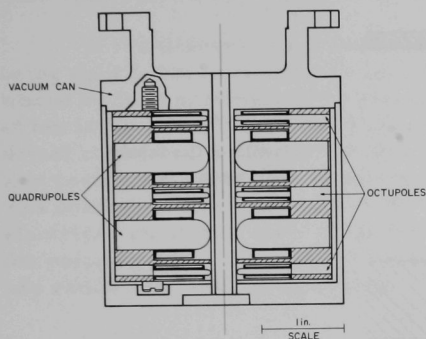


Fig. 14. Quadrupole-Octupole Magnet.
ANL Neg. No. 201-7399.

The image from a single quadrupole is focused along one diameter and defocused along the perpendicular diameter, resulting in an elliptical image from a circular object. The second quadrupole is rotated 90° from the first and defocuses the focused rays of the first quadrupole and focuses the defocused rays of the first unit. To a zero order, their effects would seem to cancel. However, just as in the optical system of a converging and diverging lens of

equal focal length, there is a net first-order focusing along the diameters. The resultant image size on the axis is partly due to spherical aberration, and this is then partially corrected by the three octupoles. The remaining image size should ideally be due to object size and diffraction, in a monochromatic beam, except for higher-order effects and other aberrations.

6.1.2 Design

Starting with the accepted number 1.14 as the ratio of radii of quadrupole bore to pole tip, trials were made with fields of the order of a few hundred gauss, object distance 10 cm, image distance 1 to 20 cm, and electrons having 50 keV energy. The following dimensions were then chosen:

Radius, lens axis to pole tip	4 mm
Radius, pole tip	4.56 mm

6.1.2.1 Magnet Structure. The poles were made hemispherical in shape. The basic quadrupole shape is a hyperbolic cylinder. However a circular cylinder is a near enough approach such that the loss in image quality is insignificant. The two sets are rotationally aligned with opposite magnetic poles adjacent. To prevent a magnetic field between these poles, a shield was placed between them. The center hole in each shield has a lobed profile that matches the quadrupole ends (as may be seen in Figs. 15 and 16). The shield was placed a distance away from the pole surface equal to the

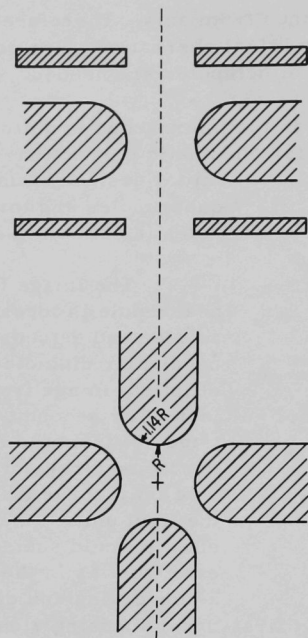


Fig. 15
Profiles of Quadrupoles
and Shields

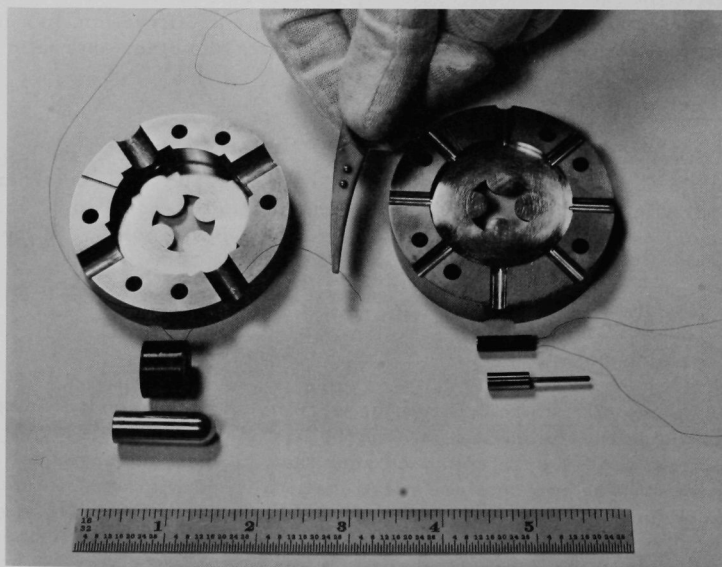


Fig. 16. Poles and Shields. ANL Neg. No. 210

distance from pole tip to lens axis (4 mm). Each tip was made hemispherical to present a similar aspect to the shield as it does to the axis.

The pole material is killed Armco iron, and the tips were polished to a radius of 4.56 mm with a radial uniformity of ± 0.0025 mm. The pole tips were examined carefully to ensure that no pits that would distort the field appeared on the surface.

A multilayer yoke structure supports the poles, each hole for a pole being split between two layers (see Figs. 16 and 17). The poles were positioned by first assembling the structure with all poles in their places but at too large radial position. Then a metal dowel was polished to a cylindrical surface of 4-mm radius with ± 0.0025 -mm uniformity. This dowel was positioned accurately down the central axis of the lens, and each pole was pushed in until it contacted the dowel, as determined by a simple electrical-continuity test. Then the stack screws were tightened to clamp the poles firmly. The stack is built with two full-length dowels to prevent any radial shift during tightening.

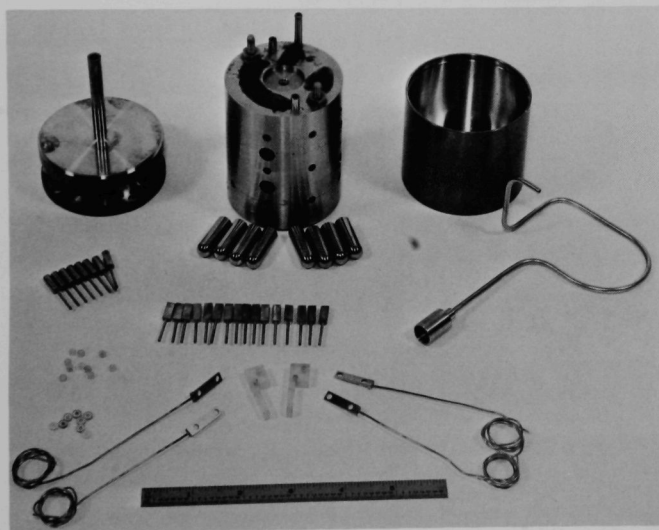


Fig. 17. Magnet Parts. ANL Neg. No. 210-707.

The coil design was based on using all the available space and fitting it to the characteristics of a selected current source. Since the power supply had a maximum output of 100 mA at 100 V, the load to utilize this fully should be $1000\ \Omega$, or $250\ \Omega$ for each of the four coils in a quadrupole. Each coil consists of 2800 turns of No. 38 single-film Teflon wire (American Super Temp. Wires, Inc.). The ampere-turn requirements are

given by $NI = 1.6 Ba$, where B is the field in gauss and a is the distance from lens axis to pole tip in centimeters. In the microscope, the bottom quadrupole (the strongest) needs a field of 600 gauss to focus 50-keV electrons on the specimen; therefore $NI = 390$ ampere turns for a magnetic circuit. Each circuit is supplied by two coils; therefore each coil requires 195 ampere turns, maximum, which then uses 70 mA current. Thus the current supply is adequate.

All the coils have exactly the same number of turns to preclude any asymmetry from unequal coils.*

6.1.2.2 Octupoles. The three sets of octupoles are similar to the quadrupoles in their cylindrical shape with hemispherical pole tips (see Figs. 14, 16, 17, and 18), but the yoke end was made larger for better support. The poles are 0.8 mm in radius with a radial uniformity of ± 0.005 mm and are also made of killed Armco iron. A few pits perhaps 0.05 mm deep were found along the cylindrical surfaces, but these were judged to be of no serious concern since they were not right at the tip and the fields from these poles are weak. The pole tips were aligned to the same dowel as were the quadrupoles (4 mm from the lens axis).

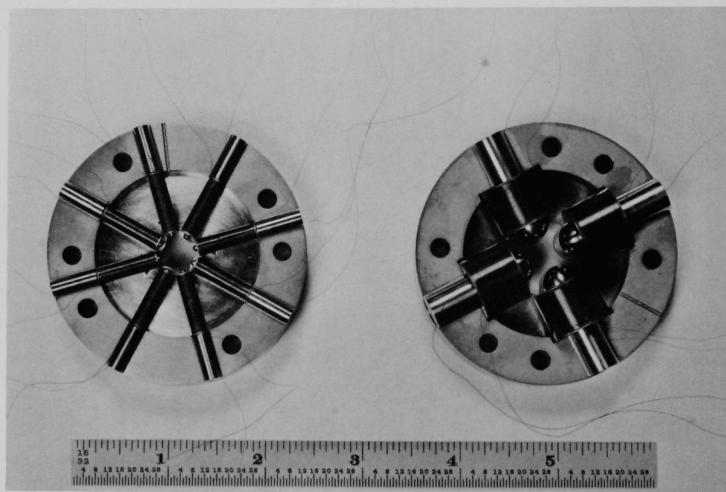


Fig. 18. Coils and Poles in Place. ANL Neg. No. 210-719.

The octupole field gradient required is of the order of 0.1 that of the quadrupoles. But the pole diameter is 0.175 that of the quadrupoles; therefore the field should be $0.1/0.175 = 0.57$ that of the quadrupoles, or

*The tedious coil winding for both quadrupoles and octupoles was done in the Particle Accelerator Division by A. W. Neubauer's group.

111 ampere turns per coil. For a current supply capable of furnishing a maximum 100 mA at 100 V, the total resistance should ideally be 1000 or 125Ω for each of the eight coils in an octupole. Space limitations, however, required that very small fragile wire is needed. Therefore, a compromise was made using No. 41 triple-film Teflon at 1600 turns per coil, giving a total resistance of 455Ω for a complete octupole.

6.1.2.3 Current Stability. The focal length of the lens is dependent on the lens current, which must then be very stable. With an object distance of 10 cm, the widest aperture (2-mm full width) represents an input half-angle of 0.01 rad. At an image distance of 3 cm, an electron at 0.01 rad angle undeviated by the lens would land on the specimen a distance $y = 13 \times 0.01 = 0.13 \text{ cm} = 13 \times 10^6 \text{ \AA}$ from the center of the image. Therefore an outer ray would be bent to move this distance at the specimen for a perfect focus. Assuming y is proportional to I (the lens current), and taking 10 \AA as the maximum permitted fluctuation (Δy), the permitted relative instability is $\Delta y/y = \Delta I/I = 10/(13 \times 10^6) \approx 10^{-6}$ or 1 ppm. If the aperture is reduced, the stability can be relaxed proportionately.

6.1.2.4 Electrical Power. At the maximum current (70 mA) in a quadrupole, the power is $I^2 R = 0.070^2 \times 1000 = 4.9 \text{ W}$. In an octupole at the same current, the power is $0.070^2 \times 455 = 2.2 \text{ W}$. The total power required for two quadrupoles and three octupoles is then 16.4 W maximum.

6.1.2.5 Encapsulation, Leads, etc. The entire pole, yoke, and coil structure was isolated from the microscope vacuum by a copper container. Figure 14 shows how the container surrounds the magnet in the form of a doughnut with a center tube for the beam. Figure 17 shows, before assembly, the two mating parts that make up the container in the upper right- and left-hand corners, and the bent tube that carries the wires to the outside in the right-hand center of the photo. After assembly, the two joints were welded by an electron beam. (One joint is at the outer circumference, and the other is where the central tube goes through a hole in the end of the outer can.) The bent tube adapter was first welded into a hole in the end of the outer can. The completed magnet is shown in Fig. 19.

The coils in each quadrupole and octupole were connected in series by welding with a very small torch and then coating the weld and adjacent wire with Sauereisen (a ceramic-like insulating material after it hardens). A pair of leads connect to each multipole, making a total of 10 wires to the outside. The container was evacuated, dry nitrogen was admitted, and the tube containing the leads was sealed with an epoxy resin forming a plastic plug through which the leads enter the tube. This was done to prevent rusting of the magnet poles.

The lead-carrying tube has a small flange at the outer end that allows a copper ring gasket to seal the flange against the microscope chamber wall where the wires go through to the outside.



Fig. 19
Encapsulated Magnet.
ANL Neg. No. 143-2425.

6.1.3 Operation and Performance

Focusing the beam was quite straightforward, despite the fact that two power supplies, one for each quadrupole, required adjustment. The operator observed the image on the storage CRT while the currents were adjusted. There was some interaction between the two supplies with respect to image clarity. A few alternations in adjustment between supplies were necessary. For very fine focusing, the line-sweep display was used (Section 3.3.5).

Hysteresis in the magnet poles was apparently quite small, since increasing or decreasing adjustments could be made near the focus with nearly identical settings.

The octupoles were turned on only after the best possible resolution was attained with the quadrupoles alone. An improvement in resolution was apparent. However, the ultimate resolution was limited by the inherent design of the quadrupoles and in practice was $\delta_x = 450 \text{ \AA}$ and $\delta_y = 150 \text{ \AA}$, part of which was due to aberrations in other components of the microscope (Section 6.1.4).

6.1.4 Computer Analysis Performed by Meads and Cohen

A digital-computer program for analyzing the linear beam properties and third-order aberration properties of quadrupole

was devised by Meads.¹⁰ Through the assistance of David Cohen* in interpretation and analysis of the computer results, a set of resolution-capability values was obtained for the original magnetic quadrupole-octupole lens built for the microscope.

Summarizing the report, the best possible resolution in two orthogonal directions corresponding to the pole gap centers are $\delta_x = 80 \text{ \AA}$ and $\delta_y = 57 \text{ \AA}$, allowing for 30% uncertainty due to source-angle distribution. A moderate end-field gradient was assumed. However, this assumption is not critical, since the worst coefficient in the series (in the spherical aberration in the y direction) changes less than a factor of 2 in going from an infinitely sharp cutoff to a very broad gradient. The calculations assumed 30-keV electrons and 1200-V tip bias.

The experimental values of best resolution were $\delta_x = 450 \text{ \AA}$ and $\delta_y = 150 \text{ \AA}$. These figures include other aberrations in the microscope, such as anode defects, possible rotational misalignment between quadrupoles, and end-shield effects, but the actual causes of the wide discrepancy from theory are not known.

Analysis of the present lens by varying parameters in the computer program indicated that the change in design that would give the most gain in resolution would be to make the poles longer axially while retaining the other dimensions.

6.1.5 Degausser

The possibility of residual magnetism producing unbalanced hysteresis curves in different poles made it desirable to have a procedure for degaussing the quadrupoles and octupoles. A circuit was designed by E. W. Johanson and his group in the Electronics Division to carry through this procedure automatically upon command.

The procedure was based on applying an oscillating current to the magnet, the current wave amplitude increasing to a maximum and decreasing again to zero. The maximum amplitude was such that the magnetism at the center of the pole core was at least as high as it ever reached in its history. At 0.067 Hz, the penetration depth is such that the core reaches 90% of its surface value. Thus, with 100 mA operating current, the degaussing current should be $100/0.90 = 111 \text{ mA}$ to ensure that the center reaches the maximum operating value of magnetism. The change in current between cycles was arbitrarily chosen to be about 3% of maximum. Therefore, the unit was designed to provide 30 linearly increasing and 30 decreasing oscillations, reaching a maximum current of 111 mA. Each oscillation takes $1/0.067 = 15 \text{ sec}$, making the time for a degaussing procedure 15 min.

*Particle Accelerator Division of Argonne National Laboratory, now at Massachusetts Institute of Technology.

The oscillations and the changing amplitudes were generated by rotating potentiometers driven by a synchronous motor through appropriate gearing. Interlocks were provided to avoid breaking the circuit to the magnet coils with power on, to prevent puncture of the insulation by an inductive potential.

Experience with the microscope soon indicated that degaussing was unnecessary since no detectable improvement in image quality was evident from using this procedure, and current settings were quite closely repeatable for achieving similarly repeatable images, indicating that hysteresis effects were small. Also, the interlocks were soon abandoned, since no evidence of puncturing appeared from switching the current supplies off during operation.

6.2 Annular Lens

An alternate lens was purchased for comparison with the quadrupole system in the microscope. For the dimensions and operating conditions involved, an RCA EMU-3G intermediate lens appeared to be the most suitable. Some of the parameters of this lens are:

Bore diameter	1.016 cm
Pole gap	0.762 cm
Coil turns	23,000 \pm 20
Current maximum	70 mA

6.2.1 Redesign

It was necessary to seal the lens for use in the ultrahigh vacuum. Holes were welded shut and a two-lead hermetically sealed feedthrough was beam-welded to the magnet case, after the coil wires were brazed to the feedthroughs.

This lens was not originally built for service as a high-resolution focusing device, and the best resolution obtainable at first was of the order of 200 Å. The obstacles in attempting to use this lens for high resolution are (1) pole-piece tolerances are too large, (2) the magnetic field is too low, but it cannot be increased because the coil would overheat, (3) the cross section of iron in the magnetic circuit is too small, and (4) the gap between pole piece and yoke is too near the poles.

The first improvement on the lens was to polish the pole bores and make them circular to ± 2.5 microns. This increased the resolution by about a factor of 2. Later, modified poles with shorter magnetic gap and smaller diameter were installed.

6.2.2 Results

Since annular lenses have been subject to exhaustive study, the characteristics of this one could be calculated and the image quality predicted. The resolution attained with the modified lens was about 40 \AA , which was in accord with the predicted best value, taking into account aberrations generated by the anode.

6.3 Electrostatic Quadrupoles

The quadrupole concept was extended to a design using electric fields. The poles are spherical ends, 3.175 mm in radius, on a rod and spaced 2.781 mm from the pole to the axis of the lens. The two quadrupoles are spaced 2.388 cm center-to-center along the axis. The poles are made of a 7% aluminum, 4% molybdenum alloy of titanium to reduce arcing possibilities (Section 5.3.1.3).

The theory is essentially the same as that of the magnetic quadrupoles, except that the forces are due to electric instead of magnetic fields and the radii of maximum effect are those in line with the poles instead of those in the gaps. No octupole correctors were included.

Construction design features a stacked set of quartz insulators and metal parts (shown in Figs. 20-22). The poles are clamped in channels of two mating quartz rings and were spaced to the proper position radially by adjusting the length of each pole piece so that the doughnut shield on the outside end of the pole is firmly against the quartz (as shown in Fig. 22). Since all materials were compatible with ultrahigh vacuums, the lens was not

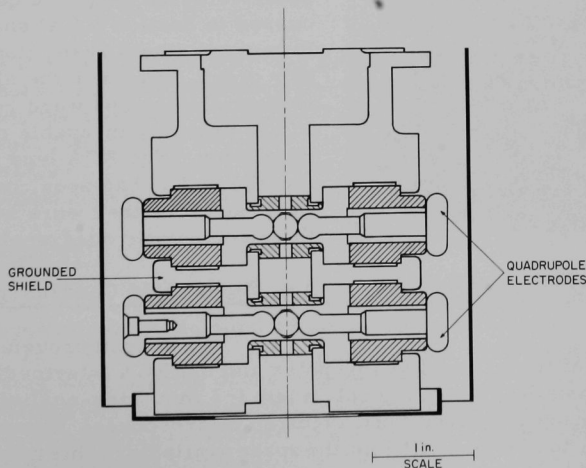


Fig. 20. Electrostatic-lens Cross Section. ANL Neg. No. 201-7403.

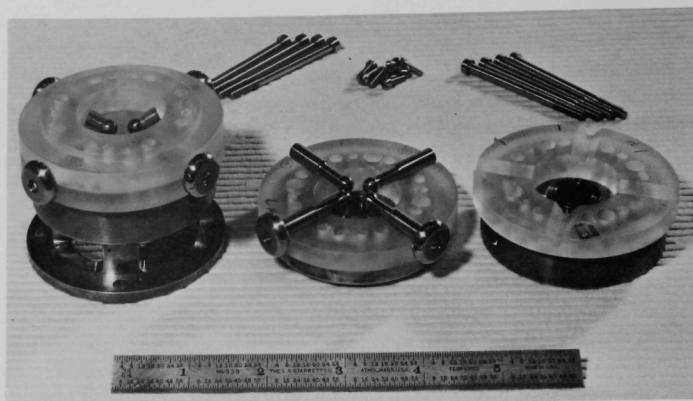


Fig. 21. Electrostatic-lens Components. ANL Neg. No. 210-1072.

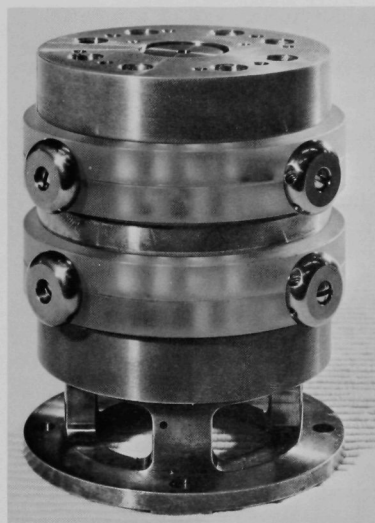


Fig. 22. Electrostatic Lens Assembled.
ANL Neg. No. 210-1073.

encapsulated. The maximum potentials required between poles is about 4 kV for 30 keV electrons and these were supplied by commercial well-regulated sources.

This system was used in the microscope for about a month, during which time it was determined that the best resolution attainable was of the order of 200 Å. Meanwhile, the Meads-Cohen analysis of the magnetic quadrupoles (discussed in Section 6.1.4) showed them to have a maximum resolution capability of this order, and since the electrostatic system dimensions were roughly similar, it was probably incapable of much better resolution. The RCA lens modifications (Section 6.2.1) had been completed by this time, so no further work was done using the electrostatic quadrupoles.

6.4 Single-field Condenser-Objective Lens

Further improvement in resolution beyond that of the original quadrupoles and the RCA intermediate lens depended on installing a short-focal-length (~ 2 mm) high-quality lens similar to objective lenses in conventional electron microscopes. Commercial objective lenses are too large to fit into the space available in this microscope, however. It has been shown^{7,8} that a single-field condenser objective, with the specimen in the central field, is capable of resolution several times better than

conventional systems with the specimen external to the field. Or, for a given resolution, the bore and gap can be made larger, thus reducing astigmatism. These lenses have not been used, because of their greater complexity, and because other limitations to resolution in microscopes would mask the gain achieved by the lens. Improvement in the other limitations recently has made the single-field condenser objective lens look attractive. Therefore this type of lens was selected for the next stage of improvement in this microscope.

6.4.1 Design

Some essential parameters applicable to the dimensions in this microscope were supplied by Reisner.⁹ The parameters and optical properties based on a bore and gap each 7.6 mm (these values were reduced in the final version) are:

	25 kV	50 kV
Spherical-aberration constant, C_s , mm	0.85	0.93
Image spread, δ/A , Å	7.9	6.2
Focal length, f , mm	2.2	2.4
Specimen location, Z_0 , mm	-1.7	-1.1
Ampere turns, NI	6400	6400

The values given for Z_0 mean that the specimen location will be approximately that distance from the geometrical center, toward the gun. With the coherence of a cold-emission source, the value of A in the equation $\delta/A = C_s^{1/4}\lambda^{3/4}$ can approach the theoretical value 0.43, thus bringing the actual image spread δ down to ~ 4 Å.

In the actual lens, the bore and gap were each reduced to 3 mm as a result of miniaturizing the specimen-handling apparatus (Section 10.4) to reduce further the aberration spread. The shorter focal length requires a higher flux concentration in the poles--it may reach 25 kG--and for that reason the magnetic circuit was made of Permendur. This alloy of nearly half iron and half cobalt has a saturation flux around 25 kG.

6.4.2 Construction

A single billet of Permendur was used for the entire magnetic structure with all pieces in the finished magnet located in the same relative positions as they were in the billet. After all the basic machining was finished, the final lapping and finishing of the pole bores and gap surfaces was done by a firm specializing in precision work. (Surface Finishes, Inc., 133 Official St., Addison, Ill.) The bore was finished to a circularity of at least 0.00002 in., and the faces to a similar flatness.

Figure 23 shows a cross-sectional drawing of the magnet. The beam is directed through the center of the magnet. The coil is divided into two similar halves, an upper and a lower, separated by a gap in the pole-gap plane for specimen-handling apparatus.

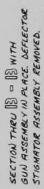


Fig. 23. Single-field Condenser-Objective Lens, Cross Section

Each coil is sealed inside a copper jacket to isolate it from the vacuum (as shown in Fig. 24). The rest of the magnet is not cased. The jacket is made of copper with 3.2-mm-thick walls, except on one end where a folded-spiral cooling channel is milled. A flat cover is placed over the channels and brazed to the case at the outer and inner circumferences. An inlet and outlet tube is then brazed on. Leakage from one channel to the next can occur, but the fit is good enough to make this a negligible factor in cooling efficiency. The heat generated may be as much as 60 W in each coil, thus making water cooling necessary. Each coil consists of 1300 turns of No. 18 Formvar-insulated wire.

6.4.3 Characteristics

Each encased coil alone has a resistance of $\sim 8 \Omega$ at room temperature. With 2 A current, the temperature reaches $\sim 55^\circ\text{C}$ after several hours in open air.

The magnet was finished and installed after the project terminated at ANL. Reports on initial operation indicate that 15 to 20 A resolution had been reached.

7. STIGMATORS

One of the more serious aberrations occurring in lenses is asymmetrical focusing resulting from defects in lens construction and material. Corrections are made in the electron beam by means of stigmators. In conventional electron microscopes, these devices are of several forms, a circular array of soft-iron screws that can be adjusted, an array of electrostatic poles around the beam that have individually adjustable potentials applied to them, or magnetic fields that can be varied by means of currents supplied to coils.

The first stigmator made for this microscope was an electrostatic unit. It was followed by a magnetic one consisting of a set of coils surrounding the electron beam so that a magnetic field is produced transverse to the beam with continuously variable intensity and continuously variable direction for the full 360° around the beam.

7.1 Electrostatic Stigmator

The first stigmator was an eight-pole unit with potentials up to several hundred volts applied to them in a sine configuration. That is, as one traveled around the electron beam from pole to pole, the potentials seen would be in the proportions 0, 0.707, 1, 0.707, 0, -0.707, -1, -0.707. The potentials were supplied through ganged sine-cosine potentiometers fed from common positive and negative potential sources. Varying the source potentials permitted the electric fields to be raised or lowered without changing the phase (angular position around the beam). The phase was changed by turning the sine-cosine potentiometers.

Mechanically, the system consisted of 0.048-in.-diam Inconel-X rods arranged in a cylindrical pattern $1/4$ in. in diameter. The effective length of the rods was 0.689 in., the rest of the rods and connections being shielded from the beam by a metal tube just inside the rod array. There were two such sets, the upper one located just below the accelerating anode and the lower one reaching into the magnetic lens (RCA intermediate) gap just above the immersed specimen (discussed in Section 10.3).

These pins served a dual function, the other one being deflection electrodes (as discussed in Section 8.2.4). The deflection sweep potentials were superposed, by capacitor coupling, on the stigmator potentials, which were directly connected to the poles.

This system worked fairly well, but had two drawbacks, both resulting in some image distortion. One defect was due to interaction and summation of the superposed potentials; the other was due to the shape of the fields produced by thin, widely spaced rods.

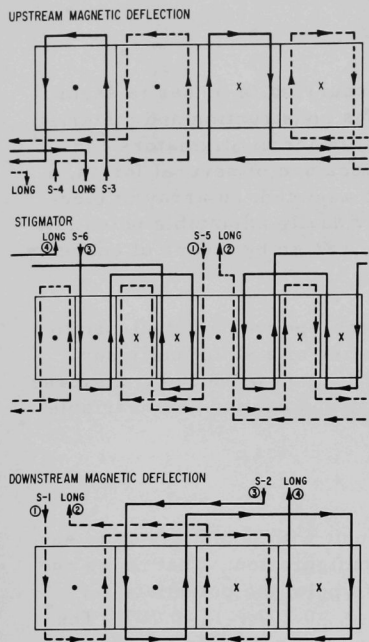


Fig. 25. Stigmator- and Deflection-coil Layout. ANL Neg. No. 143-2768.

to the right (half the distance between slots). As current S-5 is increased to its original value but in the opposite direction, the pole moves another $22\frac{1}{2}^\circ$ to the right. This process can be continued to rotate the field to any position. The field intensity is varied by increasing or decreasing both currents simultaneously and in the same proportions.

The currents are supplied through ganged sine potentiometers so that one knob rotated through 360° produces 360° magnetic rotation. Another knob controls current to the sine potentiometers and therefore controls the field intensity without affecting the angular position of the field. The maximum currents used are in the order of a few milliamperes.

The cores for stigmator and deflection coils are made of one piece of Inconel, which is nonmagnetic (see Fig. 26). The stigmator core itself is 0.400 in. diameter and 0.875 in. long. Since the stigmator fields required are quite small, each coil consists of just one turn of No. 24 Super Temp Type E Teflon-covered wire.

7.2.2 Results

The stigmator effects on the image resolution are quite marked. It is possible to remove nearly all the stigmatic defect

7.2 Magnetic Stigmator

The electrostatic stigmator was soon replaced by a magnetic stigmator in which the deflection function was separated from that of the stigmator.

7.2.1 Design of Original Unit

The magnetic stigmator consists of eight coils surrounding the beam with two separate windings. Both windings are in each of the eight slots (as shown in Fig. 25). The lay of the winding is such that every end current across a pole is compensated by an equal and opposite current across that pole, although the wires may not always lie on the same end of the pole. The stigmator is located between the two sets of deflection coils, axially.

The winding arrangement produces essentially four magnetic poles, which, by changing the ratio between currents in the two windings, rotate around the axis. From Fig. 25, with equal currents in the two windings, decreasing current S-5 to zero moves the center of the magnetic pole $22\frac{1}{2}^\circ$

as the present resolution ($\sim 40 \text{ \AA}$) shows. Operation is simple with two controls, one for phase (field direction) and one for intensity.

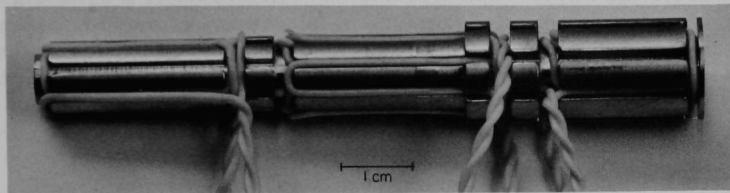


Fig. 26. Core for Stigmator and Deflection Coils. ANL Neg. No. 143-2688.

7.2.3 Condenser-Objective Lens Unit

A stigmator-deflection unit was built for the high-resolution lens, that was quite similar to the previous one (Section 7.2.1), except that it is smaller in order to fit into the space available. The stigmator core is about $3/8$ in. in diameter and $13/16$ in. long.

8. DEFLECTION

Since the microscope discussed in this report is a scanning-type device, an important part of the system is a means of moving the beam image in a raster pattern on the specimen. In addition to the usual requirements of linearity and stability in the sweep, there must be very little effect on the beam spot size.

8.1 Requirements

The display tube can show a picture 15 by 15 cm in size. The initial resolution planned was 10 Å, which should be readily distinguishable if spread over ~1 mm on the picture. Therefore the minimum scan was chosen to be 1000 Å, giving a spread on the picture tube of 1.5 mm/10 Å for a magnification of 1,500,000. At the minimum design magnification of 1,500, the specimen scan is 0.1 by 0.1 mm.

8.2 Electrostatic Deflection

Initially, electrostatic deflection was chosen over magnetic deflection for several reasons: (1) Sweep potentials were available from the storage display tubes, which use electrostatic deflection, (2) plates for deflection are geometrically simple and straightforward to fabricate, (3) phase distortion is not a difficulty, (4) frequency changes can be made more readily, (5) magnification changes are simple, and (6) digitizing the scan might be simpler.

8.2.1 Original Set

The first set of plates was mounted in two pairs, the pairs being separated axially along the beam. Each flat rectangular plate, made of Type 304 stainless steel, has a length along the beam axis of 5 mm. The gap between plates is 2 mm, and their width transverse to the beam axis is 21 mm. They are polished flat to ~0.05 mil. The first pair was centered 17.5 mm above the specimen, and the second pair 7.5 mm from the specimen. Thus for a square raster, the first pair requires less than half the deflection potentials required by the second.

The plates are supported on Pyrex insulators.

8.2.2 Single-level Set

To shorten the lens focal length, the length of the deflection system had to be reduced if it remained between the lens and the specimen. A quartz support holding four Inconel plates arranged to form a square around the beam axis was used. Because of distortion with large sweeps in this arrangement, it was soon replaced with a short-plate shielded set.

8.2.3 Short-plate Shielded Set

To reduce distortion from fields between sets of plates, a deflection system was designed with shields on both ends of the system as well as between the plate pairs. The design was based essentially on the published work of Cooper.¹¹ The resulting system has plates 2.5 mm long axially with the beam, with a gap of 1 mm, and spacing between pairs, axially, of 1.5 mm. The center shield of 0.75-mm-thick Inconel is centered in the 1.5-mm space between pairs, leaving a space of 0.375 mm from shield to plates. The bottom shield of 0.5-mm-thick copper is similarly spaced 0.375 mm from the plates; the top shield is an aperture 2 mm away. The center and bottom shield have beam apertures 0.5 mm square.

8.2.4 Stigmator-Deflector Unit

This unit used the stigmator rods as deflection plates by superposing the deflection sweep potentials on the steady stigmator potentials. (The system is described in more detail in Section 7.1.) Deflection potentials could be put on either set of stigmators, or both for double deflection. However, the unit was soon replaced by a magnetic stigmator and deflection unit (discussed in Sections 7.2 and 8.3) because of distortions produced by potential interactions and by the shape of the deflection rods as deflection plates.

8.3 Magnetic Deflection

A magnetic-deflection system was designed that separates the deflection and stigmator sections (discussed in Section 7.2). The coil schematic layout is shown in Fig. 25, and the core is shown in Fig. 26. The two sets of coils provide for double deflection.

8.3.1 Double Deflection

A double-deflection system was chosen to avoid producing distortion in the beam image. The first set of coils bends the beam away from the axis. The second set returns the beam toward the axis, which it crosses at the center of the magnetic field in the pole gap. The beam therefore pivots about the center of the magnetic field and thus avoids much of the aberration produced when the beam goes through the field away from the axis.

8.3.2 Original Design

The upper core is $17/32$ in. in diameter and $11/16$ in. long; the lower one is about $3/8$ in. in diameter and $7/8$ in. long. Each coil consists of one turn of No. 24 Super Temp Type E Teflon-covered wire. Each slot contains one wire from each of two adjacent coils. Coils and core are open and exposed to the vacuum.

Transistor converters were built to transfer potential sweep inputs (from the storage CRT sweeps) into linear current outputs for the coils.

8.3.3 Condenser-Objective Lens Unit

A stigmator-deflection unit was built for the high-resolution lens, that was quite similar to the previous one (see Section 8.3.2), except that it is smaller to fit into the space available. The system uses double deflection with the stigmator between the two sets of deflection coils. Each core is about $3/8$ in. in diameter and $13/16$ in. long.

9. APERTURES

9.1 Crossed Slits

The initial set of beam apertures, located between the accelerating anode and the lens, consisted of two sets of slits, movable at right angles to each other. The slits were 2 mm wide and 0.05, 0.1, 0.15, 0.2, 0.25, 0.5, 1, and 2 mm long. Thus a set of square apertures and a variety of rectangular apertures could be made and positioned anywhere in the beam cross section.

The slits were made in sheets of 0.25-mm-thick platinum by an electric discharge erosion method (Elox). Each of the two slit arrays was positioned through a bellows feedthrough and screw with dials marked to show intervals of 0.001 in. (Varian 954-5049).

Beam-intensity profiles were made by moving the finer slits through successive positions and measuring the intensity at the detectors.

9.2 Lower Circular Series

Later a set of six circular apertures was designed for placement in the lower part of the beam, between the lens and the deflection plates. This change in placement was done for two reasons, to see if electrons scattered in the upper part of the beam could be more effectively blocked, and to make the space occupied by the slit system available for other pieces of equipment (stigmator).

The aperture holder was designed to hold commercial electron microscope apertures, which could then be readily changed, and removal for cleaning was quite easy.

The same feedthroughs that originally operated the slits were used to position the lower apertures at somewhat increased complexity in lever mechanisms, because the slit movements were in a different plane from that of the feedthrough motions. The apertures were in a row along a slide that was pushed or retracted by one feedthrough. The slide fit loosely in its groove with 1/16 in. side clearance. A spring pushed on one side of the slide against a push arm on the other (actually positioned at 45° angle to the slide). The push arm was moved by the second feedthrough, thus providing a lateral centering adjustment for the apertures.

The slide holder, with grooves for slide and push arm, was made of fused quartz, which was also the insulator for the single-level deflection plates. The other parts near the electron beam were of Inconel, beryllium copper, or molybdenum. Platinum apertures 0.04 mm thick and 3 mm in diameter were used.

9.3 Other Apertures

9.3.1 Fixed Upper Beam

After the slit apertures were removed from above the lens and circular apertures were installed below, a fixed aperture was placed above the lens to block secondary scattered electrons. Several hole sizes were used, the largest being 1/8 in. in diameter. They were made of 0.40-mm-thick molybdenum. The reason for using molybdenum is that it can be cleaned easily by heating to redness in a vacuum and then installed in the microscope without serious oxidation. Metal oxides as well as organic contaminants can deteriorate the electron-beam pattern by collecting and retaining charges.

9.3.2 Spectrometer Entrance

A mechanism for inserting and aligning various apertures between the specimen and the spectrometer has been built, mainly for studying the focusing and aberration characteristics of the spectrometer. Longitudinal adjustment is through a screw and bellows; lateral adjustment is made through the same bellows by pushing the outer end sideways, producing lateral movement of the aperture by the lever action of the aperture slide around a pivot. This mechanism is installed and operated through the part formerly used for moving the 45° mirror. The latter was removed since there has been no occasion recently for sighting up the beam axis.

The holder is designed for five 3.175-mm-OD aperture inserts and has one open position.

10. SPECIMEN HANDLING

Specimen facilities are fairly straightforward in design with a two-gate air lock for inserting and removing the specimen, and with means for moving the specimen in two mutually normal directions in the focal plane. One unique design requirement was that of providing a gate that could be operated easily and yet make an effective seal for the ultrahigh vacuum in the microscope.

10.1 Original Specimen Holder

Standard 3.05-mm-diam specimen grids are used in a tapered grid holder, which sets in a movable block. The block is pushed by means of two bellows-type feedthroughs, at right angles to each other, for positioning the specimen in the electron beam. Two spring-loaded bumpers push the block firmly against the two feedthrough pushers so that it is firmly held in any position. The weight of the block and accessories holds it down on its bearing plate. When specimens are changed, this block is pulled out into the air lock.

10.2 Changer System

The air lock consists of a chamber with a clamped lid and a Viton O-ring seal on top, through which the specimen holder is lifted in or out, a gate valve on the side through which the specimen block is inserted or removed, a push rod for pushing or pulling the block, and a tube for evacuating the chamber.

The top lid is circular and seals a 32-mm-diam hole through which the tapered specimen holder is lifted by means of a special forceps. The lid is held in place by a U-shaped clamp and tightening screw.

The gate seals against the main chamber body by using a Viton O-ring gasket. (This and the two light pipe gaskets are the only organic gaskets in the ultrahigh vacuum; all the rest are of metal.) To get adequate gasket pressure for the seal, the gate was made of two heavy layers with a cam between them. When the cam is turned, the outer layer is blocked against a flange inside the chamber, thus forcing the inner layer against the seal ring. When the cam is released, the entire gate can be pulled down out of the way of the opening. Both operations, turning the cam and pulling the gate, are done with one handle with an operating rod through the lock chamber wall using an O-ring seal. This gate has proven to be quite reliable in use.

The push rod for inserting or removing the specimen block also slides and turns through an O-ring seal and has a key on the end which can engage a slot on the block.

The chamber is evacuated through a nominal 3/4-in. copper tube leading to the manifold connected to the sorption roughing pumps. The chamber can therefore be brought down to the roughing pump pressure, about 0.001 Torr.

Little effort was made to optimize the specimen-changing time and method, since this was not important in the early development stages of the microscope and was therefore left to be redesigned after the microscope had reached its basic design objectives.

10.3 Immersed Specimen

Using the RCA intermediate lens for focusing the beam reduced the lens focal distance and made considerable diminution of beam spot size possible. This meant removing the deflection plates and substituting deflection coils above the lens poles. (This was done in conjunction with, first, an electrostatic stigmator, and then with a magnetic stigmator, described in Section 7.) The focal plane could readily be brought to about 5 mm from the center of the pole gap without seriously overheating the magnet coils. Therefore, a specimen holder was made for inserting the specimen into the magnet bore. In addition, a method was devised for supporting the specimen holder firmly against the magnet, and isolated somewhat from the specimen block, the purpose being to reduce vibration effects producing relative motion between the specimen and the magnet.

Raising the specimen into the magnet, after locating it under the magnet, is accomplished by a wedge driven from one of the original slit feedthroughs. The specimen can still be moved, since some clearance was left around the moving parts, and the specimen holder can slide against the magnet bore, where it is held axially by spring compression.

10.4 Condenser-Objective Lens Unit

The specimen in this unit is immersed in the magnetic field in the lens gap. The principal feature is the miniaturization of the holder and adjusting mechanisms since the gap is only 3 mm long (see Section 6.4). Another innovation in this unit is the provision for withdrawing the adjusting mechanism to reduce vibration at the specimen. Toggle-type bellows feedthroughs make contact with the adjusting screws in the holder during adjustment, but when the adjusting screws are withdrawn, the specimen and holder are supported only by the lens and are not connected mechanically to the rest of the microscope.

10.5 Types of Specimen

Since the primary object of the project is to develop an instrument, specimens were chosen to show (1) sharp edges to determine rise times

and therefore beam image size, (2) characteristic electron-energy absorptions for studying the analyzing capabilities of the microscope, and (3) contrast in light-element samples without introducing foreign material (shadowing or staining).

10.5.1 Aluminum

Aluminum films of 300 to 500 Å nominal thickness were used mainly because holes and cracks furnished abrupt edges for measuring the beam spot size. This is done by noting the rise time in intensity of the primary beam through the opening in the specimen. If the sweep speed is known, the diameter of the beam can readily be calculated.

In addition, variations in film thickness make a good test for observing contrast in the oscilloscope picture.

Finally, the plasma electron absorptions at multiples of 15 eV are useful for observing energy analysis of transmitted electrons. Not only were the first three or four of these peaks observed, but the smaller peaks about midway between were also seen quite clearly with the microscope (as shown in Fig. 2).

These films, as well as the carbon films, were prepared in the Metallurgy Division by D. G. Pilney and J. K. Maurin of R. K. Hart's group and F. R. Singer of K. L. Merkle's group. A measured amount of aluminum wire (about 3 cm long and 0.4 mm thick) was evaporated by a heated tungsten wire, onto a rock salt substrate. The salt was dissolved away in water, leaving a floating aluminum film, which was then picked up on a specimen grid. The thickness was estimated by assuming a uniform 4π geometry evaporation of the wire.

10.5.2 Carbon

Carbon films are somewhat similar to aluminum in that cracks and holes furnish edges across which the beam spot size can be measured. Also, variations in thickness supply a test for contrast in a light element without shadowing with heavy elements.

In addition, the energy required to remove an inner shell electron is 283 eV and provides a test of the possibility of analyzing for carbon at that energy loss. This peak shows up quite distinctly in the energy spectrum display on an oscilloscope. Also, using only electrons suffering 283-eV loss, pictures of the specimen are displayed with good contrast. This picture is partially a "negative" of the one displayed by full-energy electrons, since thin layers produce few electrons with losses, and consequently a low signal, while thicker layers produce more. Very thick

layers, however, reduce the signal by sheer absorption and therefore appear dark when viewed by either full-energy or reduced-energy electrons.

The films were prepared by evaporating carbon onto a glass slide previously coated with a thin (a few molecules thick) layer of "Joy" surface active detergent. When the slide is dipped into water, the carbon film floats and is then lifted out on a specimen grid.

Samples of an aluminum film specimen at several electron energies are shown in Fig. 27.

10.5.3 Other Specimens

10.5.3.1 Teflon. Slices made by microtome (provided by T. N. Tahmisian's group in the Biological and Medical Research Division) were examined for energy loss peaks, one such curve being shown in Fig. 3. The carbon peak loss at ~ 290 eV is clearly evident; the fluorine K-shell loss at 687 eV is discernible as a discontinuity in the curve.

10.5.3.2 Collodion. The spectrum shown in Fig. 28 has a large peak at the characteristic loss in carbon and a small peak at 531 eV representing oxygen.

10.6 Effects

10.6.1 Contamination

In general, contamination of the specimen was negligible. In one case, an aluminum specimen was used on the order of 500 hr actual viewing time and showed no change due to contamination. This was due to the use of a vacuum in the 10^{-9} Torr region with high-speed ion pumps, and to cleanliness of all parts inside the vacuum. In one case, rapid contamination was noticed during viewing and was traced to an inadequately cleaned aperture.

Cleaning was usually done by thorough rinsing in Freon, water, ethanol, and, if possible, in an ultrasonic bath. Apertures were usually cleaned by heating them to redness in a vacuum.

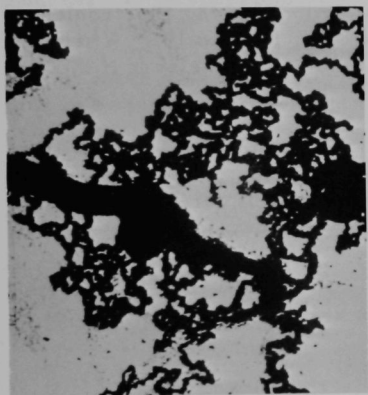
10.6.2 Ultrahigh Vacuum

Specimens apparently were not affected differently in this pressure from that experienced at the much higher pressure (10^{-5} Torr) in conventional electron microscopes.

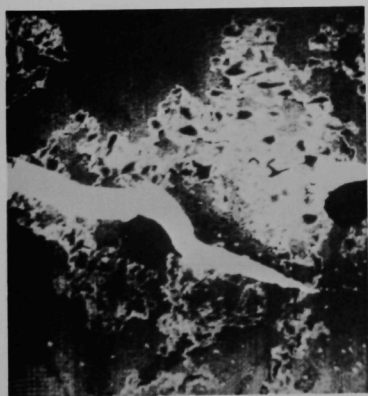
There was no appreciable difference noted in pumpdown time with an organic specimen from that with aluminum or carbon, although this operation could no doubt be improved by some redesign of the specimen changer to produce higher vacuum in the air lock.



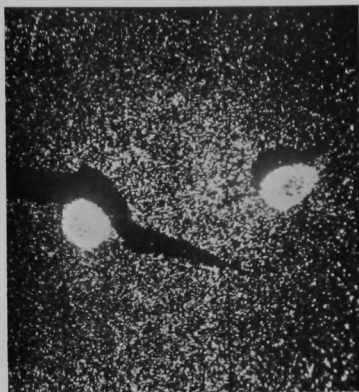
20 eV loss



9 eV loss



0 eV loss



600 eV loss



250 eV loss



100 eV loss

Fig. 27. Storage-tube Images of Aluminum, ANL Neg. No. 201-7457.

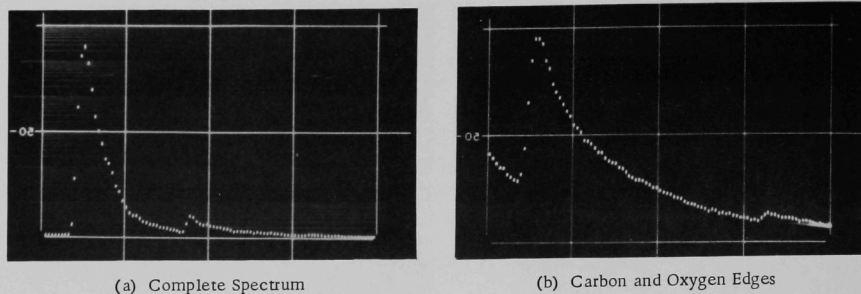


Fig. 28. Energy Spectrum of Collodion. ANL Neg. No. 201-7613.

10.6.3 Burnup

Preliminary calculations made by D. Drobnis of the Electronics Division indicated that at the beam currents used, 10^{-10} to 10^{-11} A at the specimen, burnup should not occur in most organic objects even if they were of the order of 100 Å thick.

This prediction was verified in practice, as there was generally no apparent change with the beam scanning the specimen. One exception noted was an effect of a stationary beam on the edge of certain holes in carbon. Presumably the carbon thickness tapered down to extremely small values there.

11. SPECTROMETER

The basic purpose of the microscope development being that of providing for different contrast mechanisms and some degree of specimen analysis, a means of selecting electron energies is a vital part of the system. A spectrometer design was chosen on the basis of the following requirements: (1) electron energy loss measurement accurately made, (2) reproducibility of energy loss settings, (3) stability, and (4) resolution.

11.1 Choice of Type

Hysteresis effects in iron were not compatible with the reproducibility-of-setting requirement; therefore the choice immediately was restricted to an iron-free spectrometer. An electrostatic unit was chosen over an iron-free magnetic unit, because of the sharper definition of field boundaries. A spherical plate shape was selected, because the theory had been worked out pretty well,^{12,13} and the plates could be shaped reasonably easily by optical-lens grinding techniques. Since this type of spectrometer can be made essentially for point-to-point focusing, rather than point-to-line in a cylindrical type, the output slit and detector could be kept small laterally.

11.2 Theory of Design

Several arbitrary choices were made at the beginning: (1) a central angle, or bending angle, of $\pi/2$ for ease of mechanical layout of associated parts, (2) a central beam radius of 15 cm, (3) a gap of 2 cm, and (4) a width of 10 cm. The spectrometer geometry is shown in Fig. 29.

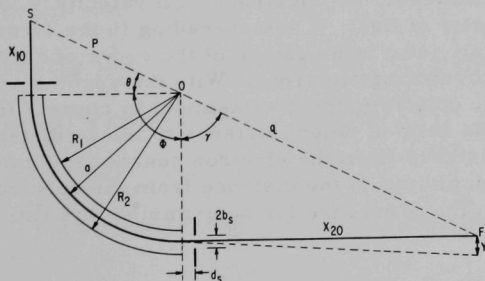


Fig. 29
Spectrometer Geometry.
ANL Neg. No. 143-2769.

11.2.1 Plate Potentials

The plate potentials required are given by

$$V_1 = 2E(1 - a/R_1),$$

and

$$V_2 = 2E(1 - a/R_2),$$

where R_1 and R_2 are the two plate radii, \underline{a} is $(R_1 + R_2)/2$, the midsurface radius, and E is the energy of the particles to be focused. In the present unit, the parameters are

$$R_1 = 13.995 \text{ cm},$$

$$R_2 = 15.995 \text{ cm},$$

and

$$E = 50 \text{ keV nominal.}$$

The potentials required are then

$$V_1 = +7115 \text{ V}$$

and

$$V_2 = -6225 \text{ V.}$$

For other electron energies, the plate potentials are proportional to the energy.

11.2.2 Focusing and Relativistic Defocusing

It can be shown¹² that for nonrelativistic particles, the source S , focal point F , and the center of curvature O all lie on a straight line (as may be seen in Fig. 29). However, for electrons with velocity v , only a few tenths that of the velocity of light, c , the spreading in the direction Y of Fig. 29 at the nonrelativistic focus can be of the order of αa , where α is the cone half-angle of entering electrons. With the spectrometer angle, Φ , fixed at $\pi/2$ radians, the only remaining adjustment to correct for relativistic defocusing was the ratio of object distance to image distance, x_{20}/x_{10} , where x_{10} is the distance from the electron source (specimen) to the spectrometer entrance, and x_{20} is the distance from the spectrometer exit to the detector slits. The procedure for determining this ratio is indicated very briefly below.

If Y_r is the distance a relativistic electron misses the nonrelativistic focus, it can be arbitrarily expressed in terms of the entrance angle spread as a power series

$$Y_r = a(k_1\alpha + k_2\alpha^2 + \dots).$$

The expression for the first-order coefficient, k_1 , has been worked out without any restriction on $\beta = v/c$, as follows:

$$k_1 = \frac{1 + \beta^2}{1 - \beta^2} \cdot \frac{x_{10}}{a} \cos \gamma \Phi + \frac{\sin \gamma \Phi}{\gamma} - \frac{2\beta^2}{1 - \beta^2} \cdot \frac{x_{10}}{a} \\ + \frac{x_{20}}{a} \left(\cos \gamma \Phi - \frac{x_{10}\gamma}{a} \cdot \sin \gamma \Phi \cdot \frac{1 + \beta^2}{1 - \beta^2} \right),$$

where γ , x_{10} , x_{20} , a , and Φ are evident from Fig. 29.

Since we wish $Y_r = 0$, we then try to make k_1 as small as possible. The other terms in the series are relatively small, since $\alpha \ll 1$. We set $\alpha = 0.01$ radian and $\beta = 0.413$ (for 50-keV electrons).

In the first trial, the condition $p = q$ was chosen, giving $x_{10} = a$ and $x_{20} = a$. The result, $k_1 = -0.255$, gave a "miss" for $a = 15$ cm, of

$$Y_r = a\alpha k_1 = 0.038 \text{ cm} = 0.38 \text{ mm},$$

which was too large for the energy resolution needed (see Section 11.2.3 below).

Choosing $q = 2p$, making $x_{10} = 0.5a$ and $x_{20} = 2a$, gave $k_1 = -0.008$ and

$$Y_r = 0.0012 \text{ cm} = 0.012 \text{ mm},$$

which was acceptable. Therefore, the dimensions were set as follows:

Object distance $x_{10} = 7.5$ cm;

Image distance $x_{20} = 30$ cm.

11.2.3 Energy Defocusing, Sensitivity, and Resolution

Velocity defocusing, Y_v , is given by¹²

$$Y_v = 2\beta a(1 + q/p).$$

However, energy defocusing was of more interest, and this quantity becomes

$$Y_E = \frac{\Delta W}{W_0} a(1 + q/p).$$

Since for relativistic focusing it was determined that $q = 2p$ was the condition required, for $W_0 = 50$ keV and $a = 15$ cm,

$$Y_E = 9 \times 10^{-4} \text{ cm/eV}$$

is then the energy defocusing for 50-keV electrons. This defocusing varies inversely with the electron energy.

The relativistic defocusing, for the selected parameters, of 12×10^{-4} cm corresponds to an error of 1.3 eV. Since the initial plan was for a resolution of 10 eV, the relativistic defocusing is acceptable.

The exit slits were designed on the basis of this resolution figure. Since a 10-eV band would spread over a range of 9×10^{-2} mm, the "closed" slit openings were made that value. The total range of the movable slit is from 0.2 to 1 cm from the fixed slit, which therefore covers the energy loss range of 220 to 1100 eV, with 50-keV primary electrons in the fixed slit.

11.2.4 End Shields

The effects of the fringing fields at the ends of the spectrometer can be compensated by a metal shield with slit width $2b_s$ at a distance d_s from the spectrometer.¹⁴ The calculations are summarized in a graph of $b_s/(a - R_1)$ versus $d_s/(a - R_1)$. A shield selected to fit these parameters makes the effective length of electrostatic deflection just equal to the physical length of the spectrometer. Actually, this work was done for a cylindrical deflector, but it was assumed that the results would be reasonably near the requirements for a small transverse angle in a spherical deflector.

Since b_s and d_s are both variables, b_s was selected as ~ 0.6 cm to give an entrance half-angle of $\sim 5^\circ$. This choice then determined the distance d_s from shield to spectrometer. The values are:

Slit width, $2b_s = 1.25$ cm,

and

Distance away, $d_s = 0.33$ cm.

The shields are at zero (ground) potential.

The effect of rounding the ends of the spectrometer plates to a radius of 3.2 mm (which was done after initial operation to avoid electrical breakdown) is given in terms of the correction, ΔS , in the effective field distance from the edge of the spectrometer:¹⁵

$$\Delta S = \frac{k}{6\pi} \epsilon^2 \left[1 + \frac{6}{5} \left(\frac{d}{k} \right)^2 \right],$$

where

$$\epsilon^{3/2} = \frac{3}{4} \pi \frac{r}{2k} \frac{(d/k)^2}{1 + (d/k)^2}.$$

For the actual dimensions, $r = 0.32$ cm, $d = 0.33$ cm, and $k = 1$ cm (one-half the spectrometer gap), the correction is $\Delta S = 8 \times 10^{-4}$ cm and is therefore negligible.

11.3 Design and Construction

11.3.1 Plates

The plates were made from commercial-grade optical fused quartz mainly for its long-term stability in shape (see Fig. 30). Using conventional lens-grinding techniques, the spherical surfaces were made smooth to about a wavelength of light (done in the Optics Shop Section of Central Shops). The plates each have a ledge on each side to provide bases for clamping them firmly to the frame. The convex plate of 13.995-cm radius has a width of 8.89 cm; the concave plate of 15.995-cm radius has a width of 10.16 cm (chord lengths). Thus the gap cross section has a width about five times the gap length to reduce field distortion from the sides to negligible values near the center of the width where the beam of interest lies.



Fig. 30. Spectrometer Plates, Frame, and Components. ANL Neg. No. 210-709.

The edges of the plate surfaces were rounded to a radius of 0.8 mm initially, but this was changed to 3.2 mm soon after experience indicated that discharges from the edges were occurring.

The conducting surface was made by evaporating Inconel onto the quartz at an elevated temperature. The plating was done by the Clausing Company of Skokie, Illinois. The plate, which is about 0.2 micron thick, adheres tightly so that it can be cleaned and wiped without danger of loosening. The plating was carried about $1/2$ cm over the edges, down the sides and ends.

Other types of plating were tried on separate pieces of quartz, but were rejected for various reasons. Fired gold-ceramic adhered well but suffered from dust settling on it during firing, leaving a bumpy surface that could not be polished without leaving open spots. Evaporated gold would not adhere well, and graphite "Dag" was also difficult to get smooth and to adhere.

There was question regarding the voltage drop across a plate coating if a substantial part of the beam fell on it. This question was resolved by a calculation that showed the voltage to be in the order of microvolts (therefore completely negligible) for a $1\text{-}\mu\text{A}$ beam.

11.3.2 Frame

Two basic requirements of the frame were rigidity and fine, stable adjustments for locating the plates accurately. The frame (shown in Fig. 30) is a heavy, welded stainless steel partial enclosure.

Each plate is held in a five-point suspension. Four points push a plate outward (apart), one at each corner against the ledge on the side of the plate. The other pushes inward at the center of the plate and consists of a threaded bolt with a locknut. The four outward-pushing points are on right-angled levers pivoted at the angle, with a 2-to-1 ratio of adjusting screw movement to plate movement. The final alignment of the plates was made using an air gauge, and the gap was adjusted to about 0.0002-in. uniformity.

The end shields (discussed in Section 11.2.4) are attached directly to the frame at their calculated locations. They are made from 0.104-in.-thick stainless steel with the slot edges rounded to full radius, i.e., 0.052 in. The slot is $31/64$ in. wide, has full rounded ends, is 4.5 in. long (direct line end-to-end), and is in the form of an arc with a $5\frac{29}{32}$ -in. radius to center.

11.4 Resolution

The design resolution was estimated from the line width in the detector with only full energy electrons going through the spectrometer, no specimen in the path. Since the energy spread in cold-emission electrons is less than 1 eV, an ideal spectrometer should show a corresponding line width in energy. This measurement can be made by using a narrow detector slit and moving it across the beam. However, sweeping the beam across a narrow slit by varying the spectrometer plate potentials produces a much clearer presentation. The slit, of course, must be at least as narrow as the resolution desired. Initially, the minimum opening was 0.1 mm, corresponding to ~ 10 eV, but the slit jaws were later honed to close with the jaws in contact.

Early measurements indicated the full-energy beam with < 1 -eV energy spread was dispersed over ~ 5 -6 eV at the slits. Assuming this spread might be due to the focus plane not coinciding exactly with the slit plane, an external magnetic quadrupole (discussed in Section 11.5) was built and placed outside the exit tube of the spectrometer. It was then possible to get an energy spread of about 0.6 eV in a total energy of 30,000 eV. The improvement in actual resolution over that of theory may be due to the effect of the end shields, which was not considered in the initial calculations.

11.5 Quadrupole Lens

To provide an adjustment between focal and slit planes, an external quadrupole was installed on the outside of the spectrometer exit tube. These focus errors may be due to slight imperfections or not having all corrections calculated, but, in particular, variations occur due to variations in specimen position or object distance.

The lens is a simple structure consisting of an octagonal yoke of steel rectangular bar, poles of 1-in. bolts, and four coils, each wound of 500 turns of No. 24 Formvar wire. By an adjustable and reversible current, the beam focus can be brought to the slit plane, regardless of whether the focal length is too long or too short. This feature of correcting in either direction is due to the fact that a single quadrupole lens has a focusing and a defocusing plane, and these planes can be interchanged by reversing the current.

This device worked well. Curves of energy spread only 0.6 eV wide are obtained, and some of this width may be due to the spread already in the incoming beam, to the slit width, and to spectrometer defects. The observed resolution in a 30-keV electron beam is a relative resolution of 1 in 50,000 or 0.002%.

11.6 Operating Experience

Miscellaneous effects and results, not all of which were obvious at first, are reported here.

11.6.1 Contacts to Plates

In the early operation, electrical contact to a plate was often lost after a breakdown occurred between plates or between a plate and ground. The contacts were spring wires bent to touch the Inconel film at the smooth convex side of the bend. A breakdown would cause a high current to flow momentarily through the contact and burn away the Inconel plating. A multiple-leaf contact was tried, but the results were the same.

A successful contact was made by making a folded pad about 5 mm square of eight layers of ~0.02-mm-thick gold foil and holding it against the plated surface with multiple springs. No contacts have failed since these contacts were installed several years ago.

Direct checks to see whether the contacts were intact were made by measuring the capacitance between plates (~50 pF) and between each plate and ground when the contacts were new. It was quite clear from these measurements which, if any, contact had failed whenever trouble was indicated. (Opening the microscope to measure the contact resistance was a major task.)

11.6.2 Cleaning by High Voltage

When the microscope is exposed to the atmosphere and then closed, difficulty is experienced for some time with discharges between plates or between plates and ground. The fastest cleanup occurred by (1) backfilling with dry nitrogen before opening the system, (2) holding the pressure at $\sim 10^{-2}$ Torr, (3) putting a series resistor of 1 M Ω in the plate line, and (4) maintaining the average discharge current at $\sim 10 \mu\text{A}$. As cleanup current decreases, the potentials are increased until they are well above operating level. For operation at 7 kV, the cleanup potential is carried up to ~ 10 kV, sometimes 12 kV. Usually 10 to 20 min is sufficient time for cleanup.

11.6.3 Apparent Gain in Energy

An energy spectrum that has a "tail" reaching to higher energies than that of the primary electrons is puzzling at first glance, since there is no apparent reason for electrons to gain energy. However, these appear to be simply due to defects in focusing by the spectrometer, and they can be nearly eliminated by proper adjustment of the external quadrupole lens.

12. ENERGY SLITS

Selection of precise energies of electrons requires a slit to limit the band accepted to a width as small as or smaller than the energy resolution desired.

12.1 Requirements

The initial design was for a variable band from 10 to 100 eV in width, which with the spectrometer dispersion of 9×10^{-4} cm/eV, required that the slit openings be variable from 0.09 to 0.9 mm. Actually, they will open to 1.0 mm.

To compare information at two energies, two slits are necessary. One is fixed in position, and the other movable from 2 to 10 mm from the fixed one, to cover a difference of 220 to 1100 eV between beams (at 50-keV accelerating potential).

12.2 Design

The slit mechanism is shown in Fig. 31 looking in the direction that the electrons go. The lower- and upper-slit opening adjustments are made and measured by two small micrometers, operating through stainless steel bellows. The upper slit is moved by another, and larger, micrometer through another bellows, and carries along the entire small micrometer and bellows mechanism which opens and closes the slit.

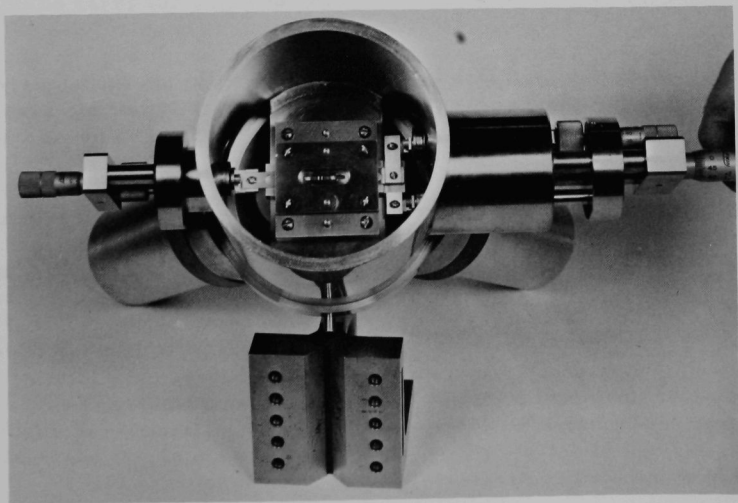


Fig. 31. Detector-end Structure, Showing Location of Energy Slits. ANL Neg. No. 210-716.

The two scintillation detectors are about 1 cm back of the slits, and to avoid possible crosstalk, either from scattered electrons or from optical pulses, a pair of shades was installed. These are flat 0.1-mm-thick stainless steel shim stock slides between the two scintillators, and fastened at one end to the inner slit jaw (jaw nearest the other slit). The movable slit pulls its shade as it moves, bending it around the edge of the scintillator. The shades are held taut and prevented from buckling by extension springs attached to the other end.

The fixed jaws are made of beryllium copper, and the movable jaws of Inconel since the latter slides on a frame made integral with the fixed slits. Both slits are 2 mm long.

12.3 Rework for Higher Energy Resolution

Experience with the microscope made it apparent that higher energy resolution would be desirable, and it was shown from the highly monochromatic primary beam that the spectrometer was capable of high resolution. Therefore the slit stops were moved so the slits would close in contact. This left a slit width that was due only to imperfections in the honed slit jaws and was shown to be somewhat less than 1 eV in bandwidth at the narrowest setting.

13. DETECTORS AND LIGHT PIPES

After the electrons are dispersed according to their energies by the spectrometer, and the desired ones are selected by slits, conversion to an electrical signal is the next step. The signal can be pulses from individual electrons, or it can be a current when electrons are collected at a faster rate.

13.1 Choice of Detectors

The ultrahigh vacuum posed an environmental restriction on the type of detectors used. After some trials, it was decided that small CsI or plastic (Pilot B) detectors may evaporate slowly enough to be satisfactory. The lower detector, at the fixed slit, is a sheet of Pilot B scintillator about 6 x 10 mm cemented with clear epoxy resin to the light pipe. The upper detector is a sheet of cesium iodide about 12 x 10 mm cemented to the upper light pipe. This one is larger to cover the area scanned by the movable slit.

As of this writing, the Pilot B detector has operated satisfactorily for three years. The present cesium iodide detector has been operating about half that length of time, the original one having dissolved during a period when excessive moisture entered the microscope accidentally.

13.2 Light Pipes

To carry the scintillation light to the photomultiplier, a quartz light pipe is used for each detector. Each pipe has a tapered shape to match the scintillator area to that of the photomultiplier face and is aluminized on all surfaces except the two active faces to prevent light escaping. The two pipes are not identical, the upper one having a larger face to carry the larger movable-slit detector.

The light pipes go through the chamber wall and thus serve as the vacuum seal. Each pipe is circular, about 25 mm in diameter at the vacuum seal, and has a flange that is pressed against a Viton O-ring to form a seal with the chamber. The photomultipliers are therefore outside the vacuum.

13.3 Photomultipliers

Both photomultipliers are Amperex XP1010, which are 10-stage units with S-11 spectral response. The active cathode surface is 32 mm in diameter.

13.4 Experience

The seal between light pipe and vacuum chamber was initially designed to be a gold ring. However, even with a well-fitting support ring around the light pipe, one quartz pipe cracked. Viton O-rings were then substituted. The concern was whether the required vacuum of 10^{-9} Torr would be attainable, but it turned out that this vacuum was readily reached using Viton seals.

The loss of a CsI detector through its hygroscopic absorption of water followed an event in which water was lying in the microscope chamber. This water came from a leak in the cold baffle (caused by water freezing in it, as discussed in Section 16.4). The detector has remained intact through the numerous exposures to atmosphere from opening the microscope chamber.

The two photomultipliers are the original ones, which have been operating over four years.

14. DISPLAY SYSTEM

The types of display used, specimen image, energy loss image, color composite, and energy spectrum are described in Section 2.6. The equipment used is described in the following paragraphs. A more detailed discussion of the image display system is in Ref. 16.

The image-display circuits were designed and checked out by W. K. Brookshier, and the optical and signal level requirements were calculated by Dr. J. Gilroy, both of the Electronics Division.

The dual-channel display console is shown in Fig. 32. The far left rack is a multichannel analyzer used to accumulate and improve the signal-to-noise ratio of low-level-energy spectra (discussed in Section 3.3.4).

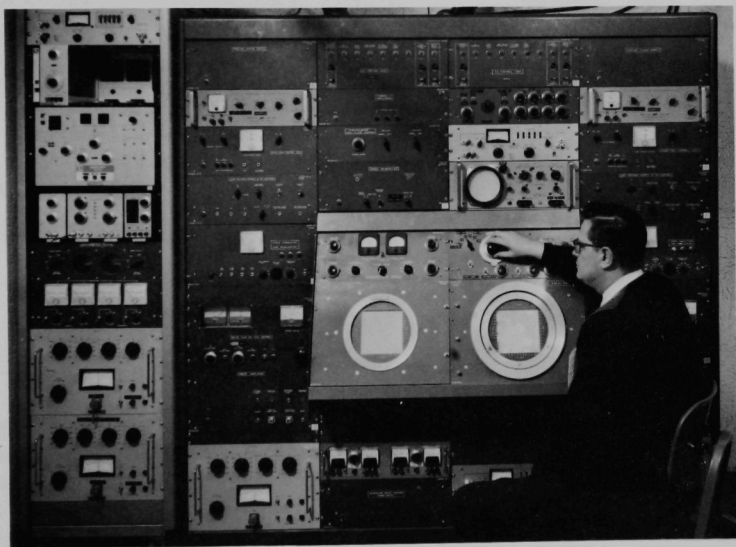


Fig. 32. Display Console Showing Multichannel Analyzer at Left. ANL Neg. No. 143-2072.

14.1 Image Display

The image-display output is a yellow-black picture on a cathode-ray-tube raster, 6 x 6 in. square. The storage tubes used for this service make it possible to accumulate signals from successive sweeps and to retain a picture on the tube face for a considerable length of time (days).

14.1.1 Requirements

Besides the obvious needs, such as resolution in the image display, there is the need to process very weak signals, since the electron beam intensity at selected energy losses in the specimen can be very small, perhaps of the order of 10^{-14} A. The system must be able to count electrons at this level as well as measure currents at higher levels. It should also be possible to integrate signals over a long time span in order to produce acceptable image displays. The latter requirement was met by using storage cathode-ray tubes, which, because of their storage capability, permit the use of very slow sweep rates and correspondingly long dwell times per picture element.

Two displays are necessary to show simultaneously the images from two energy loss values, using the two detectors in the microscope.

14.1.2 Storage Tubes

The storage tubes selected for image display are Hughes Tonotron Type H-1069 AP20. Some characteristics of this tube are

10-in. diameter

Electrostatic focus and deflection

Green-yellow display

6 x 6-in. raster

450 lines of resolution per raster width

14.1.3 Electronics

The electronic equipment in the display section consists of three functional systems, (1) signal processing, (2) storage tube power, and (3) sweeps. The two channels have separate signal processing and storage tube power systems, but one sweep system supplies both channels. A block diagram of Channel 2 is shown in Fig. 33.

14.1.3.1 Signal. From the anode of the photomultiplier (discussed in Section 13), an electrical signal goes into a video preamplifier mounted close to the multiplier tube. Long leads connect the preamplifier low-impedance output to the video amplifier mounted in the display console.

The preamplifier (the circuit of which is shown in Fig. 34) has current ranges from 10^{-8} to 10^{-4} A, each delivering a nominal 1-V output. The risetimes vary from 7 μ sec on the 10^{-8} A range to 0.04 μ sec on the two upper ranges. A conventional tube rather than an electrometer tube is used for the input stage to obtain greater bandwidth. It is operated with grid currents in the range 10^{-10} to 10^{-9} A. Drift is less than 10 mV/hr on the higher ranges.

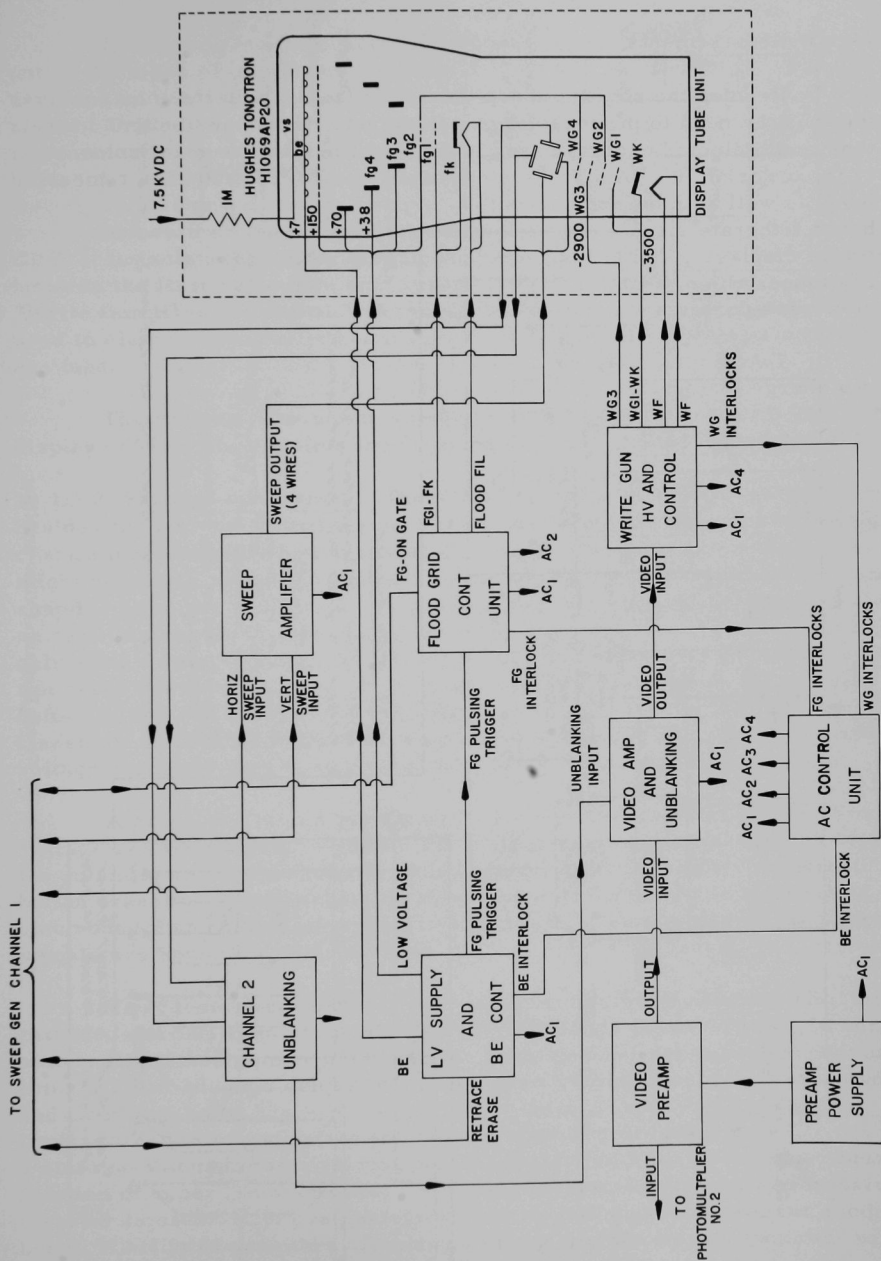
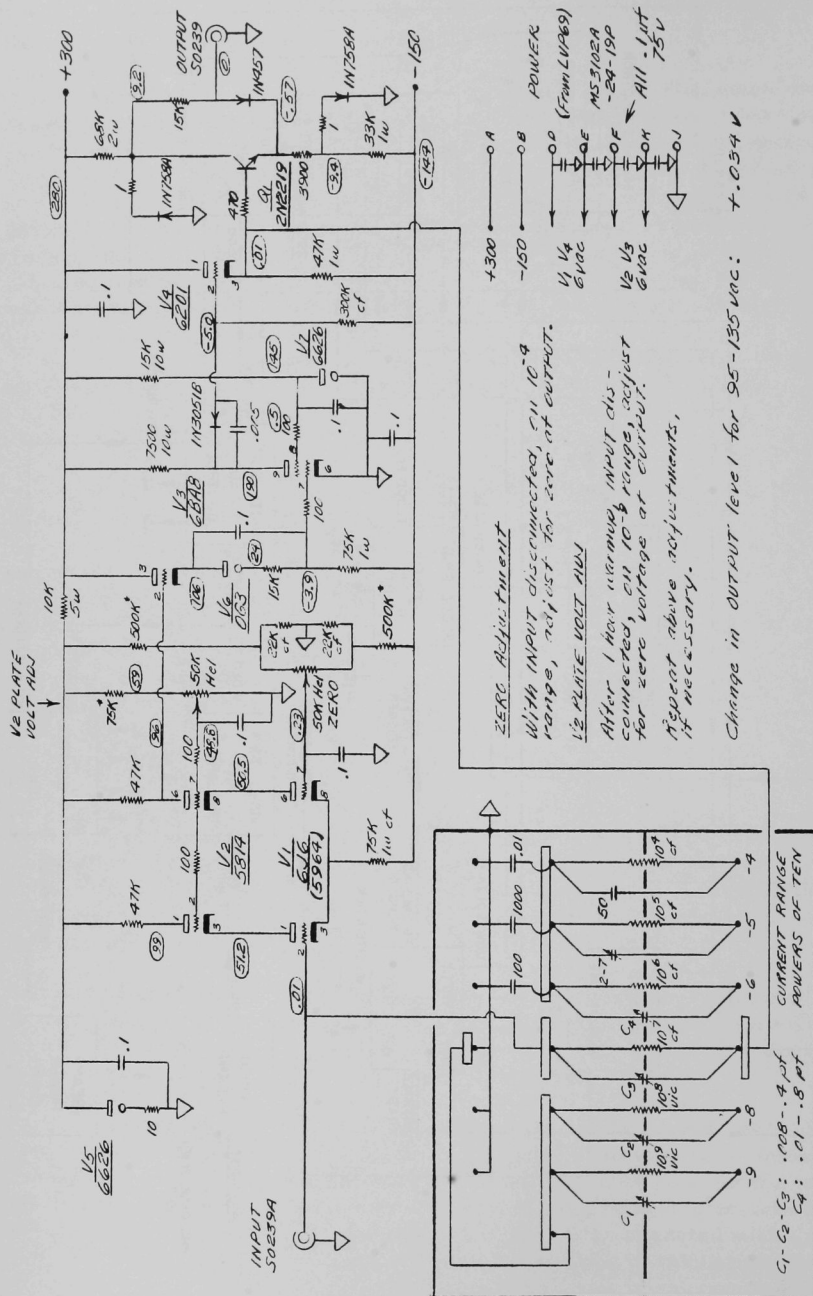


Fig. 33. Block Diagram of Channel 2 Display. ANL Neg. No. 143-1705.



The video amplifier accepts an input signal of 0 to +2 V from the output of the video preamplifier and amplifies it by a factor of five. The unit develops an unblanking signal from differentiation of the horizontal sweep signal. Unblanking permits the writing beam to function only when the beam is scanning, to protect the storage tube from damage. It also blanks the horizontal and vertical retrace sweeps.

Before the output signal from the amplifier is applied to the storage CRT, it is isolated from its ground reference and added to the bias required between the first write grid and cathode. This is done by the unit called "Write Gun HV and Control." A manual write-gun clamp level control is used to clamp off the write beam during startup to avoid damage to the storage tube.

The preamplifier power supply is a well-regulated unit located in the display console and supplies the dc potentials remotely to the preamps.

14.1.3.2 Storage-tube Power. There are 16 electrodes in the storage tube besides the four deflection plates. There are some possibilities of damaging certain tube elements by not having all the electrodes properly biased, as might happen in applying potentials in the wrong sequence or if certain power supplies were not connected. To prevent such misapplication of potentials, an "AC Control Unit" is provided that allows certain powers to be supplied only after a delayed time from the application of other powers. Also, there are cable interlocks with other chassis requiring that they be connected before power can be applied to the tube. In particular, the flood gun is biased off until other power has been on for 2 min. Also, the write-gun high voltage cannot be turned on until a number of other conditions are met.

A group of five low potentials to the tube are supplied by the "Low Voltage and BE Control" supply. The BE (backing electrode) control adjusts the potential on it, which acts as a brightness control. A one-shot erase button erases a stored picture by supplying a positive bias to the backing electrode. For continuous erase, a pulse train of single-shot erase bias signals are applied to the electrode.

The "Flood Grid Control Unit" supplies the flood filament, the flood cathode, and one flood grid. A view switch permits the flood beam to illuminate the stored picture for viewing. With the flood beam on, the storage time is about 30 sec. For extended storage of the picture, the view switch and flood-gun beam are cut off. An intermediate condition involving a trade-off between brightness and storage time can be obtained by the use of a storage-extension feature, which cuts off the flood-gun beam for a variable fraction of time. This unit also has a gate to turn on the flood gun whenever a raster is under way, even though other controls may be set to cut off the beam. This is to provide a visible display during the writing process, provided other conditions permit visible brightness.

14.1.3.3 Sweep System. The sweep system consists of a sweep generator, a sweep control unit, and two sweep amplifiers, one for each channel.

The sweep generator provides horizontal and vertical sweeps, at 20-V amplitude, to form a raster of 1000 lines in 10, 1, or 0.1 sec. The rasters may be individually generated or repetitive. This unit requires horizontal unblanking signals from a differentiated output to the deflection plates of the tube, in order to prevent the writing beam from being on unless the beam is being swept across the tube face. The 10-sec raster was modified after initial operation of the microscope to have 600 lines, each synchronized to the 60-Hz power-line frequency. This removed some of the loss of resolution due to stray 60-Hz magnetic fields (discussed in Section 19.1.3).

A sweep control unit permits adjustments in amplitude and position to the sweep signals sent to the microscope. The sweep potentials applied to the deflection plates inside the microscope are derived from those applied to the storage tube. A step attenuator reduces the potentials applied to the microscope plates, decreasing the scan distance and thus increasing the magnification, since the scanned area on the specimen is always imaged on a 6 x 6-in. raster. The steps available and the nominal area scanned in the initial design of the specimen and deflection plates, at 50-keV electron energies, are as follows:

Specimen Area	Magnification
100 x 100 μ	1,500
50 x 50 μ	3,000
20 x 20 μ	7,500
10 x 10 μ	15,000
5 x 5 μ	30,000
2 x 2 μ	75,000
1 x 1 μ	150,000
5000 x 5000 \AA	300,000
2000 x 2000 \AA	750,000
1000 x 1000 \AA	1,500,000

Both the horizontal and vertical deflection plates receive balanced (push-pull) signals, such that the average potential of a pair remains constant. For a sweep length of 100 μ at the specimen, the signal levels are 150 V peak-to-peak on each plate, which corresponds to a signal of 300 V peak-to-peak between plates.

Electrical positioning of the raster on the specimen is accomplished by the use of a steady dc potential difference between a pair of deflection plates, upon which the sawtooth sweep signals are added. This has the same effect as a fine mechanical adjustment of specimen position, and covers a range of about $\pm 50 \mu$.

The first model of sweep control used signals taken from the storage-tube deflection potentials and applied them directly to the microscope deflection plates. The signals to the microscope were thus affected by adjustments made to obtain proper operating conditions for the storage tube. A later model was then built which buffered the connection between display and microscope so that either system could be adjusted independently without affecting the other.

A Normal-Reverse switch was incorporated in the newer unit to reverse the connections between pairs of deflection plates in the microscope. This effectively rotates the image on the screen by 90° .

Four sweep amplifiers are included in the system--one horizontal and one vertical for each pair of deflection plates. Each amplifier takes the 20-V peak-to-peak output signals from the sweep generator and converts them to the 300-V peak-to-peak push-pull output signals required for the deflection plates.

14.2 Energy Spectrum

A spectrum of intensity (number of electrons collected) versus energy loss provides a fingerprint of the elements present in the specimen (covered in Sections 2.6.4 and 3.3.3). In this display, the deflection sweeps to the microscope are shut off and a focused electron beam impinges on the specimen area of interest. Voltage ramps are superposed on the electrostatic spectrometer potentials, thus sweeping the dispersed spectrum of electron energies across a detector slit. The sweep potentials are synchronized with the horizontal sweep of an oscilloscope. The signal strength picked up by the detector is applied to the vertical deflection of the oscilloscope, thus producing the spectral curve.

Samples of energy spectra are shown in Figs. 2 and 3.

14.2.1 Circuits

Ramp voltages to the spectrometer plates are applied by connecting the sweep output from the oscilloscope through a capacitor to the voltage supply to each spectrometer plate. This is done at the grounded side of each power supply to avoid using high-voltage capacitors. Detector signals are taken directly from the low-impedance output of the preamplifier to the oscilloscope. Switches were eventually installed to make it simple to change the mode of display from storage-tube image to energy spectrum.

14.2.2 Multichannel Analyzer

If the energy-spectrum sweeps are repetitively applied to a multichannel analyzer instead of to an oscilloscope, the signal-to-noise ratio can be improved (as discussed in Section 3.3.4).

For the microscope, an RIDL Designer Series analyzer with 400 channels is used.

14.3 Color Display

Having two energy slits and detectors at the output of the spectrometer makes it possible to display two images simultaneously, one in each channel. These images are of the same specimen area, but represent results of looking at two different losses of energy in the electrons. For example, a "conventional" image made from electrons having no energy loss can be displayed on one storage tube at the same time as an image is displayed on the other storage tube made from electrons having lost 283 eV (energy required to remove a K-shell electron from carbon), to show the location of carbon compared to the overall density picture. Or, two different energy losses can be chosen, corresponding to characteristic absorption energies of two elements, and displayed to show simultaneously the comparative locations of the two elements in the specimen.

If the two images can be made to apparently coincide, one superposed over the other, the relative location of details in them is more easily seen. By using two contrasting colors, one for each channel, such a composite image clearly delineates the two images in superposition. Two schemes for forming color composites have been tried successfully. The first system used optics to combine the images from the two storage tubes, and the second used a color-television monitor to combine the two images in one picture tube.

14.3.1 Optical Composite

The two storage-tube faces lie about 2 ft apart in the same plane. Using three ordinary mirrors and a partially transmitting mirror permits the two images to be superposed and be made congruent. A system was designed and tested for producing such composites from the microscope by Dr. J. Gilroy of the Electronics Division (see Fig. 35).

Two mirrors are used in a periscope configuration to transfer the image from one storage tube to a position about halfway between the tubes. The image from the second tube is similarly transferred to the same position as the first, but the second mirror in this case is partially transmitting so that the first image can be seen through it, along with the second image reflected from it. Because the second periscope is farther from its tube face than the first in order to get the partially transmitting mirror above its counterpart in the first periscope, its image would appear smaller than the other if they were midway between the tube faces. The images are made the same size by moving the two mirrors and the images toward the second tube face. When the mirrors are adjusted properly, the images are precisely congruent, and there are no parallax problems.

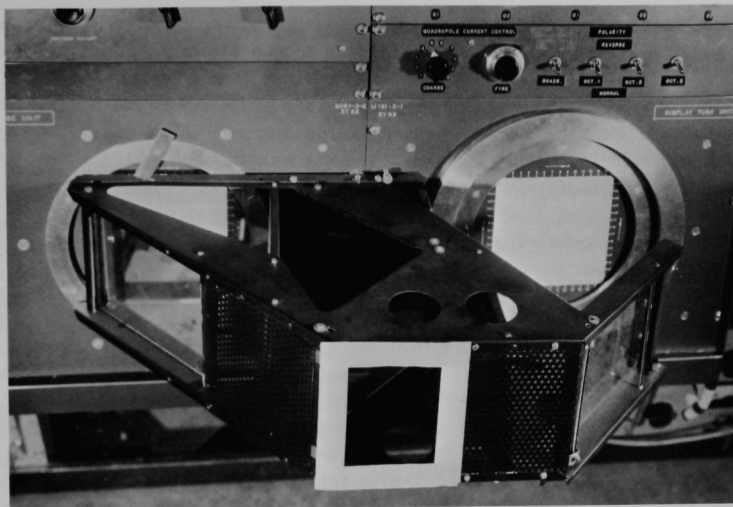


Fig. 35. System for Producing Color Composites by Optical Method. ANL Neg. No. 143-1837.

A red filter is placed over one tube face, and a green filter over the other. The tubes have P20 phosphor, which appears greenish yellow. There is enough red radiation from the phosphor to provide a distinctly red image through a red plastic filter. There is also a bright green image through a green filter. Several photos of the composite color image have been made, and the results are highly satisfactory, with areas of red, of green, and of various mixtures of the two appearing in different areas of the specimen.

14.3.2 Color-television Composite

A color composite can be made on a color-television tube face by applying the spectrometer detector signals to the electron-beam intensity controls in the television tube. Signals from one detector preamplifier modulate one color gun, and those from the other modulate another gun. Superposition of images is inherent in this system.

This system was designed by W. K. Brookshier of the Electronics Division and was built around an RCA Model TM21D Color Monitor, a high-quality television color receiver used in television studios as monitors of the transmitted pictures. The modifications necessary were the substitution of a different decoder unit and the addition of a color sweep control.

The raster sweeps are all operated at standard television frequencies. Since the color-picture-tube phosphor does not have long persistence, it cannot be used to accumulate signals from successive sweeps. Also, a

complete raster is made in $1/30$ sec; therefore, the total signal is only $1/300$ th that received in one 10-sec scan on the storage-tube display. For low-level signals, the signal-to-noise ratios will likely be poor, and they cannot be improved by cumulative methods within the system. However, photographing the picture-tube image for a number of successive raster sweeps enables time integration to be done photographically. Up to this time, the system has only been tested and the image is quite satisfactory. When it is put into routine use, photographic integration will probably be used to improve signal-to-noise ratios on low-level signals.

14.3.2.1 Decoder. The decoder unit fulfills several functions. In normal television reception, horizontal and vertical synchronization pulses from the broadcasting station ensure that the interlaced scanning is properly synchronized. In microscope use, these synchronization pulses are absent; therefore they must be supplied, along with blanking pulses. A 157.5-kHz oscillator output is divided by 5 and 2 to produce a standard 15.75-kHz horizontal frequency, and by factors of 5, 7, 5, 5, and 3 to provide the vertical 60-Hz frequency. The 157.5-kHz frequency also supplies a built-in dot generator for convergence adjustments. The 60-Hz vertical-sweep frequency can be locked to the power line so that line frequency pickup in the microscope will produce a stationary pattern. The decoder also furnishes 20-V peak-to-peak sawtooth outputs to the color sweep control for amplification to the levels required to drive the microscope deflection system.

The unit also accepts the signal outputs from the microscope detector preamplifiers into three available channels, one for each color: red, green, and blue. With two detectors at present in the microscope, three pairs of primary television colors can be selected: red-green, red-blue, or blue-green. In addition, inputs can be combined to give three more pairs of colors: red-cyan (blue and green), green-violet (red and blue), or blue-yellow (red and green). If, in the future, three detectors are built into the microscope, there will be no choice of display colors, since the red, green, and blue inputs will all be used.

14.3.2.2 Color Sweep Control. This unit accepts the 20-V peak-to-peak sawtooth waveforms at the horizontal rate of 15.75 kHz and at the vertical rate of 60 Hz. They are amplified to 300 V peak-to-peak at each of four output terminals to drive the deflection plates in the microscope. Output cathode followers permit driving capacitive loads up to 500 pF at each terminal.

Attenuation controls are provided on both horizontal and vertical sweeps. They operate in 1-0.3-0.1 sequence through four decades.

15. CAMERA SYSTEM

15.1 Storage-tube Photography

Photographs of the image on the storage tube can be made by means of a Polaroid camera mounted on a simple bracket from the storage-tube panel. Since a picture can be stored for a considerable length of time (hours), there is ample time to set up and adjust the camera when a good picture is obtained. Many pictures have been made over the years since the microscope was first started. When better quality pictures were desired, the Graphic Arts Department supplied a camera and operator to take pictures of the storage-tube image.

This system has several weaknesses. The resolution on the storage tube is about 80 lines/in. or less than 500 lines over the 6-in. raster. The picture has a rather high contrast from dark to bright, with a limited range of greys in between. The camera and bracket are physically in the way of viewing the tube comfortably and of operating the controls. To alleviate these problems, a separate oscilloscope-camera system was built.

15.2 Remote Camera

To overcome the drawbacks of photographing the image on the storage tube (discussed in Section 15.1), a separate remotely-operated system was designed by D. J. Keefe and E. L. Williams of the Electronics Division.

15.2.1 Capabilities

The system was designed to have high resolution, to provide a wide range of tones, to be convenient to operate, and to be well protected from failure or error in operation.

The resolution with present electronics is 200 lines/in. on a 3 by 3-in. raster for a total of 600 lines. Nominally, this resolution appears to be little better than that of the storage tube. However, the improvement in picture quality is quite apparent. The CRT is capable of producing line widths <0.001 in. By expanding the raster time from 10 to 30 sec, the present CRT electronics would permit a resolution of 1800 lines/raster. This will require some changes in the sweep systems for the microscope. The reason for the present resolution is that the line sweeps in the raster are keyed to the power-line frequency, for 60 lines/sec. Keying the line frequency to every 3rd or 4th sweep to give 180 or 240 lines/sec is a solution that would require little change in microscope equipment, but does require raising the high-frequency cutoff point of the amplifier. This point is approaching the limit of straightforward electronics, because the amplifier must be capable of passing dc signals and it must supply large currents to the deflection coils.

The tonal range of the CRT is much better than that of the storage tube, and adjustment is convenient once a calibration has been made. For this purpose, a monitor oscilloscope is located in the operating console for the microscope. In the camera CRT, the signal modulates the beam intensity; in the monitor CRT, it is applied to the Y deflection. Both CRT's share the same X sweep along with the storage tube. The monitor Y deflection is thus a measure of the brightness of the spot in the camera CRT. Readings on the monitor are then correlated with the black, greys, and white in the developed film from the camera system. From then on, when a scene of interest appears on the storage tube, the amplifier bias is set to give lower readings on the monitor at the "black" level, and the amplifier gain is then adjusted to give upper readings just at the "white" level on the monitor. This ensures a proper tone range on the developed picture, as long as that particular type of film is used.

Convenience of operation depends on which camera is used, the Polaroid or the 70-mm magazine unit. In either case, the bias and gain adjustments for proper tonal range and shutter operation are controlled from the operator's console panel. If the 70-mm camera is used, film advancement is also controlled from the console, making it possible to take a reel of pictures without being near the CRT-camera system. The Polaroid film must be advanced manually in the usual manner.

15.2.2 Cameras

A 70-mm drum-loaded-magazine Beattie-Coleman camera is used for normal pictures. The film is advanced electrically by remote control at the microscope console. It uses a Carl Meyer 125-mm $f/2$ lens. The camera is mounted on a transverse sliding back, so that two cameras can be used conveniently.

A Polaroid camera is mounted on the sliding back, for use in getting quick pictures without waiting to develop a 70-mm roll.

15.2.3 Cathode-ray Tube

The cathode-ray tube was chosen for high resolution and good tonal qualities. The tube is a Westinghouse WX-30233P unit with line width less than 0.001 in. everywhere in a raster about 3 x 3 in. The flat face is 5 in. in diameter, and it uses 40° magnetic deflection.

15.2.4 Dark Box

The CRT is mounted inside a simple plywood box painted flat black inside. Since the lens has a short depth of focus when focused on an object the size of the CRT raster, adjustments were provided in the CRT mount to align the tube both for axial position and axis tilt (the latter to bring all the raster into focus if part of it is in focus).

15.2.5 Circuits

The system requires (1) power supplies for the CRT elements, (2) sweep drives, (3) control, (4) protection, and (5) monitor scope. Figure 36 is a block diagram of the system.

The power supplies used for the CRT are (1) a 30-kV Sorenson Model 5030-4 for the high-voltage anode, (2) a 5-kV NJE S327 for the focus anode, (3) a 500-V unit for Grid No. 2, (4) a 6.3-V filament supply, and (5) a cathode bias of nominally 43 V. Other supplies are ± 35 , ± 15 , and ± 10 V, for the control and sweep functions.

The remote-control circuit provides for taking pictures, advancing the film, and indicating lights. A green indicator on shows that the system is ready for taking a picture (film is advanced, etc.). A red light on indicates that the shutter is open and a picture is being taken. The shutter is opened and closed automatically, when a picture is called for, at the beginning and ending of a raster.

The control system, in addition to the remote operating features, has three other functions: (1) modification of the video input to match the intensity operation of the CRT, (2) modification of the deflection voltages, supplied from the microscope console, to match the requirements of the CRT, and (3) modification of the unblanking input signal to synchronize the retrace.

The sweep drives perform five major functions: (1) supplies the horizontal and vertical drive currents, (2) provides protection for the CRT if either horizontal or vertical sweep fails, (3) provides control logic and drive circuitry, (4) provides the clamping network for protection circuits and unblanking signals, and (5) provides protection for the CRT from unsafe conditions of voltage in the control power supply. Figure 37 is a block diagram of the sweep-drive circuit.

Protective circuits are included that prevent the electron beam from burning a spot or line on the phosphor. If either horizontal or vertical sweep fails, the CRT is biased off. Also, if the regular cathode bias supply fails, a battery supplies the bias to hold the beam off until the high voltage dies away. The cathode is run at positive bias, so blanking is done by clamping the grid to ground. To unclamp the grid, a differentiated signal is required from both vertical and horizontal deflection coils. The battery is kept charged by a trickle charger. If the charging current becomes excessive, a meter relay shuts off the high voltage. Other relays protect against failure of the bias supply or relay supply.

The monitor consists of a Tektronix 360 oscilloscope and power supply. Its main purpose is to set the video signal levels to get the proper scale of tones on the finished photograph (see Section 15.2.1). In addition, it can be used to monitor eight signal points in the system for checking

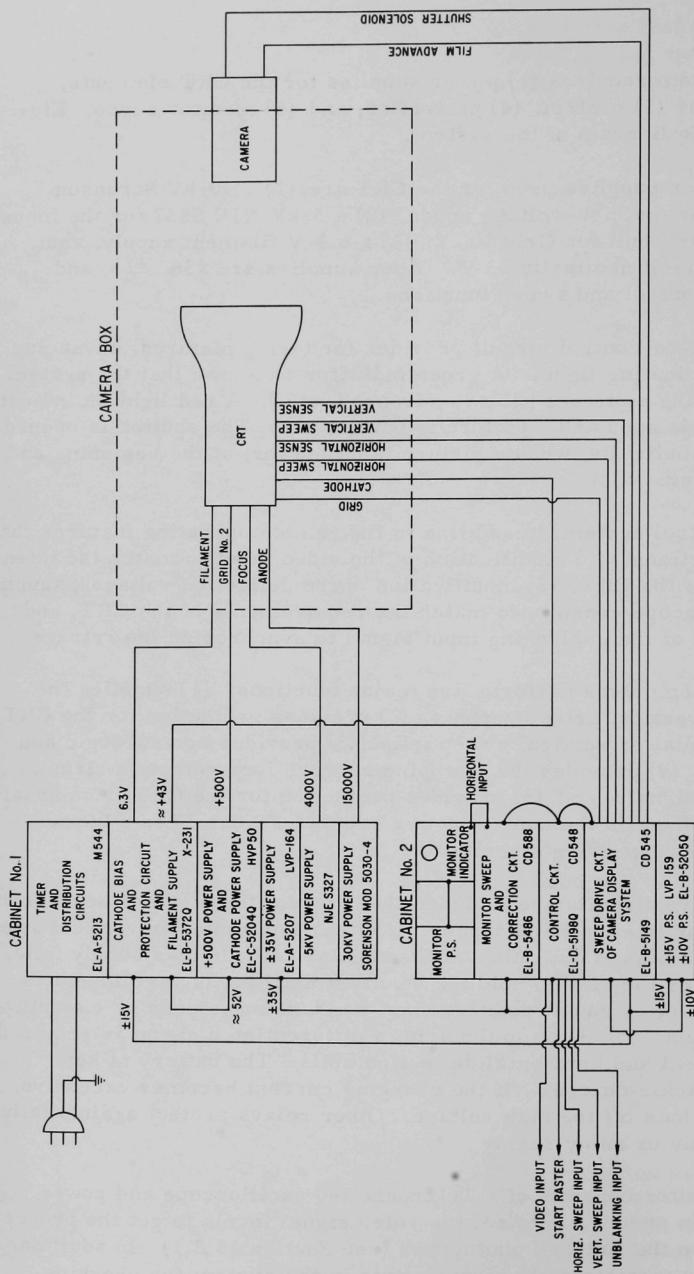


Fig. 36. Camera-system Block Diagram, ANL Neg. No. 143-2879.

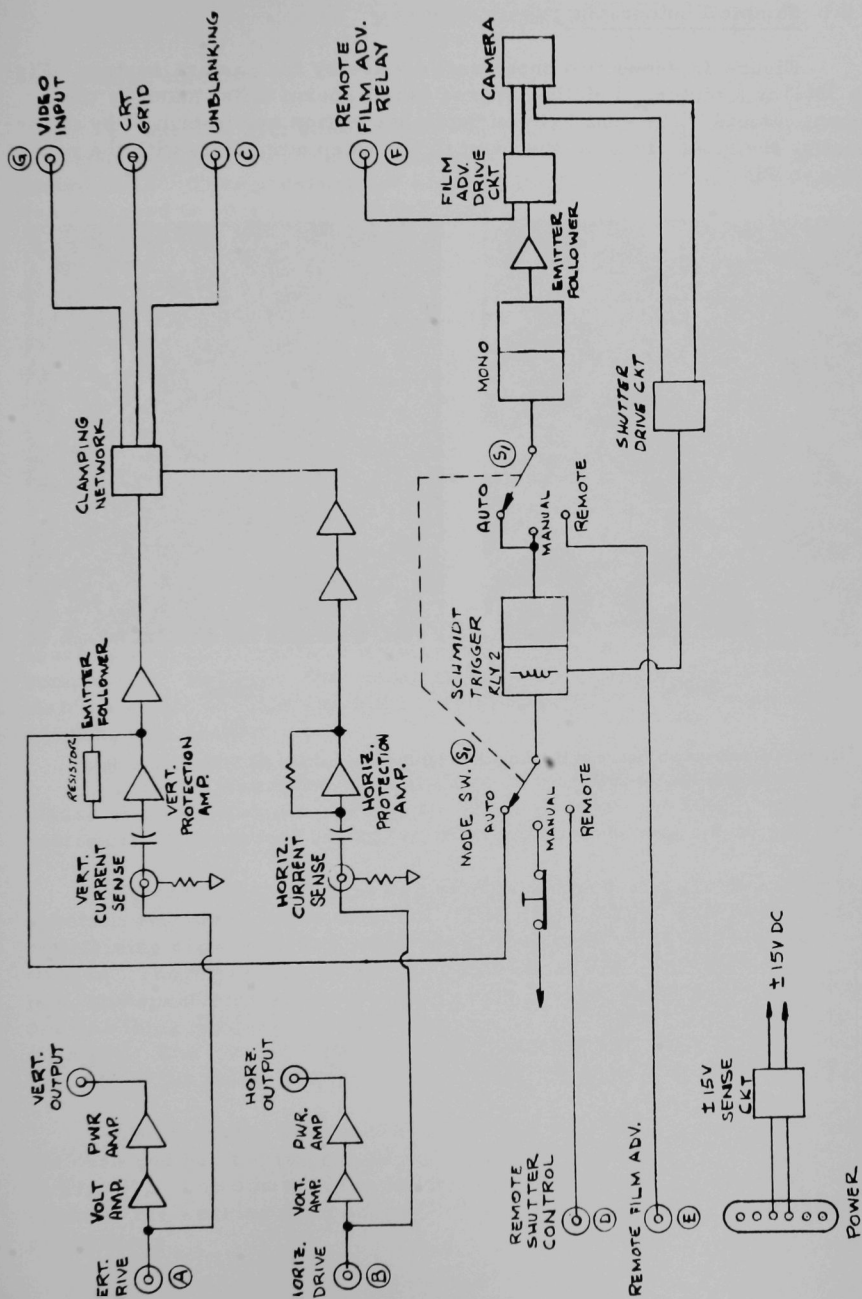


Fig. 37. Sweep-drive Block Diagram

15.2.6 Sample Photographs

Figure 38 shows two photographs made by the camera system. Figure 38(a) is a picture of *Helix Aspersa* (snail sperm tails) taken by the 70-mm camera. The contrast and depth perception are improved by differentiating the video signal at the input to the video amplifier, with the result shown in Fig. 38(b).

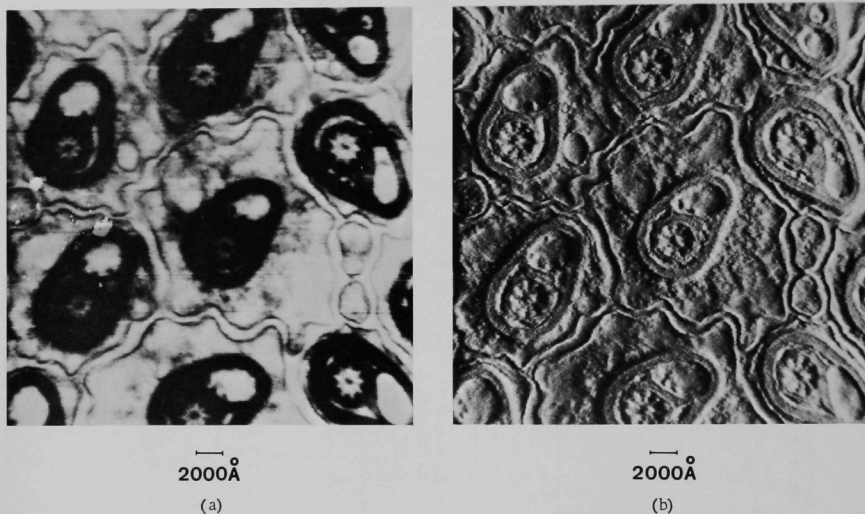


Fig. 38. Camera-system Picture of *Helix Aspersa*. (a) Direct signal and (b) Differentiated signal. ANL Neg. No. 143-2677.

16. VACUUM SYSTEM

16.1 Requirements

To operate with stability and reliability, a cold-emission source of electrons requires an ultrahigh vacuum environment. The figure generally quoted is 10^{-9} Torr pressure for continuous operation; so the microscope was designed to operate at that pressure.

In principle, it is possible to pump differentially, keeping the tip area at 10^{-9} Torr and the remainder of the microscope at a higher pressure. The only opening necessary between the two volumes is a beam aperture which can be of the order of 1 or 2 mm diameter. However, it was calculated that the pumping capacity needed would be quite large, and there was no assurance at such low pressures that the required vacuum could be attained. Since it appeared to be reasonably straightforward to accommodate the remainder of the system to 10^{-9} Torr pressure service, it was decided to build the entire microscope to operate at that pressure.

16.2 Chamber

16.2.1 Design

Initially, it was planned to build the microscope in a modular optical bench type of configuration, which would have some advantages for changing components. However, the actual design became essentially a microscope inside a single vacuum chamber. There were two primary reasons for adopting this design.

First, it was apparent that pumps would be necessary at several places along the column, and the ion pumps needed are heavy, cumbersome devices to move around for lining up components to which they are attached.

Second, the tolerances required in lining up the anodes, magnet, and spectrometer were of the order of 0.0002 in. Setting these tolerances and maintaining rigidity to that order were somewhat uncertain using demountable flanges. Therefore, the magnets, deflection system, specimen holder system, and spectrometer were built rigidly attached to a center base plate of 3/4-in.-thick stainless steel, which was in turn rigidly attached to the chamber. The magnet structure with apertures was built directly onto the top side of the plate, and the spectrometer directly to the bottom side.

The chamber is a split box, one half of which is rigidly mounted to the base and has the ion pumps and liquid nitrogen baffle attached (as shown in Fig. 39). The other half is movable when the flange is unbolted, and it contains the working components and mechanisms as well as electrical connections.

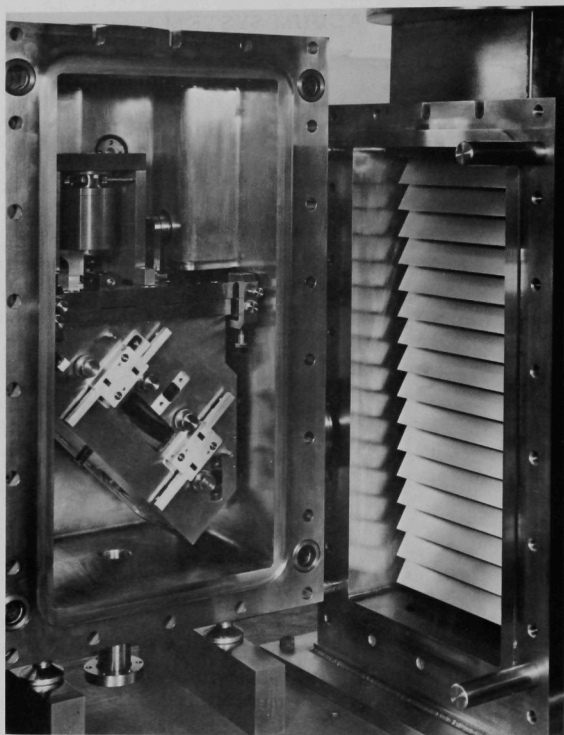


Fig. 39. Microscope Chamber. ANL Neg. No. 210-715.

The chamber main flange has approximately $10\frac{1}{2} \times 22$ -in. inside dimensions. Each flange half is made of $7/8$ -in.-thick stainless steel plate. The seal is a simple corner type with a 0.040-in.-diam gold wire gasket.

The detector extension of the chamber has about a 4-in. inside diameter with a grooved Vactite-type termination to which is attached a gate valve. The valve isolates the detector-slit section in order to change detectors without complete loss of vacuum in the microscope. (Actually, except for a few occasions in the first days of operation, this valve has not been needed and would no doubt have been left out had its lack of use been foreseen.)

Flanges other than the main one, the cold trap seal (see Section 16.4), and the gate-valve attachment, are all Varian Conflat units. Three 6-in.-ID flanges are used, one at the top to hold the high-voltage insulator, and two on the back side for the ion pumps. Twelve 1-in.-ID ($2\frac{3}{4}$ -in.-OD) flanges are used: two for slit adjustments, two for specimen motion, two for

spectrometer potential feedthroughs, two for windows (one at the emission tip level, one to look up the column axis), one for adjustment of the spectrometer entrance diaphragm, one to move a 45° mirror into the column for visual inspection, one for a vacuum gauge, and one for the roughing pump system.

16.2.2 Materials

The chamber is made of Type 304 stainless steel with $3/8$ -in.-thick walls. All welds and inside surfaces were polished down to eliminate surface conditions and defects that might outgas.

This material is a rather clear-cut choice for an ultrahigh vacuum system. In addition, a nonmagnetic material was required which was reasonably well satisfied by Type 304 stainless, although we found evidence of permanently magnetized spots on such material.

All the Varian Conflat fittings use OFHC copper gaskets. The main flange, cold-trap flange, and high-voltage insulator use gaskets made of gold wire 0.040 in. in diameter. The two Vactite gate-valve flanges use copper gaskets. Three Viton O-ring gaskets also face the vacuum volume, one on each of the two light pipes and one on the air-lock gate.

16.2.3 Components

All the movable feedthroughs are actuated through bellows seals. Although changes are made frequently, there are usually six Varian linear-motion feedthroughs with 1 in. travel readable to 0.001 in. in the system.

Three bellows (Flexonics) are used for the slit controls as described in Section 12. Another $2\frac{13}{32}$ -in.-ID Flexonics bellows is between the top flange and the high-voltage insulator flange to permit adjusting the emission tip laterally and longitudinally to the beam axis.

The electrical feedthroughs are commercial units with standard $2\frac{3}{4}$ -in.-OD vacuum flanges. Two single high-voltage units are used for the spectrometer-plate potentials, and an eight-conductor unit is used for deflection plates, stigmators, etc.

Conductors to the quadrupoles and octupoles are led through a tube to the magnet coil chamber. The tube has a small copper-gasket-seal fitting, which seals against the main chamber wall. The inside of the tube leads directly to outside atmosphere. The magnet and coils are isolated from the vacuum by a copper container, and the conductors connect directly to the coils without feedthroughs. This system avoids any outgassing from the coils, and lead-ins, to the vacuum system.

16.3 Pumps and Gauges

Two primary considerations in choosing a pumping system were the requirement to reach 10^{-9} Torr pressure in a reasonable time and the necessity to keep the microscope free of contamination.

The low pressure is required for stable operation of the cold-emission tip. One can perhaps struggle along at a decade higher pressure with frequent flashing of the tip. This has been done in the operation history of the microscope, but it is not a satisfactory procedure. Fluctuations in the beam current show up in the picture intensity with a resultant poor image.

The spectrometer plate surfaces were felt to be particularly sensitive to the effects of very thin films of contamination due to charges being built up on these insulating materials. The surfaces collect many electrons from the beam going through the spectrometer, and any insulating material would quickly become charged. Any charges in this area would distort the focusing by the spectrometer, and the resolution of the spectrometer depends on this sharp focusing ability. Therefore, ion vacuum pumps were chosen for their freedom from contaminating products.

16.3.1 Roughing Pumps

To avoid any possible oil or mercury contamination from roughing pumps, sorption pumps were selected to reduce the chamber pressure from atmospheric pressure to about 10^{-3} Torr. Two standard Varian VacSorb pumps are used in succession. The first pump reduces the pressure to 1 to 10 Torr, and the second reduces it to the point where the ion pumps can be started. These pumps each contain 3 lb of synthetic zeolite, are chilled with liquid nitrogen for pumping, and are regenerated by baking at $\sim 300^{\circ}\text{C}$ for several hours.

To shorten the roughing time (to half of the original $1\frac{1}{2}$ -2 hr), a mechanical roughing pump was added. Oil contamination was avoided by using a liquid-nitrogen vapor trap along with a long (~ 30 ft), small tube between the pump and the microscope. After mechanical pumping, one sorption pump is usually sufficient for the remainder of the roughing stage. After several years of using this system, there is no evidence of oil contamination in the microscope.

Valves between each pump and the roughing manifold are $1\frac{1}{2}$ -in. Viton-sealed, bellows-sealed-drive, high-vacuum units (Varian Right Angle Valves). The manifold is connected to the microscope chamber through a bakeable valve with copper seal and bellows drive. This valve is closed to a measured torque, which is increased slightly until eventually a new copper seat is necessary (Varian Right Angle Bakeable Valve).

Pumping controls were mounted on a separate rack and included, for roughing, a Bourdon-tube gauge and a General Electric viscosity-drag type meter. A thermocouple gauge mounted in the roughing manifold then measured the pressure down to about the roughing limit.

16.3.2 Ion Pumps

Ion pumps were chosen for final pumping, because there is no possibility of contaminating the system with organic materials. There is a risk of titanium atoms coming out of the pump, but these can be stopped by a baffle, which is the cold baffle in this microscope.

Two 400-liter/sec Varian VacIon pumps operate in parallel to the microscope chamber. The weight of these pumps is carried by the microscope base to avoid having the vacuum flanges carry the load. One pump has a built-in heater, which is used occasionally for baking. The other pump is baked by operating it at 10^{-4} to 10^{-5} Torr, where its internal power usage is of the order of 1 kW.

Stray magnetic fields from these pumps were of the order of 1 G near the electron beam before shielding was installed. Various shields were used, including perforated Mumetal cylinders around the beam area, and a 1/2-in.-thick steel plate between the microscope chamber and the pumps. This plate is outside and, of course, does not cross the 6-in.-diam pump connections; however, it appeared to reduce the field near the beam.

16.3.3 Nonmagnetic Pumps

Search for a nonmagnetic, noncontaminating, silent pump led to the purchase and testing of an Orb-Ion electrostatic ion pump. As of this writing, however, this pump has not been installed.

After some modification (changing flanges to Varian Conflat, etc.), the pump was tested and found to have the desired pumpdown rate and base pressure (in the 10^{-10} -Torr decade). However, to install it on the microscope requires a 90° bend, which deteriorates the pumping speed. This is due to the fact that these pumps must operate in a vertical position, because the cathode core is a thin rod supported only at one end and it would sag if operated horizontally. Another possible drawback is the high-frequency oscillation generated by the pump.

16.3.4 Gauges

No indicator is used for pressures from atmospheric pressure down to about 100 Torr. At this point, a General Electric viscosity type gauge indicates the pressure down to about 0.1 Torr, at which point a thermocouple (TC) gauge is capable of indication. The TC gauge indicates pressure down to about 5×10^{-3} Torr and, with decreasing accuracy, to

At the TC-gauge lower limit, the ion pumps are turned on. Although in principle, the ion gauge should begin to indicate at about the TC-gauge limit, it was the experience at the microscope that the next decade (10^{-3} to 10^{-4} Torr) was a range in which the pressure is unknown. There are gauges that cover this region, such as an ion gauge operating in the Pirani mode, but none were installed in the microscope. It is not normally necessary to know the pressure, except as an indicator of trouble such as a leak. With experience, pumpdowns were routinely successful, and, in fact, the ion gauge was eventually removed to make room for a magnet-cooling-liquid feedthrough.

The ion-pump current is a fairly accurate measure of the pressure in the range 10^{-6} to 10^{-10} Torr, ranging from ~ 100 mA to ~ 0.1 μ A. For some time now, this has been the only indicator of pressure used in the microscope below 10^{-3} Torr.

16.4 Cold Trap

To speed up the pumpdown time by removing condensable vapors rapidly, a liquid-nitrogen-cooled baffle was installed. It consists of two vertical tubes hanging from the tank with baffle plates mounted between them. The entire structure is of stainless steel.

The top flange of the tank seals to a mating flange on the microscope, using a gold wire gasket, which is a ring 11.5 in. in diameter. The microscope vacuum around the tank provides thermal isolation except for the contact at the flanges.

The baffle plates are shaped with an open U cross section and are spaced so that the baffle blocks any straight line through it, primarily to prevent titanium atoms ejected from the pump from reaching the operating components of the microscope.

One failure of the trap occurred when the weld at the bottom of one of the vertical tubes broke, due to freezing of water that had accumulated in the tube to a depth of about 2 in. To prevent this occurring again, whenever the microscope is opened to atmosphere, tubular heaters are first dropped into the tubes, all nitrogen is boiled away, and the tubes warmed to $\sim 120^{\circ}\text{C}$. This procedure further prevents condensation on the outside (vacuum side) of the baffle system when opened, making the subsequent pumpdown much easier.

16.5 Procedures and Experience

Discussed here are some of the unusual experiences, pitfalls encountered, and comments about equipment and components.

16.5.1 Pumpdown

Early experience with troubles during pumpdown were usually associated with leaks in the gold-wire seals. Basically, the flanges and gaskets were well designed, and the solution was generally adequate tightening.

Outgassing was not serious after dry nitrogen was used for back-filling. Extreme care in cleanliness was followed for everything installed inside the vacuum system.

Bakeout was discontinued after the initial one at over 200°C (see Section 17.3), since operating vacuum could be reached in a reasonable time (4 or 5 hr).

16.5.2 Electrical Conditioning

After pumpdown, high voltages need to be brought up gradually and with protection against discharge damage. After some trials and a few jarring breakdowns, the procedure adopted is to bring the high voltage up gradually with a 100-megohm resistor in series. When the system appears stable at operating potential, the resistor is removed. No resistor is used for operation because current variations would produce potential variations in electron energy with loss of focus and resolution in the image.

Spectrometer potentials require "conditioning" also after each opening of the microscope. These were quite troublesome in the first few months of operation, but gradually improved with usage, and later conditioning could be done in 10 min. This is normally done during pumpdown while the pressure is in the 10^{-3} to 10^{-5} Torr range, as cleanup is much more efficient there than at lower pressures.

16.5.3 Sorption Pumps

One problem involving the sorption pumps was the appearance of zeolite granules in the manifold and microscope chamber. A few misoperations of the valves probably allowed a blast of gas into the microscope. When procedures were more carefully controlled and a safety screen was installed in the neck of the sorption pumps, no further trouble was experienced.

Recent procedure has been to let the mechanical pump run until the pressure reaches <0.1 Torr. Then one sorption pump can reduce the pressure to the ion pump starting point a number of times before bakeout is necessary.

The zeolite has been changed several times, more as a measure of preventive maintenance than of any clear evidence that the material was failing.

16.5.4 Ion Pumps

The ion pumps operated without rebuilding or disassembly for at least 4 years including some hundreds of pumpdowns and were in service most of the time. A few failures occurred in the electrical feedthroughs. Failures occurred in the cable plug that connects to the feedthrough. These were attributed to deterioration from bakeout temperatures.

Occasional servicing to remove emission-point growth on the titanium anodes is necessary. This condition is noted by an abnormally high pump current for the pressure actually present, due to electron emission from points. These points are eliminated by connecting a 14- to 15-kV source to the pump anodes and leaving it for 15-30 min. At this potential, emission current from the points is high enough to destroy them.

That baffle protection between pumps and system is necessary as evidenced by the discoloration on the cold baffle side facing the pump. The stainless steel has a dark burned appearance, due probably to ejection of titanium atoms and to glow discharges that occur at $>10^{-3}$ Torr pressures, which often flash in the system beyond the pump.

16.5.5 Flanges and Seals

The three gold wire gaskets (main body flange, cold trap tank, and high-voltage insulator) are made in Central Shops by cold welding and then smoothing the weld. At first some leaks occurred, but later they proved completely reliable when sufficient torque was applied to the flange bolts.

The three Viton O-ring seals (air-lock gate and two light pipes) were quite reliable, except that a few failures of the gate gasket occurred after bakeouts that may have reached 200°C. The rings were found to have deformed to the shapes of their contacting surfaces.

All the Varian Conflat seals were satisfactory, with no failures when they were properly tightened.

17. BASE AND ACCESSORIES

This section describes miscellaneous parts of the microscope and various outside pieces of equipment used in connection with microscope operation.

17.1 Base

The base was made rigid to avoid any possible bending that might affect microscope alignment and also to support the heavy components. The two ion pumps weigh ~700 lb, and the microscope chamber itself is quite heavy. The complete microscope, with base, weighs nearly 1 ton.

The base top is a plate of 7/8-in.-thick steel. Sides of 1/2-in.-thick steel are welded to the top, along with a 3/8-in.-thick back. The front is left open, except for a sturdy cross brace near the bottom, for access to the sorption pumps and valves. A slot was cut in the top through which the vacuum roughing tube extends to the sorption pumps and permits the front chamber to be moved out for opening the chamber without removing this tube. The top dimensions are $30\frac{1}{2} \times 44$ in., and the surface is 37 in. above the floor, without antivibration mounts.

17.2 Telescope

A telescope was provided for looking along the electron beam axis from below the specimen up to the emission tip. It is mounted horizontally, and a 45° mirror is pushed into position through a bellows feedthrough to permit viewing up the axis. The mirror consists of an aluminum coating on a stainless steel block and is located between the specimen and the spectrometer. During microscope operation, it is retracted out of the way of the electron beam.

The telescope is a Gaertner M522-C laboratory telescope with modified mounting and equipped with an auxiliary lens to reduce the working range to a span of 30-60 cm. At 30 cm the specimen is in focus at ~22X magnification, and at ~60 cm the top anode and emission tip are in focus at ~12X magnification.

The telescope is mounted on a rigid arm attached to the base and has lateral and angular adjustments. Vacuum-tight windows at the telescope level and emission tip level permit illumination and viewing of the microscope interior.

The telescope was very useful in the first operations of the microscope for noting positions of the various parts of the specimen and for checking alignment of the first anode. However, it was not needed for later operation and has been removed, along with the lower window and the 45° mirror, the latter to make room for a below-specimen set of apertures.

17.3 Bake-out Oven

For baking the microscope at 250°C to achieve 10^{-9} Torr vacuum readily, an oven was built that could be placed over the entire operating part of the microscope, excluding the ion pumps, which can be heated independently.

The oven was a rectangular chamber, with open bottom, that set directly on the base top. The sides were of 1-in.-thick Marinite-36. Flat heaters aggregating a power of 4000 W were attached directly to the walls. The box was divided for ease of installation.

The oven was used for the initial pumpdown, and temperatures in the microscope reached well over 200°C. Subsequent pumpdowns were found to be satisfactory without baking at high temperatures, so the oven was not used again and was eventually dismantled.

17.4 Test Fixtures for Gun

Three test fixtures for testing filaments have been constructed. The first has a 4-in.-diam chamber long enough to accommodate the high-voltage insulator and anodes. The end plate can be changed to have a fluorescent screen, an extension, or an electrode as desired. The unit is mounted on the flange of a 400-liter/sec ion pump and has provision for roughing pump connections.

This chamber was used mainly to observe the direction and pattern of the electron emission from the tip to see if it was suitable for use in the microscope. It was also used to observe the focal properties of the gun with anodes by providing a movable fluorescent screen in an extension tube.

The first chamber's usefulness for gun studies made a second unit necessary for checking tips routinely. This is a much smaller unit, being made essentially of $2\frac{3}{4}$ -in.-OD flange fittings with a 30-liter/sec ion pump.

With increased usage and studies of different types of tip material, it became necessary to build a third fixture to test up to five tips with one pumpdown. This is a simple chamber with a fluorescent screen on one end and a plate with feedthroughs for five tips on the other. An 8-liter/sec ion pump is attached.

The fluorescent screens were made using commercial high-vacuum flange windows, coating them with stannous chloride vapor to form a conductive surface for the electrons to escape, and depositing a commercial fluorescent layer.

17.5 Filament-forming Fixtures

The filament has five bends, which are formed in three steps using three separate forming jigs. The first one makes a square U-bend, and the second bends the U bottom piece into the filament V, with the original U legs now in one straight line. The third jig bends the two legs.

For welding the 5-mil-diam tip wire onto the 8-mil filament, a jig was made, with grooves to hold the wires in position. They are welded together in a small electric resistance welder using 1/8-in.-diam molybdenum electrodes with 1/16-in. tip diameter, applied at 8-oz force. A 2.8-J discharge pulse is used.

18. POWER SUPPLIES

18.1 High-voltage Supply

The microscope was built for an operating potential of 50 kV. The high-voltage supply (see far left cabinet in Fig. 1) purchased has a range of 10 to 80 kV at 0.5 mA output. The unit, a Canalco Model 80, operates internally at 70 kHz and has a dc output regulation specified at 50 ppm including ripple, but in tests appears to have a short-term regulation of 10 ppm.

Several modifications were made as the needs developed. The output voltage range is covered by a rotary switch providing 32 increments that vary from a few hundred volts at the low-voltage end to several thousand at the high end. For gun-focus studies, continuous voltage adjustment was needed, so a multiturn potentiometer was added to the divider network for this purpose. Later a selsyn drive was put on this potentiometer with the drive unit on the operator's panel at the microscope.

The power supply is located approximately 20 ft from the microscope to avoid possible magnetic effects on the electron beam.

Service experience on the supply has been good. A few failures have occurred involving electronic components, such as a divider string resistor opening up, and tube failures. The original high-voltage cable and connector failed after about two years of operation and was replaced by a cable rated for 100-kV operation.

18.2 Tip-bias Supply

The bias anode is set at a potential to cause cold emission of electrons from the source tip. This potential depends on the size and nature (materials or adsorbed layers) of the tip and on the emission current. It therefore must be adjustable and stable, since the current is a sharply rising function of voltage once emission begins. The magnitude is usually 1 to 3 kV positive with respect to the tip. Also, since this anode and associated circuits are at nearly full accelerating potential with respect to ground, this system must be built to ride on the high-voltage level without leakage or danger.

Leakage currents from the bias system must be kept very low, no more than a few nanoamperes, to avoid disturbing the high voltage at the tip. Energy resolution as well as focusing depend on an energy spread in electrons that is very low, hopefully no more than a few tenths of an electron volt.

18.2.1 Original Divider

Initially, the bias potential was obtained from a voltage divider between the high voltage and ground. The total resistance is 200 M Ω with a Kelvin-Varley-type divider covering the range -45 to +50 kV (0 to +5 kV bias) in 100-V steps (at 50-kV accelerating potential). The resistors and switches are all immersed in a Plexiglas box filled with transformer oil.

This unit was used only a short time, because of leakage currents around the terminals. Although these currents were small, they were sufficient to cause some instability in beam current and energy. While the divider was being repaired, a simple battery unit was used which proved to be satisfactory, so the divider was not used again.

18.2.2 Battery Bias Supply

Except for the short initial period using the divider previously described, batteries have been used to supply the first anode bias. Two rotary switches are used, one for 300-V steps using small dry batteries each with 300-V output. The other switch provides 22.5-V steps from another set of batteries.

The first unit was a simple box containing batteries, switches, and an electrometer. After occasional experiences with corona leakages, a unit was built with corona shields. Four doughnut-shaped shields with a 250-kV operation rating are used, providing three between-shield spaces, one for the batteries, one for the switches, and one for the electrometer. This eliminated all leakage problems in that part of the system. This system is enclosed in a large Plexiglas box.

18.2.3 Electrometer

Part of the tip emission current is collected by the first anode and is the amount of current supplied by the batteries. Since this current is a few microamperes or less, the battery life approaches its shelf life. The current in this loop is measured by an electrometer inside the tip bias box. The electrometer is battery operated with ranges of 10^{-10} to 10^{-7} A full scale, and was designed by D. Keefe in the Electronics Division. In addition, a microammeter is connected in series with the electrometer to indicate currents up to 20 μ A. This current is watched carefully during operation because it shows when erratic emission starts at which time flashing is necessary.

The part of the emission current that is not intercepted by the bias anode is supplied by the high-voltage power supply and circulates in that loop of the circuit. The beam current to the specimen is included and is of the order of 10^{-9} A. This current is not measured.

18.3 Spectrometer Supplies

18.3.1 Requirements

Two potential supplies, one positive and one negative, are needed for the two spectrometer plates. The potentials required (see Section 11.2.1) for 50-keV electrons are +7115 and -6225 V and are proportional to the electron energy.

The stability needed is calculated as follows: A permissible movement, ΔeV , at the energy slit of the electrometer is selected. The ratio $\Delta eV/V_0$, where V_0 is the electron energy, is the relative stability required because of the direct proportionality between spectrometer potential and electron energy. Initially, a 10-eV energy resolution was decided upon, and one-fourth of that or 2.5 eV was selected as a maximum permissible instability. Therefore, the stability required was $2.5/50,000$ or 0.005%. These specifications were met by Fluke 410A supplies, which have adjustable outputs up to 10,000 V.

Later, reworking the spectrometer energy slits and adding an external quadrupole permitted the resolution to be improved to ~ 0.6 eV, implying a stability somewhat better than a part in 10^5 . In fact, there is no apparent short-term movement of the peak at maximum resolution, whereas an instability of two parts in 10^6 could probably be seen as a movement of the peak.

18.3.2 Modifications

18.3.2.1 Tracking. The ratio of radii of the inner to the outer spectrometer plate is very nearly $7/8$. Therefore the outer (negative) potential is $7/8$ that of the inner plate.

Frequent resetting for different energies, for changes in primary electron energy, and for tracing out energy curves makes it difficult to set one reading at $7/8$ the other. Therefore, this supply was modified to give an output potential which is $7/8$ of the knob readings. Therefore, both supplies are always set to identical readings, making operation much simpler.

The modification was straightforward. Regulation started from a voltage divider in the supply with 10,010 k Ω total resistance with sampling voltage tapped 247 k Ω from the low-voltage end of the string. This 247-k Ω resistance was changed to 282 k Ω ($8/7 \times 247$) by adding a 35-k Ω resistor. Then 35 k Ω was removed from the other leg of the divider. A trimming potentiometer at the tap then is used for final alignment.

18.3.2.2 Simultaneous Operation. Tracking and searching for energy information are much more satisfactory if changes can be made using a single control and making it continuous. This was done by inserting a 100-k Ω linear multiturn potentiometer into the divider string, between the high-voltage terminal and sampling takeoff point, of each power supply. The two potentiometers are ganged together mechanically so as to be turned simultaneously by one knob. The potentiometers are mounted in a panel on the microscope operating console and are mounted so as to withstand 10 kV between them and ground and 20 kV between potentiometers.

The divider string has a resistance of 1 k Ω for each volt output. Therefore, the 100-k Ω potentiometer adds from 0 to 100 V to the reading on the power-supply panel of the positive supply, and each division on the 10-turn dial represents 0.1 V. The output of the negative supply tracks at 7/8 times the readings.

18.3.2.3 Overvoltage and Reversing. To reduce electrical discharges between spectrometer plates after the microscope is opened to atmosphere, it is helpful to apply potentials well above the operating range and to reverse the polarity of them.

The power supplies were modified to supply about 12 kV by switching in a resistor parallel to the string between sample tap and ground, thus lowering the potential at the sample point. This forces the regulator to its upper limit and supplies the higher voltage at the terminals.

A separate panel contains reversing switches between the power supplies and the spectrometer plates to aid in the electrical cleaning-up process. These switches are ceramic-frame-type rotary units designed for high voltages.

18.4 Magnet Supplies

18.4.1 Requirements

The stability needed for the focusing-lens currents is of the order of 10^{-6} (calculated in Section 6.1.2.3). The best rated current stability in a commercially available supply known to us at the time was 0.001% in 8 hr, in the Princeton TC-100.2R unit with maximum output 100 mA at 0 to 100 V compliance voltage.

Five Princeton supplies were purchased, one for each of the two quadrupoles and for each of the three octupoles.

Stability over hours is not particularly important with this microscope; however, short-term stability over 20-30 min is necessary. Tests on these supplies indicate that short-term stability, ripple, and noise add up to the order of 10^{-6} of maximum current.

The quadrupole coil parameters were selected to give a total resistance of $1000\ \Omega$ per quadrupole to take advantage of the maximum current, 100 mA, at maximum potential, 100 V, available from the power supply. Each octupole has a resistance of about $450\ \Omega$, but calculations indicated that the octupole current requirements would be only a few milliamperes and maximum utilization of the power supply would not be necessary. Number 41 B & S gauge wire is used in the octupoles, and increasing the resistance would require using still smaller wire with its attendant delicate handling.

A Princeton Model TC-602CR current supply is used for the $5\ \text{\AA}$ lens. This unit is rated 2 A maximum current at 0 to 60 V compliance voltage, with rated stability of 0.002% over an 8-hr period. The two coils were wound to have a total resistance of $16\ \Omega$.

18.4.2 Modifications

18.4.2.1 Degausser Operations. The reset circuits of the five original current supplies were changed to allow the degausser to control the power supplies, in particular to keep the currents on during degaussing. As degaussing was soon found to be unnecessary, these modifications were no longer used.

18.4.2.2 Rotatable Wheels. In the Model TC-602CR supply, a factory modification was made to have the current-setting wheels continuously rotatable (except the highest-step wheel). These are considerably easier to operate than those that must be backed through their range when the limit is reached.

18.5 Tip-flasher Supply

A pulser was built to supply a pulse of current to heat the tip and clean it of foreign molecules. The unit, designed by P. Michaud and A. Quigley of the Electronics Division, provides an adjustable current up to 10 A at 5 V and an adjustable pulse length of 0.2 to 2 sec.

The first unit had a built-in transformer and flashing required shutting off the high voltage, changing connections, flashing, and restoring operating potential. Later, a transformer with 60-kV isolation between primary and secondary was mounted in the tip bias supply box and connected permanently to the filament. This makes it possible to flash the tip during operation (discussed in Section 4.3.3).

19. ENVIRONMENT

The interactions between the microscope and its environment are generally such as to degrade its performance. Temperature effects may become serious as the ultimate resolution of design is approached, but no serious adverse effects have been noted. A reasonably well regulated temperature in the room should be adequate. Electric fields in the area have been of no concern, since they are blocked from the interior of the microscope by its metal case.

The two most disturbing environmental elements are fluctuating or oscillating magnetic fields and mechanical vibration. These have required extensive study and will probably require more effective solutions as resolution is improved.

19.1 Magnetic Field

If the primary electron beam moves outside its prescribed deflection pattern, the result is similar to increasing the size, and perhaps the shape, of the focused beam image with consequent loss of resolution. A varying magnetic field component perpendicular to the beam can produce such a movement.

For example, using 50-keV electrons, the path in a transverse magnetic field B is a circle of radius R (cm) = $772/B$ (gauss). Over a 10-cm path, a 1-G field deflects the electron 0.64 mm, or a 1- μ G field deflects it 6 Å. Thus, for 5 Å resolution it appears that short-term variations in magnetic fields must be below 10^{-6} G in magnitude.

A perfectly stable magnetic field, provided it is not so large as to bend the beam into apertures (~ 1 G), is not troublesome, since the effect is to simply shift the raster at the specimen. Similarly, slow variations, changes in the order of a raster period, would distort the image and may or may not be objectionable, depending on the accuracy of reproduction desired.

Fast fluctuations move the spot over an area larger than the beam image supposedly covers and therefore degrade the resolution. These variations must be reduced to low magnitudes, or compensated for--which is possible in some cases to a limited extent (60-Hz compensation described in Section 19.1.3).

19.1.1 Measurements and External Generators

The ac magnetic field was measured with a coil composed of half of the secondary of an automobile ignition coil. This coil was connected directly to an oscilloscope. The coil was calibrated by comparing its

reading, simultaneously in the same location, with that of a Bell Gaussmeter using a Hall probe, which was in turn checked against magnets supplied for that purpose. The coil has a sensitivity of 1.02 V peak-to-peak for a 60-Hz magnetic field of ± 1 G amplitude.

The measured fields around the microscope area in Building 818 varied from less than 1 to 20 or 30 mG, and the direction of the field varied with location.

Earlier measurements were considerably higher, and the generators of these high fields were found to be circulating currents in steam piping between Buildings 818 and 827, and in piping to the steam heater in the microscope room. These currents were eliminated by installing an insulating separator at a coupling in each line.

Some obvious methods of reducing stray fields were put into effect by removing the high-voltage power supply, the vacuum-pump supplies, and other equipment some distance away (10-20 ft).

19.1.2 Microscope Shielding

The beam inside the microscope was shielded with Mumetal cylinders and plates of various configurations to suit the different components used. The shields were placed to reduce the field only between the gun and the specimen. Beyond that point, small ac fields are less serious in that signal strength only is affected when high-energy resolution with narrow detector slits is desired. Large fields, ac or dc, can cause trouble, because of possibly diverting desired electrons from the detector slit and diverting unwanted ones into the slit, but none of this affects spatial resolution in the specimen.

Shields were perforated, particularly around the emitting tip area, to reduce the impedance for gas flow in pumping. They were annealed by the Lindberg Steel Treating Company after all work on them was finished.

Outside the microscope a 1/2-in.-thick steel plate was placed between the ion pumps and the microscope body to reduce the stray dc field from the pumps. This reduced the field near the beam from the order of 1 G to a small fraction of a gauss. Although this field is steady, it was large enough to deflect the beam too far, particularly when small apertures were used.

19.1.3 Compensation

Assuming the 60-Hz field is uniformly repetitive and is from the power line, the picture image can be improved considerably by keying the horizontal sweeps in the deflection to the same phase of the ac line. Any vertical deviation due to the field then occurs at similar positions along the horizontal sweeps, resulting in a picture slightly bent or "humped" uniformly

from top to bottom. Any horizontal deviation similarly appears as a picture slightly stretched and compressed in the horizontal direction, but this distortion is again uniform from top to bottom.

Synchronization of the horizontal sweep to the line frequency was incorporated into the system so that one sweep was made for each cycle of the power line. The 10-sec picture generation then was made with 600 lines rather than the original 1000. However, the improvement in picture quality was quite evident as a result of removing the randomness of deviations of the beam on the raster area.

Another form of compensation is to nullify the fields by adding equal but opposite-direction fields by means of coils. This system was tried using two pairs of rectangular coils outside the microscope and applying power-line currents appropriately adjusted. (No coils were used to produce a field parallel to the electron beam, since such a field does not deflect the beam.)

A servo operation of such compensating field coils has been considered and may be required ultimately. This would consist of a pickup to measure the fluctuating fields and a controller to apply appropriate currents to the compensating coils. This type of system would not be limited to power-line compensation, but could in principle correct for all varying magnetic fields.

19.2 Vibration

Mechanical vibration can degrade the resolution for essentially the same reason that fluctuating magnetic fields do. That is, the electron beam moves, with respect to the specimen, outside of its prescribed deflection pattern.

Vibration can show up in several places. The emission tip is thin and long and can easily acquire a cantilever-type vibration. This tip is then a moving source for the beam, and the focused image executes corresponding motions, thus increasing the effective spot size.

The other vulnerable spot for deleterious vibration effects is at the specimen, with relative motion between it and the lens and beam. Other components are less susceptible because they can be mounted more rigidly.

Attempts to measure the intensity and frequency of vibrations in floors did not produce results that were very helpful in solving the problem of vibration, except to avoid placing the microscope in high-vibration locations.

The first location in Building 21 was not very satisfactory. Although the concrete floor was directly on the ground, considerable vibration was apparently transmitted through connection paths to large fans and machinery

in Building 17 nearby. The microscope was then moved to the vault attached to Building 818. This room has a thick concrete floor set on the ground and not rigidly connected to Building 818. For resolutions down to 50 Å or so, which was attained in this location, vibration did not seem to be a serious problem.

Spring shock mounts were used as feet for the microscope. These were chosen from commercially available units (Barry Controls) suitable for the load imposed on them.

In Building 21, where vibration was serious, various other ways of mounting the microscope were tried, none of which were successful. Among those tried, one was a set of inflated tires from a Cushman vehicle.

The Building 818 vault proved to be much quieter and, from the vibration standpoint, was satisfactory for the resolution attained at that time (50 Å). Interestingly enough, the best freedom from vibration occurred when the microscope was supported rigidly on the concrete floor, using jack screws.

A design for suspending the microscope on long elastic ropes was made, but had not been constructed at the time of the termination of the project at ANL. The suspenders are shock-absorber cords made of multiple rubber-band filaments covered with a stretchable woven tube. These are used for exercisers and for holding delicate cargo in aeroplanes. Resonance at 1 Hz requires an elastic extension of 10 in. Therefore an overhead frame was designed to use cords about 5 ft long.

ACKNOWLEDGMENTS

Many people were involved in one way or another with the design and construction of the microscope. It would be difficult to try to give proper credit to everyone, and no attempt at such will be made. However, a few people had unusual responsibilities and should be singled out for their outstanding contributions to the project.

The mechanical portion of the microscope was designed primarily by J. M. Nixon, and construction was carried out under the supervision of E. G. Sundahl, both of Central Shops.

The electronics part was designed and constructed under the supervision of W. K. Brookshier of the Electronics Division. Design problems generally concerning specimen-beam interactions and signal detection were solved by J. Gilroy and R. J. Epstein of the Electronics Division.

The original idea, basic concepts, and continuous development of ideas, as well as much of the hardware designs were, of course, those of A. V. Crewe. I was associated essentially as project manager for the design, construction, and development of the microscope.

REFERENCES

1. J. W. Butler, "Digital Computer Techniques in Electron Microscopy" *Proc. Sixth Intern. Cong. for Electron Microscopy*, Kyoto, pp. 191-192 (1966).
2. R. Gomer, *Field Emission and Field Ionization*, Harvard University Press, Cambridge, Massachusetts (1961).
3. R. D. Young and E. W. Muller, *Experimental Measurement of the Total-Energy Distribution of Field-Emitted Electrons*, *Phys. Rev.* 113, 115-120 (1959).
4. J. P. Barbour, F. M. Charbonnier, W. W. Dolan, W. P. Dyke, E. E. Martin, and J. K. Trolan, *Determination of the Surface Tension and Surface Migration Constants for Tungsten*, *Phys. Rev.* 117, 1452-1459 (1960).
5. P. A. Sturrock, *Static and Dynamic Electron Optics*, The University Press, Cambridge (1955).
6. A. Septier, *Etude experimentale des aberrations d'ouverture d'un system de deux lentilles quadrupolaires magnetiques*, *Compt. Rend.* 245, 1905-1908 (1957).
7. W. Glaser, *Strenge Berechnung magnetischer Linsen der Feldform $H = H_0/[1 + (z/a)^2]$* , *Z. Physik* 117, 285-315 (1941).
8. E. Ruska, *Current Efforts to Attain the Resolution Limit of the Transmission Electron Microscope*, *J. Roy. Microscop. Soc.* 84, Pt. 1, 77-103 (1965).
9. J. H. Reisner, Broadcasts and Communications Products Division, Radio Corporation of America, Camden, N. J., private communication.
10. P. F. Meads, Jr., *The Theory of Aberrations of Quadrupole Focusing Arrays*, Ph.D. dissertation at the University of California, Berkeley (May 15, 1963); available as Lawrence Radiation Laboratory Report UCRL-10807 (1963). A summary was published in *Nucl. Instr. Methods* 40, 166-168 (1966).
11. H. G. Cooper, *Design of a High-Resolution Electrostatic Cathode Ray Tube for the Flying Spot Store*, *Bell Sys. Tech. J.* 40, 723-759 (1961).
12. E. M. Purcell, *The Focusing of Charged Particles by a Spherical Condenser*, *Phys. Rev.* 54, 818-826 (1938).
13. C. P. Browne, D. S. Craig, and R. M. Williamson, *Spherical Electrostatic Analyzer for Measurement of Nuclear Reaction Energies*, *Rev. Sci. Instr.* 22, 952-965 (1951).
14. M. G. Inghram and R. G. Hayden, *Mass Spectroscopy*, Nuclear Science Series Report No. 14, NAS-NRC Publication 311, pp. 8-9 (1954).
15. R. G. Herb, S. C. Snowdon, and O. Sala, *Absolute Voltage Determination of Three Nuclear Reactions*, *Phys. Rev.* 75, 246-259 (1949); Appendix I, "Determination of Effective Entrance and Exit Planes of Analyzer," [p. 257] and Appendix II, "Ideal Analyzer Relations," [pp. 257-258].
16. W. K. Brookshier and J. Gilroy, *Display System for Use with a Scanning Electron Energy Analyzing Microscope*, *IEEE Trans. Nucl. Sci.* 12, 104-110 (1965).

PERMANENT NATIONAL LAB WEST



3 4444 00008281 8

x

